REGULATORY MECHANISMS GOVERNING THE ESTABLISHMENT OF CELL POLARITY AND MITOTIC SPINDLE ORIENTATION IN THE *DROSOPHILA* NEUROBLAST

by

JONATHON FREDRICK MAUSER

A DISSERTATION

Presented to the Department of Chemistry and Biochemistry
and the Graduate School of the University of Oregon
in partial fulfillment of the requirements
for the degree of
Doctor of Philosophy

June 2014

DISSERTATION APPROVAL PAGE

Student: Jonathon Fredrick Mauser

Title: Regulatory Mechanisms Governing the Establishment of Cell Polarity and Mitotic Spindle Orientation in the *Drosophila* Neuroblast

This dissertation has been accepted and approved in partial fulfillment of the requirements for the Doctor of Philosophy degree in the Department of Chemistry and Biochemistry by:

Tom Stevens	Chairperson
Kenneth Prehoda	Advisor
Bradley Nolen	Core Member
Raghuveer Parthasarathy	Core Member
Christopher Doe	Institutional Representative

and

Kimberly Andrews Espy	Vice President for Research and Innovation; Dean of the Graduate School

Original approval signatures are on file with the University of Oregon Graduate School.

Degree awarded June 2014

DISSERTATION ABSTRACT

Jonathon Fredrick Mauser

Doctor of Philosophy

Department of Chemistry and Biochemistry

June 2014

Title: Regulatory Mechanisms Governing the Establishment of Cell Polarity and Mitotic Spindle Orientation in the *Drosophila* Neuroblast

The *Drosophila* neuroblast undergoes repeated asymmetric cell divisions that produce one daughter cell that assumes a neuronal fate and another that remains a neuroblast. During mitosis, the neuroblast polarizes the conserved Par polarity complex to the apical cortex, which is responsible for segregating fate determinants to the basal cell cortex. Polarity is accompanied by orientation of the mitotic spindle through the proteins Pins, Mud, and Dlg to ensure that the cleavage furrow properly segregates the fate determinants. The adaptor protein Inscuteable coordinates these two pathways. In my work, I have addressed how asymmetrically dividing cells are dynamically polarized during the cell cycle and how the resulting polarity is coupled to spindle position.

To address how neuroblast polarity is dynamically controlled, I identified the protein Inscuteable as a continuously polarized cue for Par complex localization during mitosis. Inscuteable and Bazooka, a member of the Par complex, interact directly and form a complex that is regulated by the mitotic kinase Aurora A. Regulating this interaction allows for cell-cycle dependent establishment of polarity and for the subsequent loss of polarity after the cell divides.

To investigate how Par complex directed polarity is connected to spindle position, I investigated the effect of Inscuteable binding on the spindle orientation ability of the protein Pins. When bound to Inscuteable, Pins' spindle orientation activity becomes repressed. Inscuteable competes with Mud for Pins binding and represses the Gai-Pins-Mud signaling pathway. Function of the parallel Pins-Dlg pathway remains unaffected. This repression behavior may allow differential timing of spindle attachment (through Dlg) and spindle shortening (through Mud) pathways that ensures correct alignment of the mitotic spindle.

I was able to model the spindle orientation behavior of Pins using a synthetic protein containing activation sites that have different affinities for the activator. Changing the number and affinities of these activation sites leads to different response profiles that mimic the ultrasensitive behavior of Pins using a non-cooperative mechanism. Together, these regulatory mechanisms cooperate to allow for spatial and temporal control of polarity and for physical connection of polarity to the mitotic spindle.

This dissertation includes previously published and unpublished co-authored material.

CURRICULUM VITAE

NAME OF AUTHOR: Jonathon Fredrick Mauser

GRADUATE AND UNDERGRADUATE SCHOOLS ATTENDED:

University of Oregon, Eugene
University of Portland, Portland, OR

DEGREES AWARDED:

Doctor of Philosophy, Chemistry, 2014, University of Oregon
Master of Science, Chemistry, 2011, University of Oregon
Bachelor of Science, Chemistry, University of Portland

AREAS OF SPECIAL INTEREST:

Biochemistry
Cell Biology

PROFESSIONAL EXPERIENCE:

Graduate Research Fellow, Department of Chemistry, University of Oregon,]
Eugene, Oregon, 2008-2014

Graduate Teaching Fellow, Department of Chemistry, University of Oregon]
Eugene, Oregon, 2008-2009, 2011-2014

Undergraduate Research Assistant, Dr. Angela Hoffman, Department of
Chemistry, University of Portland, 2006-2008

GRANTS, AWARDS, AND HONORS:

National Institutes of Health Molecular Biology and Biophysics Training Grant
Appointee, University of Oregon, 2009-2010

Graduate Student Award for Excellence in the Teaching of Chemistry
Department of Chemistry & Biochemistry, University of Oregon.

PUBLICATIONS:

Mauser, J. F. and Prehoda, K. E. (2012) Inscuteable regulates the Pins-Mud spindle orientation pathway. PLoS one 7(1), e29611

Lu, M. S., Mauser, J. F., Prehoda, K. E. (2011) Ultrasensitive synthetic protein regulatory networks using mixed decoys. ACS Synthetic Biology 1(2), 65-72

ACKNOWLEDGMENTS

I wish to express my sincere gratitude to my mentor and Ph. D. advisor Dr. Ken Prehoda for his guidance during my time in graduate school and for his assistance in preparing this manuscript. His constant encouragement and guidance of my professional development throughout my time in his lab has had an immeasurable impact on my life and will be invaluable as I achieve my future scientific goals. I would like to thank my thesis committee for giving their input and feedback on my research over the years and for offering their professional advice on developing my career. I would like to thank the members of the Prehoda and Doe laboratories for their helpful discussions, and for generously sharing reagents and equipment. Specifically, I would like to thank Mike Drummond for his friendship and for his technical assistance with tissue preparations and in planning *Drosophila* genetics experiments. I would like to thank Nick Smith for his early influence on me that attracted me to the Prehoda Lab, and to Chris Johnston for being an effective role model and for his friendship. I am very grateful to the Department of Chemistry and Biochemistry for being very accommodating of my desire to develop as a teacher and for providing me ample opportunities to teach and to meet many wonderful students. Finally, I would like to thank all of the members of the Institute of Molecular Biology for their friendship and for making my time at University of Oregon memorable and pleasant. This work was supported by NIH grants R0l GM068032 and R01 GM087457 awarded to K. Prehoda and NIH Molecular Biology/Biophysics Training Grant to J.F. Mauser.

I dedicate this work to my family for always being supportive in all of my pursuits and in believing in me throughout the process of earning my Ph. D. My parents' early influence on me was what made me interested in science and I would not be where I am now without them. I dedicate this to my wife, Meghan, whose love and support during every day of graduate school has been truly invaluable.

With you by my side, anything is possible.

TABLE OF CONTENTS

LIST OF FIGURES

Figure Page

APPENDIX A

LIST OF TABLES

CHAPTER I

INTRODUCTION

From the moment of fertilization to the moment of death, nearly all tissues in the body rely on the correct function of many different types of polarized cells. The cells lining the digestive tract absorb nutrients, skin cells replenish themselves, white blood cells fight invaders, and neurons extend their axons up to a meter to reach the tip of your toe. Despite the variety of tasks they perform, all polarized cells utilize a surprisingly common set of components in order to accomplish their biological functions. In order to accomplish each of these tasks, cells must undergo a common cell process, known as cell polarity, in which subcellular contents are organized to allow for specific functions to be performed at defined regions of the cell.

Loss of these key polarity components can lead to a disruption of cell orientation control. Skin cells, which usually divide in a controlled manner to add layers to the skin begin to pile up and resemble cancerous growth (Royer and Lu, 2011). White blood cells lacking cell polarity are unable to mature and lead to overproliferation in bone marrow, causing Leukemia (Grabher et al., 2006). Neurons seeking their terminal targets form incorrect branches and never find the cells they intended to innervate (Shimizu et al., 2011; Barnes et al., 2007). Thus, the establishment and regulation of cell polarity is central to many key functions cells perform.

Cell polarity is the process by which a cell organizes its contents to specific regions

of the cell in order to perform cellular tasks. All polarized cell types rely on establishing and maintaining the asymmetric distribution of a core set of protein polarity factors. This process involves both defining the region of the cell that exhibits polarity as well as maintaining a polarized localization of components at that region. Often this process involves the highly regulated coordination of many other cell processes, such as signaling cascades, cell trafficking, and the assembly of function of the cytoskeleton.

These asymmetries can be generated by a variety of different mechanisms and may be activated in a context-specific manner in a process known as symmetry breaking.

There are many ways polarity is established in cells. Unicellular organisms such as yeast develop a small spot on their cell membrane that is utilized to localize cell division machinery and to set the axis of the next cell division. Animal cells can utilize this mode of polarity to allow for cell motility, but can also exhibit different types of polarity that allow for the advent of additional functions. Dividing zygotes and stem cells generate large broad regions of polarized components on the membrane to allow for cell-type differentiation. Over the course of evolution, functional mechanisms of establishing polarity have been selected for and improved. Extant polarization mechanisms are therefore very likely to have many commonalities across species and cell types.

In natural systems, polarity is frequently observed to be oriented towards some signal or cue. These cues can include regulated physical landmarks within the cell as well as signaling gradients from the extracellular environment (Wang et al., 2014; Kato et al., 2011; Moore et al., 2013). Different types of intrinsic and extrinsic cues can lead to different manifestations of polarity. Cells that exist in a stable intercellular signaling gradient, such as in the presence of tissue Wnt signaling, adopt a permanent polarized

localization parallel to the signaling gradient (Strutt, 2001). Many cells exhibit exquisite temporal and spatial control of polarity. Cells undergoing chemotaxis, for example, polarize their movement a directional manner. If the chemical signal moves the cell needs to redirect its polarized motion quickly and efficiently to continue the chase (Gambardella and Vermeren, 2013).

Loss of polarization cues in a statically polarized cell type can lead to depolarization of the cells and reversion to a cancer-like state. In order to avoid detrimental depolarization events, polarized cells exert robust control of the localization and activity of the polarity machinery within the cell. Many common cellular factors that influence the ability for a cell to become polarized have been identified and these share many common mechanistic motifs. How these components are regulated to give rise to the various manifestations of cell polarity in the cell is a major topic of study in modern cell biology.

GENERAL MECHANISMS OF CELL POLARITY

Yeast Polarity

To establish polarity, a cell must localize polarity machinery specifically to one region of the cell. Perhaps the simplest mechanism that could give rise to this behavior would be the direct recruitment of polarization factors to a small region of the cell membrane. The brewer's yeast *Saccharomyces cerevisiae* offers one of the oldest functional mechanisms to generate this type of spot polarity. Yeast cells utilize a regulated structural cue, the budding scar from a previous cell division, to orient their polarity axis. For a yeast cell that simply needs to grow another bud to proliferate, utilizing a mark from a previous division makes a lot of sense; the machinery is likely still localized there from

the previous event. However, establishment of polarity along this axis is not absolutely required. In systems lacking a bud scar, polarity can still arise at random positions on the membrane with budding fidelity completely unaffected (Irazoqui et al., 2003). Thus, expressing a structural cue can override more stochastic mechanisms for generating polarity.

Yeast cell polarity is established as a function of entry into mitosis and occurs via the specific activation of the Rho GTPase Cdc42. Before polarization is induced, during interphase of the cell cycle, Cdc42 exists in its GDP-bound inactive form and is uniformly distributed in the cell. Upon entry into mitosis, the master regulator of the cell cycle, Cdk1, activates Cdc24, a guanine nucleotide exchange factor for Cdc42, which localizes to the bud scar (McCusker et al., 2007). Cdc42 is switched to its active state by being induced to bind GTP and goes on to bind specific effector proteins, such as Bem1 (Peterson et al., 1994). Bem1 and Cdc42 go on to activate other cellular factors and, importantly, trigger the actin cytoskeleton to push on the membrane, thus growing a daughter cell bud. Cdc42 also coordinates the intracellular trafficking machinery to fill the bud with the correct cargoes. After cell division, Cdc42 returns to its symmetric, inactive localization (Slaughter et al., 2009).

Cdc42 polarization is thought to follow a simple model which may be represent one of the earliest functional mechanisms for establishing cell polarity (Chau et al., 2012). Activation of a small number of Cdc42 molecules on the cell cortex causes the recruitment of factors that subsequently recruit and activate other nearby Cdc42 molecules. Cdc42-mediated activation of the actin cytoskeleton can explain one potential way this system might work. Cdc42-mediated recruitment of the actin cytoskeleton directs intracellular

trafficking machinery to deliver more Cdc42 to the polarized cortex. Depletion of Cdc42 from the cytoplasm prevents spurious polarization at other sites on the membrane (Johnson JM, Jin M, Lew DJ, 2011).

Simple spot polarity is also utilized to allow for regulation of directed cell movement. Fibroblasts are cells that secrete collagen fibers to form the extracellular matrix and are required for processes such as wound healing. To accomplish this task, they need to migrate to the site of an injury and then be triggered to deposit extracellular matrix components. Responding to cell signaling pathways such as PDGF/Akt, the fibroblast polarizes Cdc42 and other GTPases, such as Rac, at spots oriented toward the source of the signal (Higuchi, 2001). The presence of Cdc42 and Rac greatly enhances the rate and mode of chemotaxis in fibroblasts presumably by favoring formation of specific types of actin filament (Monypenny et al., 2009; Kurokawa et al. 2004). However, the direction of movement is not controlled by Cdc42. Rather, flows of cytoskeletal proteins emanating from the source of the intracellular signal are thought to trigger the change in direction (Heath and Holifield, 1993).

In order to study the basic mechanistic elements of cell polarity in an unbiased way, several groups have used computational approaches to determine possible physical requirements for the establishment of various types of cell polarity (Wedlich-Soldner et al., 2003; Meinhardt and Geirer, 2000; Altschuler et al., 2008; Ma et al., 2009). Recapitulation of observed phenotypes *in silico* has granted many unique insights into natural systems and common themes have been better appreciated.

Computer modeling of yeast polarity reveals that a simple positive feedback loop can fully explain the natural behavior and that simple feedback mechanisms are capable of

establishing small regions of cell polarity (Altschuler et al., 2008). Simple feedback models work well only for small cells that contain relatively few molecules and the polarized domains they generate are small and quite unstable (Goryachev and Pokhilko, 2008). Small regions of polarity function very well if directing function to only a small region of the cell cortex, as in yeast budding. In more complex systems that must efficiently segregate components into daughter cells, however, spot polarity is insufficient to generate equal-sized domains on the cell cortex and is easily overwhelmed by even small variations in concentrations of the key players.

Recent work in the field of synthetic biology has utilized computational models to generate theoretical mechanisms of polarity establishment and coupled these predictions with biological experiments to test predictions (Chau et al., 2012). By examining commonalities in natural systems, a two-component system consisting of polarizing species vs. regulating species was established. Polarizing species were allowed to interact with the cell membrane using one variable and their diffusion was limited by the presence of other neighboring molecules. Presence of the regulatory component could alter these variables in many conceivable ways. The nature and magnitude of the interactions between the two components was systematically changed and tested for ability to generate polarity on a one-dimensional surface.

Thousands of parameter sets and different arrangement of interaction network nodes were tested to determine if these schemes could give rise to cell polarity. From all of the theoretical networks possible, three common motifs were capable of polarization: positive feedback, positive feedback with simple inhibition, and mutual inhibition. However, these individual motifs were sensitive to variation in concentration of the

components. At low concentration regimes, polarity is weak and exists only in small spots on the cortex. Robustness at low concentrations was found to be greatest when multiple motifs were combined and allowed frequent spots of polarity to form *in silico*.

To test this hypothesis, the predicted mechanistic motifs were combined and used to engineer synthetic signaling pathways. Yeast strains were generated that expressed engineered components from mammalian systems. These yeast generated the membrane lipid PIP3, which is not normally made in yeast, on one spot on the cortex and then utilized a protein that only binds PIP3 as a readout. While individual motifs work, they are unstable and do not occur as frequently as those observed in nature. Utilizing a combination of all three mechanistic motifs generated the most polarized PIP3 on the membrane (Chau et al., 2012). Notably, these polarized domains still existed as small spots and occurred in random positions on the cell cortex. Thus, while we know enough about polarity to generate it from modular components, we may only be able to create the simplest polarities. Mastering other modes of polarity will likely require additional understanding of the factors and complicated regulatory mechanisms of many different model systems.

The Cdc42 mechanism on its own is not sufficient to establish broad regions of polarity required for efficient differentiation in multicellular organisms that need to bisect a large cell during mitosis. Multiple elementary polarity mechanisms have been combined over the course of evolution to allow for polarity to solve the specific problem large cells present. The ancient Cdc42 mechanism has been maintained in animal and fungal lineages, but has gained enhanced effectors that allow for the combination of Cdc42 positive feedback with other mechanisms, such as mutual exclusion. The connection of additional polarity apparatus to Cdc42 has enabled cell polarity to become much more robust in larger

cells.

Animal Cell Polarity

In yeast, the positive feedback driving Cdc42 polarization is able to establish polarity over short time spans and small regions of the cell. To solve the challenges offered by large animal cells to generating polarity, the Cdc42 mechanism has been refined by introducing interactions with a novel set of effector proteins known as the Par complex. This complex consists of the PDZ-domain containing proteins Par-3 and Par-6 as well as the serine/threonine kinase aPKC. Binding of Par-6 to active Cdc42 is thought to activate aPKC which leads to the phosphorylation and displacement of aPKC substrates, such as Lgl and PAR-1 from the cell cortex (Hurov et al., 2004; Atwood et al., 2007; Atwood and Prehoda, 2009; Motegi et al., 2011), generating a region of polarity in the cell.

Addition of this additional machinery allows for the layering of regulatory mechanisms, such as mutual inhibition, on top of the simple Cdc42 polarization mechanism. Computational simulations predict that combining the positive feedback model of Cdc42 with other regulatory motifs can lead to increased robustness of polarity (Chau et al., 2012). In multicellular organisms, such as the worm and fly, the advent of the Par complex allows for broader and longer-lasting regions of polarity than are observed in yeast.

The zygote of the nematode worm *Caenorhabditis elegans,* has been a powerful model system for understanding cell polarity. The polarization of this cell occurs in two distinct phases: the establishment phase and the maintenance phase (Cuenca et al., 2003). To establish polarity, this system utilizes a physical cue, the location of the sperm's entry

into the cell, to induce formation of an anterior-posterior polarity axis with the point of sperm entry considered the posterior (Goldstein and Hirn, 1996). Fertilization triggers the polarized contraction of the actinomyosin network towards the anterior side of the cell through the inheritance of sperm factors such as the RhoGEF ECT-2 (Motegi and Sugimoto, 2006; Schonegg and Hyman, 2006). Similar to yeast, where cytoskeletal activity directed trafficking apparatus to deliver more Cdc42, the cortical flows of cytoskeletal proteins away from the point of sperm entry are responsible for polarizing the Par complex and Cdc42 at the anterior cortex (Munro, 2004).

The polarity maintenance phase is marked by the addition of a mutual inhibition mechanism between anterior aPKC and PAR-1 and PAR-2 at the posterior (Benton and St. Johnston, 2003; St. Johnston and Ahringer, 2010; Hao et al., 2006). aPKC removes PAR-1/2 from the anterior cortex and likewise, PAR-1 removes PAR-3, and thus the entire Par complex from the posterior cortex. Loss of either of the key effectors of these polarized domains results in spreading of the opposite domain across the cell cortex (Motegi et al, 2011; Gotta et al., 2001).

Interestingly, coupling the Cdc42 positive reinforcement motif with a mutual inhibition motif is not sufficient to generate polarity in computational simulations (Goehring et al., 2011). In order to emulate the polarity observed in *C. elegans* zygotes, positive feedback for both anterior and posterior complexes must be added to the simulation. In this model, the anterior and posterior domains reinforce their own localization in a similar mechanism as that observed in yeast cells for Cdc42. Actin polymerization is involved in reinforcing Cdc42 localization and the driving the Par complex toward the anterior cortex (Goehring et al., 2011). The posterior cell cortex seems

to be reinforced by a microtubule dependent mechanism that both recruits PAR-2 to the posterior cortex and protects it from displacement by cytosolic aPKC (Motegi et al., 2011).

The oocyte of the fruit fly *Drosophila melanogaster* also serves as a simple insect model system for this kind of broad cellular polarity, where each set of polarity components occupies roughly half of the total cell cortex. The two model systems resemble one another in many ways, but also differ in the length of time they remain polarized. Both cells exhibit broad polarity oriented along an anterior-posterior axis and are composed of very similar components. Similar to the *C. elegans* zygote, actin dynamics are required in the *Drosophila* ooctye for Cdc42 polarization and formation of anterior polarity. The Par complex grants the ability to maintain the polarized cortex over time. (Liebfried et al., 2013; Vanzo et al., 2007). Whereas the *C. elegans* zygote is triggered to polarize from factors at the sperm entry site, the oocyte experiences a nearly continuous signaling gradient from its sheath of nurse cells (Tian and Deng, 2008). This continuous signal leads to polarity that is established before fertilization and persists for relatively long periods of time.

Continuous physical cues within the cell can also lead to this type of constitutive polarity behavior. The polarization and activity of Cdc42 is required for dynamic Par complex polarization during cell divisions and during cell motility, but Cdc42 is also thought to be the most upstream polarity component in very stable polarities, such as those observed mammalian and *Drosophila* epithelia (Hutterer et al., 2004; Joberty et al., 2000). Epithelial cell types establish a ring of apical cell-cell junctions that allows cells within the tissue to physically connect and to communicate with one another. These junctions are targeted, assembled, and positioned in a polarity dependent manner (McKinley et al., 2012;

Harris and Tepass, 2008).

Cell junctions serve as a structural mark that allows cells to be divided into apical and basolateral regions. The apical region contains the Par complex and Cdc42 and is responsible for nutrient intake, exocytosis, and responding to environmental cues in its surroundings. The basolateral region is thought to act as a region that allows anchoring of the epithelial layer to adjacent cells and to the underlying basement membrane. Once the ring of junctions has been assembled, polarity machinery is recruited to the junctions and an apical-basal polarity axis is established.

Par-3 is positioned at the cell-cell junction by binding of its PDZ domains to adherens junction signals such as the adhesion protein E-cadherin (Achilleos et al., 2010; McKinley and Harris, 2012). In contrast to other systems, aPKC, Par-6 and Cdc42 are decoupled from the localization of Bazooka in epithelia. Baz becomes localized with the cell-cell junctions while aPKC/Par-6/Cdc42 form a domain over the entire apical margin of the cell and do not colocalize with Baz. This behavior is thought to occur by competition for Baz binding by elements of the epithelial polarity regulators Crumbs and Stardust and by aPKC phosphorylation of Bazooka (Krahn et al., 2010; Morais-de-Sa et al., 2010). The decoupling is thought to contribute to junctional maturation and also may relieve aPKC inhibition by Baz (David et al., 2013; Iden et al., 2012). Despite their lack of colocalization in epithelia, interactions between aPKC/Par-6/Cdc42 and Par-3 are indispensable in correct epithelial formation (Horikoshi et al., 2009). The persistence of polarity in the oocyte and epithelia indicates that the presence of a permanent cue can lead to long-lived polarity behavior.

The increasing number of regulatory components in this system requires only

minimal adjustments to the polarity mechanism *in silico*. In computational simulations of epithelial polarity, establishment of a polarized apical domain can be well modeled by modifying the *C. elegans* positive feedback/mutual antagonism model to utilize cooperativity. Cooperativity is a feature of signaling pathways by which inputs can be converted to outputs in a nonlinear manner. As in yeast, positive feedback behavior is still required for the apical polarity components to localize, but basal components must be cooperatively removed in a nonlinear fashion to achieve a valid reproduction of epithelial polarization behavior (Fletcher et al., 2012). Computational models have not yet been adjusted to accommodate the differential localizations of Par-3 and aPKC. Par-1 is known to directly repress only Par-3 localization. The band of Par-3 may act as a buffer or as a barrier to diffusion that assists in the maintenance of polarity for extended periods of time. During the cell divisions of epithelial cells, both of the daughter cells from this division inherit cell-cell junctions from their parent cell, which act to re-establish correct junctions with their neighbors (Baker and Garrod, 1993). Thus, new epithelia inherit polarization cues from their parent cell, and this is used to maintain polarity.

However, permanent cues do not necessarily lead to persistent polarity. Planar cell polarity machinery is commonly utilized in epithelia to orient cells along the organismal body axis. Planar cell polarity allows for the formation of highly patterned tissues such as kidney nephrons, insect wings, and sensory stereocilia in the mammalian cochlea (Zallen, 2007). This type of polarity is indispensable for biological processes that require coordination between multiple cells in a tissue, such as during the developmental processes of gastrulation and axis elongation (Gong et al., 2004). Failure to correctly control planar cell polarity can lead to conditions such as deafness or polycystic kidney disease (Rida and

Chen, 2009; Kibar et al., 2007).

Planar cell polarity functions by utilizing tissue signaling gradients as polarization cues and aligning specific receptors, such as the G-protein coupled receptor *Frizzled* or the receptors Fat and Daschous to this gradient (Zallen, 2007; Strutt and Strutt, 2009). This axis of planar cell polarity often persists over the organism's entire life. However, in these cells, polarity is dynamically established as a function of the cell cycle. In planar cell polarity pathways, the permanently localized cue is regulated as a function of the cell cycle. Activation of the *Frizzled* receptor, for example, recruits factors such as Strabismus (Stbm), and causes localization of the Par complex to the opposite pole of the cell. The regulation of this permanent cue, therefore helps to explain dynamics of the Par complex in a system that contains permanent cues for cell polarity.

The *Drosophila* sensory organ precursor is a type of stem cell in the developing fruit fly that utilizes planar cell polarity to generate sensory bristles on the wings and notum of the adult fly. These organs comprise a portion of the peripheral nervous system and the differentiation of a single cell eventually gives rise to specialized daughters such as the hair shaft, hair socket, nerve cell, as well as other supporting cells (Bellaiche et al., 2001; Roegiers et al., 2001). The formation of the entire sense organ begins with the division of the pI SOP progenitor. Similar to the *C. elegans* zygote, the Par complex in the pI SOP cell localizes broadly to the posterior cell cortex and segregates aPKC substrates such as lethal giant larvae (Lgl) and Numb (Nb) to the anterior cortex. Once the cell completes division, the Par complex is maintained in the posterior daughter cell, termed pIIa, which goes on to develop the shaft and socket cells of the sense organ. Numb is segregated to the anterior daughter cell, termed pIIb, which divides twice more to become the neural lineages of the

sense organ.

During cytokinesis, E-cadherin molecules form junctions between the pIIa and pIIb cells. The pIIa cell, which obtained the majority of the Par complex, utilizes these junctions to divide once more in the same orientation at the pI cell divided and form the shaft and socket cells of the bristle. The pIIb cell, however, overrides the junctional cue and rotates its axis of polarity perpendicular to the axis the pI cell utilized (Le Borgne et al., 2003).

The pIIb cell undergoes dramatic changes in polarity compared to its parent pI and sister pIIa cell (Roegiers et al., 2001). The difference in behaviors is due to the initial polarization behavior of the pI cell and the effects of segregating neural fate determinants specifically into the anterior daughter cell. These determinants are effectively able to override the normal programming associated with planar cell polarity and establish a new mode of establishing polarity. The identity of the factor that reorients this cell came from groundbreaking work in another stem cell model system, the *Drosophila* neuroblast. These two cell types were found to share a common component, Inscuteable, and likely share a common mechanism for establishing polarity.

NEUROBLAST POLARITY

Like sensory organ precursor cells, many stem cell types are derived from epithelial layers and exhibit markedly different cell polarities from the cells that surround them in the tissue. The *Drosophila* neuroblast undergoes repeated asymmetric cell divisions that produce one daughter cell that assumes a neuronal fate, and another that remains a neuroblast. During mitosis, the neuroblast polarizes the Par complex to the apical cortex that leads to the segregation of fate determinants such as Numb, Lgl, and Miranda to the

basal cell cortex. Each neuroblast division results in a self-renewed neuroblast as well as a differentiated ganglion mother cell (GMC) that can subsequently divide to form two neurons or glia. Thus, a small number of neuroblasts are sufficient to generate thousands of neural cells over the course of organismal development. Correct segregation of differentiation factors into separate daughter cells requires both a strong cell polarity as well as the alignment of the mitotic spindle along the cell polarity axis. Failure to establish polarity or to align the mitotic spindle can result in incorrect segregation of fate determinants to the daughter cells, leading to developmental defects.

Drosophila neuroblasts begin their development as epithelial cells in the early embryonic neuroectoderm (Prehoda, 2009; Egger et al., 2008; Doe, 2008). Individual cells are induced to differentiate into neuroblasts due to their expression of factors that inhibit Notch signaling. Notch signaling in many contexts is responsible for maintaining epithelial identity (Bhat, 1998). Among these neuroblast specific factors are proteins such as the transcription factors *scute* and *achaete* that repress the expression of the Notch receptor and promote the expression of the Notch inhibitor Numb among many other products.

The deactivation of the Notch pathway allows for differentiation of neuroepithelial cells into neuroblasts. The early neuroblast, having been transformed from an epithelial cell, still contains many features common to epithelia, such as cell-cell junctions constitutively localizing the polarity machinery. As the neuroblast assumes its identity, it begins to delaminate from the neuroectoderm into the embryonic interior, but its cell-cell junctions remain intact, leaving an apical "stalk" and resulting in the initial polarization of the Par complex to the apical cell membrane.

In nearly all other polarity models, Cdc42 is considered either upstream or is

codependent with the Par complex for polarization. In neuroblasts, however, the localization of Par-3 is upstream of Cdc42 polarity. Mutants of Par-3 fail to polarize Cdc42 and instead remain symmetric (Atwood et al., 2007). Independent Cdc42 polarization and activation is followed by recruitment of aPKC/Par-6 to this location and establishment of apical-basal cell polarity. Neuroblasts rely on both intrinsic and extrinsic cues for the correct alignment of their cell divisions. Neuroblasts both *in situ* and in dissociated clusters exhibit a strong correlation between their division axes over the course of multiple divisions, with multiple GMC daughter cells generated over a small arc of the neuroblast cortex (Siegrist & Doe, 2006).

After the first division, epithelial cell-cell junctions are lost and the Par complex depolarizes. Since the neuroblast must divide again and repolarize the Par complex in the absence of junctional cues, this switch of polarity modes from persistent to dynamic polarity presents a unique look at how a changing cellular context can affect the type of polarity a cell exhibits. Since the Par complex must be polarized in a similar location at the beginning of every subsequent division, this phenomenon implies that, similar to other systems, there may be some regulated, continuously polarized mark on the cell cortex that signals for Par complex localization at the onset of mitosis.

COUPLING POLARITY TO SPINDLE ORIENTATION

Polarized cell processes often coordinate with other cell pathways, such as cell trafficking or cytoskeletal growth. Alignment of cytoskeletal components, such as the actin cytoskeleton or the mitotic spindle, to the axis of polarity is among the most common coordinations observed in polarized cell types. This coordination between cytoskeleton and

polarity underlies complex biological behaviors such as cell-type differentiation.

Yeast cells that polarize via the Cdc42 mechanism need to ensure that duplicated chromosomes are correctly drawn into the developing bud. Cdc42 activity is responsible for marking the location of the new daughter cell and for directing the actin cytoskeleton to push outwards to form the bud. The actin cytoskeleton that results from Cdc42 activity is co-opted in order to orient the mitotic spindle into the bud. Bim1 and Kar9, elements at the tips of astral microtubules are drawn into the developing bud by the motor activity of myosins which utilize the polymerized actin cytoskeleton as tracks to pull the mitotic spindle into alignment with the developing bud (Miller et al., 2006, Siller and Doe, 2009). Microtubules in the bud are captured by the protein Bud6, and then undergo Dynein-mediated spindle shortening to obtain robust spindle alignment (Lee et al., 2003, Sheeman et al., 2003). Thus, in this system, polarity is coupled to spindle orientation through a set of common regulatory elements, namely Cdc42 and actin. This common node for both processes is perhaps the simplest way to generate pathway crosstalk.

Animal cells, such as the *C. elegans* zygote or the *Drosophila* oocyte, which exhibit broad cell polarity domains that meet at the midzone of the cell, are sensitive to misalignment of the mitotic spindle. In order to ensure that these two broad domains are correctly segregated, the mitotic spindle must be tightly aligned along the long axis of the cell and the cleavage furrow must efficiently separate these domains at their interface. To accomplish the coordination of polarity and spindle orientation, a complex enriched at the anterior cortex and consisting of GPR-1/GPR-2 and Gai is utilized to trigger spindle alignment (Siller and Doe, 2009; Werts et al., 2011). In depolarized animal cell types, the GPR/Ga complex will always overlie one of the poles of the mitotic spindle. Creating a

link between polarity and the spindle complex is the key to robustly oriented cell divisions.

Similar to Cdc42, evolution has utilized the activity of a small G-protein, Ga, and its effector proteins to initiate a biological function. Activation of Ga on the anterior membrane of the zygote occurs through polarized function of the GEF Ric-8 and the effector proteins GPR-1 and GPR-2 . The activation of GPR-½ by Gai induces the binding of the spindle adaptor LIN-5 and induces mitotic spindle orientation along the anterior-posterior axis by activating dynein-mediated spindle shortening pathways (Park et al., 2008).

Alignment of the spindle orientation pathway with polarity axis may occur through the utilization of an extracellular signaling gradient, such as that observed in the *Drosophila* oocyte, which activates Ga at the anterior polarity axis. Extrinsic cues have been observed in the *C. elegans* zygote, though it is unclear how this gradient would align with the point of sperm entry (Werts et al., 2011). Utilization of a common signaling gradient, rather than a common factor, as in yeast, may also be sufficient to allow pathway coordination.

Proliferating epithelia present an interesting exception to the general trend of aligning the mitotic spindle to the axis of polarity. *Drosophila* follicular epithelia localize the Pins/Ga (*Drosophila* GPR-1/2 homologs) spindle orientation to the basolateral cortex and not to the apical cortex. This arrangement aligns the mitotic spindle parallel to the tissue axis. The cleavage furrow bisects the apical domain, containing the Par complex, and both daughter cells inherit molecularly symmetric contents. The subsequent division of the cell allows for lateral growth of the epithelial layer.

Stem cells derived from epithelial layers tend to break from the basolateral

alignment of the mitotic spindle observed in standard epithelial models. In addition to directing the orientation of cell growth in tissues, core planar cell polarity machinery is utilized in SOP lineages to perform asymmetric cell divisions. In the pI SOP cell, the planar polarized receptor acts to orient the mitotic spindle to the polarity axis. In contrast to other model systems such as the *Drosophila* oocyte, the spindle orienting Pins/Gai components do not localize with the polarity machinery, but on the anterior pole of the cell. Alignment of spindle orientation with polarity, therefore, does not necessitate the colocalization of components, but merely that the localization of the two components exist along a common polarity axis.

In the pIIb SOP cell, which undergoes dramatic reorientation of its polarity and cell division axes, the polarity machinery is once again colocalized with the spindle orientation machinery, but along an apical-basal axis instead of the anterior-posterior axis of the parent pI cell. This behavior is also observed in the neuroblast, which also exhibits apical-basal polarity. In both the pIIb cell and in delaminated neuroblasts of the developing larval central nervous system, Par complex polarity is observed first during prophase of mitosis. Mitotic spindle formation is tightly correlated to this same event. By metaphase, when polarity is strongest, the mitotic spindle has become robustly aligns to the Par-complex. After cell division, polarity components become depolarized and the mitotic spindle breaks down.

To couple the orientation of the mitotic spindle to the polarity axis in these cell types, the Par complex is thought to recruit the Pins/Gai spindle orientation machinery through the novel factor Inscuteable. While there are many important factors involved in establishing polarity and coordinating the mitotic spindle, the scaffolding protein

Inscuteable has been thought to play an important role as a bridge between the two pathways. Inscuteable mutant neuroblasts exhibit defects in both cell polarity and in spindle orientation, suggesting the importance of Inscuteable to both systems.

THE ROLES OF INSCUTEABLE

In both the pIIb SOP cell and the neuroblast, Inscuteable has been shown to play a key role in both reorientation of cell polarity as well as in coupling the mitotic spindle to this axis (Kraut et al., 1996; Orgogozo et al., 2001). In *Drosophila*, Inscuteable is expressed in cell types that generate neural lineages, such as pIIb SOP cells and neuroblasts. Inscuteable has a mammalian ortholog, mInsc, which seems to be expressed more broadly in many different types of tissues. Wherever mInsc is expressed in mammals, it is sufficient to reorient the cell polarity and spindle axis to generate stratified and differentiated tissues (Postiglione et al., 2011; Zigman et al., 2005).

Drosophila cells expressing Inscuteable also exhibit narrow arcs of apical cell polarity that are not typically observed in other types of polarized cells. In contrast to the *C. elegans* zygote and *Drosophila* oocyte, in which the polarity domains meet at the midzone of the cell, Inscuteable-expressing cells form tight crescents over approximately 25% of the cell membrane. This phenomenon is likely to be Inscuteable-dependent and could contribute to high-fidelity segregation of daughter cell components by localizing them tightly at the poles of the cell, rather than meeting in the middle of the cell. Given the high correlation between unique polarity/spindle orientation behaviors and the expression of Inscuteable, understanding the mechanisms by which these changes occur can shed light specialized mechanisms of high-fidelity asymmetric cell division.

Inscuteable is an ankryin-repeat domain containing protein that associates directly with both Pins and Baz and is thought to physically bridge the two complexes and to coordinate their outputs (Knoblich et al., 1996; Wodarz et al., 1999). Inscuteable mutants exhibit defective spindle orientation and polarity maintenance, consistent with its roles in both processes (Schober et al., 1999; Siegrist and Doe, 2007). During delamination, recruitment of Inscuteable follows a standard linear pathway, where induced polarity of Par-3 recruits Insc during mitosis. Polarized Insc subsequently recruits Pins and the spindle orientation machinery.

However, after fully delaminating, Insc, Baz, and Pins form increasing mutual dependencies on each other. In delaminating mutants of Insc, Baz still correctly localizes to the apical stalk but after delamination is complete, Baz fails to localize to the apical membrane. In Baz mutants, Inscuteable fails to localize and is becomes distributed to the cytoplasm. For example, the Pins-Inscuteable complex is fully codependent in larval neuroblasts. Without pins, Inscuteable never localizes. Without Insc, Pins never polarizes (Izumi et al., 2004). The location of Baz during the first division, therefore, may serve to mark where a perpetual cue is to be formed that will take over after delamination.

Inscuteable also causes very interesting phenotypes when misxpressed in different tissues. In SOP cells, Inscuteable is expressed specifically in the pIIb lineage and not in the parent pI cell. When Inscuteable is expressed in the pI SOP cell, Inscuteable localizes with Pins at the anterior cortex of the cell instead of localizing with the PAR complex at the posterior. Strikingly, Inscuteable does seem to bridge polarity and spindle components, as the Par complex also localizes at the anterior cortex with Pins and Insc (Roegiers et al., 2001). Similar to a neuroblast, Inscuteable expression in the pI cell is sufficient to reverse

cell polarity and to couple Pins and Baz during mitosis. This cell, interestingly does not rotate its polarity axis perpendicular, but simply inverts the anterior-posterior polarity axis. Expression of Insc in the pIIb daughter cell, however, does lead to axis rotation. Inscuteable alone, therefore, is not sufficient to induce this change in the pI SOP cell.

When misexressed in epithelial cells, however, Inscuteable is sufficient for axis reorientation and it performs this task robustly. In epithelia such as the optic lobe, Inscuteable is recruited to the apical margin of the cell during interphase and is not localized to the basolateral junctions where Pins is localized, as in SOP cells (Egger et al., 2007). Inscuteable also does not localize strongly to adherens junctions where Baz is presumably localized. If Insc does not localize where its binding partners localize, how does Inscuteable become apically restricted? Pins is absolutely required for Insc recruitment to the apical cortex, indicating that Insc may be reorganizing Pins to the apical cortex with it (Kraut et al., 1998; Yu et al., 2000). During mitosis, Inscuteable does seem to serve as a bridge between polarity components during mitosis, but this bridge does not seem to be active during interphase.

The complicated phenotypes of different mutants coupled with the puzzling differences between the localization behavior of Insc when misexpressed in different cell types has made understanding the roles of Inscuteable in polarity and spindle orientation difficult to analyze. Common themes for Inscuteable function between cell types abound, but these analyses are confounded by unique differences that exist. Observations that both pIIb cells and delaminated neuroblasts only exhibit polarity during mitosis serve to challenge the passive adaptor model for Inscuteable function. If the Par complex becomes symmetric during interphase, how does it know to re-establish polarity at similar positions

during subsequent divisions? Inscuteable may be serving a more regulated role than previously believed for its role polarity establishment in fully delaminated neuroblast systems.

QUESTIONS REMAINING IN CELL POLARITY

-How do larval neuroblasts become polarized?

-How does the cell cycle machinery interact with polarity components?

-How do stem cells remember their polarity axis between divisions?

-How is spindle orientation linked to cellular polarity in the neuroblast?

Much is known about the mechanisms governing cell polarity from groundbreaking work in multiple model systems. Despite the variety of context-specific differences, there is likely to be shared common mechanisms that are observed even in the most unique types of polarized cell. This work will illustrate my work in studying the *Drosophila* neuroblast and the regulatory mechanisms governing the establishment of its polarity and coupling polarity to the mitotic spindle. Rather than a simple bridge, Inscuteable is an active regulatory element required for the correct function of asymmetric cell division.

In this dissertation, I describe how I utilized a mixture of cell biological, biophysical, and biochemical methods to investigate the regulatory mechanisms controlling the establishment of cellular polarity in the *Drosophila* neuroblast and how this polarity axis is connected to the orientation of the mitotic spindle. In chapter II, I will discuss the role of Inscuteable in localizing Bazooka during mitosis. Inscuteable serves as a continuously polarized landmark on the cell cortex that binds Bazooka during mitosis. At the end of the cell division, the Inscuteable-Bazooka complex is disrupted by phosphorylation by Aurora A during the exit from the cell cycle. This chapter contains

previously unpublished co-authored material. Chapter III will detail the spindle orientation roles of Inscuteable. Inscuteable competes for binding to Pins with the mitotic spindle component Mud. This competition prevents premature microtubule shortening, but has no effect on microtubule targeting and cortical attachment pathways. Once the spindle is attached, Mud is able to outcompete Inscuteable and robustly orient the spindle. This chapter contains previously published co-authored material. Chapter IV will describe a mechanism that models the ultrasensitive spindle orientation activity of Pins. Activation of Pins may not require cooperative activation behavior, but may instead utilize a simple decoy domain mechanism to prevent early activation of spindle orientation. This chapter contains previously published co-authored material. Lastly, in Chapter V I will provide the contributions to the fields of cell signaling and stem cell biology that this dissertation has made.

BRIDGE TO CHAPTER II

In the preceding chapter, I described the relevance of the *Drosophila* neuroblast model system and the components involved in its asymmetric division. I described the model where Inscuteable acts as a physical connection between the cell polarity and spindle orientation complexes. I also introduce the challenge to this model presented by the dynamic cell polarity observed in the neuroblast. In the following chapter, I explain my work in describing the cell cycle regulated localization behavior of the Par complex and the role of Inscuteable in establishing and maintaining Par complex polarity. I also will speculate on why dynamic polarity may be an important phenomenon that allows for high-fidelity production of daughter cell lineages.

CHAPTER II

THE ROLE OF INSCUTEABLE IN THE MAINTENANCE OF AN APICALLY POLARIZED PAR-COMPLEX

This chapter contains unpublished co-authored material

Author contributions: Jonathon Mauser and Ken Prehoda designed research; Jonathon Mauser performed research; Jonathon Mauser and Ken Prehoda analyzed data; and Jonathon Mauser and Ken Prehoda wrote the paper.

INTRODUCTION

Formation of a correctly polarized apical domain in the *Drosophila* neuroblast is a crucial event during the establishment of apical-basal polarity. In wild-type organisms, recruitment of the Par-complex (consisting of Par-3 (Bazooka), aPKC, Par-6, and Cdc42) to the apical portion of the neuroblast results in the displacement from the apical cell membrane of cortical fate determinants, such as Miranda (Mira), Lethal Giant Larvae (Lgl) and Numb (Nb). These factors subsequently become localized to the basal cortex of the neuroblast and are segregated into the basal daughter cell after mitosis. Failure to establish a functional apically polarized domain results in a molecularly symmetric division of the

neuroblast. Inability to sort differentiation factors in these mutants results in over proliferation of neuroblasts in the developing central nervous system and developmental lethality (Wang et al., 2007; Betschinger et al., 2006; Lee et al., 2006).

Previous genetic studies have described the molecular pathway that leads to the polarization of aPKC in neuroblasts. Bazooka (PAR-3) is considered the most upstream component of the pathway and will correctly localize in the absence of any other member of the PAR-complex (Atwood et al., 2007; Rolls et al., 2003; Petronczki and Knoblich, 2001). The presence of activated Cdc42 where Bazooka localizes allows for the localization of aPKC and Par-6 and establishment of apical-basal polarity. The correct localization of Bazooka, therefore, is the crucial step in defining the polarity axis. Previous studies in multiple model systems have identified several factors that may be involved in the localization of Bazooka, including the basally localized kinase PAR-1 and the protein phosphatase PP2A (Krahn et al., 2009; Huynh et al., 2001) as well as the cell scaffolding protein Inscuteable.

Inscuteable is thought to act as a bridge between the Pins complex and the Par complex. The physical connection between the complexes is thought to be sufficient to allow coupling of polarity to spindle orientation. Inscuteable mutant neuroblasts exhibit defective localizations of the Par complex machinery after delamination as well as spindle orientation defects (Wodarz et al., 1999; Schober et al., 1999). In delaminating embryonic neuroblasts, Inscuteable is dependent on Bazooka for its localization. In the absence of Bazooka, Inscuteable fails to localize to the apical delamination stalk. Conversely, if Inscuteable is lost, Bazooka is still able to be localized to the delamination stalk, yet fails to form robust crescents once delamination is completed. Weak crescents of Bazooka can

occasionally be observed in an *inscuteable* mutant (Wodarz et al., 1999; Schober et al., 1999), indicating that the role of Insc is to maintain Bazooka polarity after delamination. In an embryonic system, Bazooka seems to form a cue for the initial apical recruitment of Insc, but without Insc, Bazooka cannot localize stably post-delamination. The roles of the genetic and physical interactions between Insc & Baz that promote polarity maintenance, therefore, are unclear.

Neuroblasts are known to exhibit a stereotyped cell division axis that persists over the course of multiple sequential divisions (Siegrist et al., 2006). The Par complex is known to form crescents with Inscuteable during prophase of mitosis in the dividing neuroblast, at which time it becomes active and begins to displace Miranda and other aPKC substrates from the apical region of the cell (Siegrist and Doe, 2005; Betschinger and Knoblich et al., 2004). Bazooka may exhibit polarity dynamics in this system, repeatedly polarizing to a similar location on the cell cortex over the course of multiple divisions. Alternatively, it may be persistently localized at the cortex and undergo compaction into a robust crescent. The precise signal for this repeated localization behavior remains unknown and the temporal localization dynamics of the Par complex in neuroblasts, so far, remain poorly characterized.

The pI SOP cell, another *Drosophila* model system for asymmetric cell division, exhibits a cell-cycle dependent regulation of cell polarity machinery similar to neuroblasts. In this cell, the Par complex is localized to the cytoplasm during interphase and forms crescents by prophase (Wirtz-Peitz et al., 2008; Roegiers et al., 2001). Mechanisms that have been proposed to control this temporal behavior involve the mitotic kinase Aurora A at the G2/M transition. Aurora activation allows aPKC to form a complex with Bazooka

and provides the missing localization cue for Par-complex localization at the posterior cortex. pI SOP cells, however, do not express Inscuteable. Misexpression of Insc in the pI cell causes relocalization of the Par complex to the anterior cortex, suggesting an upstream role for Insc in dynamically polarizing cell types.

What roles this dynamic polarization behavior might play in the correct divisions of the neuroblast remain to be described. Inscuteable serves as a key point of focus due to its key interaction with Inscuteable after neuroblast delamination. We sought to explain the role of Inscuteable in the maintenance of Bazooka localization during later stages of development by investigating the mechanism of Bazooka recruitment to the apical cortex in wild-type larval neuroblasts and then comparing the localization behavior to a system depleted of Inscuteable.

MATERIALS AND METHODS

Fly Stocks & Genetics

Wild-type (*w1118*) and transgenic fly stocks used were obtained from the Bloomington Drosophila Stock Center. Transgenic RNAi lines were generated by the Transgenic RNAi Insertion Project (TRiP). Inscuteable RNAi (35042), Bazooka RNAi (31523), and Aurora A RNAi (35763) lines were crossed to *Inscuteable-GAL4* driver. All mutant chromosomes were balanced over CyO actin:GFP, TM3 actin:GFP, Ser, e, or TM6B Tb. All crosses were performed at 25°C. Live imaging experiments utilized *worGal4* (Albertson and Doe, 2003) and *UAS-His2A-mRFP* (Emery et al., 2005) crossed to *UAS-EmGFP-Insc* (gift from C. Doe) or *UAS-Bazooka-GFP* (gift from T. Harris).

Live imaging

Second or third larval brains were prepared for imaging as previously described (Siller *et al.*, 2005). 21 Z steps were collected at 1 μm intervals every 60 sec. Live imaging was performed using a spinning disk confocal microscope equipped with a Hamamatsu EM-CCD camera (Hamamatsu, Japan) using a 63 × 1.4 numerical aperture oil immersion objective. A linear photobleaching correction was added, using the intensity of a region outside the cell as a reference. Latrunculin B treatment was performed on the strain using a final concentration of 100 μM, with live imaging beginning before treatment.

Molecular cloning, protein expression and purification

Constructs encoding the functional region of Inscuteable have been described (Schober et al., 1999; Tio et al., 1999, Knoblich et al. 1999). Residues 252–600 of Inscuteable, including the central Ankyrin-repeat containing region, were used for all experiments. Constructs of Bazooka and Aurora A were prepared by PCR from cDNA followed by sticky-end vector ligation. MBP-fusion constructs were prepared utilizing the pMAL-c2 vector and hexahistidine-tagged constructs were prepared by ligation of insterts into a pBH4-based vector.

MBP-fusion proteins were purified on amylose resin (New England Biolabs), washed with three bed-volumes of PBS+1% Triton X-100 and one bed-volume of PBS. Proteins were eluted using PBS+1M Methyl-α-D-glucopyranoside (Sigma-Aldrich).

Hexahistidine-fusion proteins were purified on Ni-NTA agarose resin (Qiagen). The incubated resin was then washed with a large excess of cell lysis buffer (50 mM NaPO4/150 mM NaCl/10 mM imidazole). Samples were then eluted with elution buffer (50 mM NaPO4/150 mM NaCl/300 mM imidazole).

Echinoid (Ed) fusion constructs were made in pMT-V5 (Invitrogen, Carlsbad, CA), replacing the Ed cytoplasmic domain with a visualization tag and the protein of interest at the COOH terminus (e.g., Ed-GFP-Insc). HA-tagged constructs were cloned into pMT-V5 containing an NH2-terminal HA tag.

Transfection and S2 Cell Experiments

S2 cells were grown in Schneider's media (Sigma) supplemented with 10% fetal bovine serum and seeded at ~2×10^6 cells per well of a six-well culture dish on the day of transfection. S2 cells were transfected with 0.4–1 μg total DNA with Effectene (QIAGEN), and gene expression was induced 16–24 hr after transfection with the addition of 500 μM $CuSO_4$ for 24–48 hr. RNAi was performed as described in Johnston et al. (2009).

In Vitro Binding Assays

MBP pull-down assays were performed incubating 50uL of amylose resin with saturating concentrations of MBP fusion proteins in 1xPBS for 30 minutes. These reactions were followed by three washes in 1x PBS+ 1% Triton X-100. The final wash buffer was removed and 50uL of 30uM 6xHis tagged substrate was added to the beads

and incubated at room temperature for 15 min before washing, elution, and analysis by gel electrophoresis and western blotting against the 6xHis tag.

In Vitro Kinase Assays

Recombinant MBP Aurora-A was purified from bacteria. Substrates were diluted to 10uM in the assay buffer (50 mM Tris-HCl, pH 7.5, 100 mM NaCl, 10 mM $MgCl_2$) and incubated at 30 °C for 5 min. The reactions were initiated by adding 1 mM ATP spiked with [γ-^{32}P] ATP ($\sim 1.0 \times 10^5$/nmol of ATP). The reactions were incubated at 30 °C for an additional 10 min. These samples were then resolved on a 12.5% SDS-PAGE gel, dried, and exposed to a phosphor imaging cassette for five minutes.

Immunofluorescent staining and antibodies

The brains of second-instar larvae were dissected and fixed for 20 minutes in 4% paraformaldehyde in 1x PBS + 1% DMSO. Transfected S2 cells were allowed to settle onto coverslips for an hour at room temperature. The media was removed and the cells were fixed paraformaldehyde in 1x PBS + 1% DMSO. Samples were washed three times for five minutes each at room temperature in 1x PBS + 0.3% Triton X-100. These were then blocked for 30 minutes at room temperature in 1x PBS + 0.3% Triton X-100 + 1% bovine serum albumin. After blocking, primary antibodies in blocking buffer were applied overnight at 4°C with constant shaking. Primary antibodies used for these studies include: rabbit phospho-Histone H3 (1:20000; Santa Cruz), rat α-tubulin (1:1000; Sigma-Aldrich), Guinea Pig bazooka (1:1000; Chris Doe), mouse HA (1:1000; Covance), rabbit aPKC (1:500; Santa Cruz), Guinea Pig Miranda (1:1000; Chris Doe), rabbit Inscuteable (1:1000;

Chris Doe). We used fluorescent-conjugated secondary antibodies from Jackson ImmunoResearch or Molecular Probes. Images were collected using a Leica TCS SP2 confocal using a 63×/1.4NA objective. ImageJ, Adobe Photoshop and Illustrator software were used for data analysis and figure formatting.

Image Processing and Quantification

To obtain integrated intensities from movies, the cytoplasm or apical surface (defined by the region of the membrane where the metaphase crescent will later exist) were selected in ImageJ with the freehand selection tool. The grey values of all pixels in the selection were then integrated. To obtain crescent/cytoplasmic ratios from Ed-expressing S2 cells, the induced polarity crescent or cytoplasm (excluding the nucleus) was selected using the freehand selection tool and the average intensity was measured in ImageJ. These ratios were calculated and quantified using GraphPad Prism.

To generate cortical profiles of cells, the cell cortex was selected using the freehand selection tool. Selection began at the basal cortex, as determined by the center of the GMC daughter cell pool, and continued around the apical circumference of the cell. This selection was then straightened using a 5-pixel width straighten function and averaged by scaling in ImageJ. Images were subjected to maximum entropy thresholding in ImageJ to highlight regions of maximum gray values.

RESULTS

To investigate the specific roles of Inscuteable in establishing and maintaining Bazooka polarity, we first undertook an observational approach to characterize the

mechanism of Bazooka enrichment at the apical cortex of wild-type neuroblasts. Bazooka has been previously described to form crescents at the apical cortex of the neuroblast during prophase and metaphase, which disappear during anaphase (Wodarz et al., 1999). We used confocal microscopy to visualize the localization of Bazooka in both fixed preparations of larval brains as well as with neuroblast-specific UAS-GFP-Bazooka expression. During interphase, Bazooka is diffusely localized in the cytoplasm and as puncta on the membrane, whereas it localizes to the apical surface of the neuroblast during and after prophase (Figure 1A). In contrast to previous reports, we find that Bazooka does not truly disappear from the cortex during anaphase, instead spreading uniformly over the cell cortex during equatorial constriction and becomes increasingly weak during anaphase/telophase.

To visualize the cortical populations of Bazooka as a function of the cell cycle, we generated cortical profiles of neuroblasts at different stages of the cell cycle by selecting the cell border and straightening the selection using ImageJ (Figure 1B). During interphase, cortical Bazooka exists as multiple discrete puncta that are randomly distributed across the membrane. By prophase, Bazooka forms one large continuous region in the apical region of the cell that persists into metaphase (Figure 1C). We observed from the cortical profiles we generated that metaphase crescents seem to occupy a smaller proportion of the total cellular cortex than those observed in prophase. We measured the signal from the crescents as a function of total cortical circumference and determined that crescents in prophase are broad, occupying ~40% of the cell surface (Figure 1D). During prometaphase and metaphase, the crescent compacts to ~25% of the cell cortex, and subsequently expands over the cell cortex during telophase, becoming

nearly uniformly cortical by cytokinesis. After the cell division is resolved, the cortical Bazooka returns to the cytoplasm and to cortical puncta (Data not shown). In subsequent divisions, the Bazooka crescent forms crescents at approximately the same position on the cell cortex (Appendix A, Fig S1A), similar to what was previously observed in clustered neuroblast cell culture (Siegrist & Doe, 2006).

The sudden appearance of the Bazooka apical crescent during the onset of mitosis could occur by multiple different mechanisms, including direct cytoplasmic recruitment to the apical cortex or by the coalescence of cortical puncta into an apical domain. To investigate this, we quantified movies of dividing UAS-GFP-Bazooka expressing neuroblasts to determine the relative levels of polarized Baz versus the population existing in the cytoplasm at each time point in the movie. Bazooka begins to enrich at the apical cortex at approximately the point where nuclear chromatin begins to compact at the onset of prophase (Figure 1E). By prometaphase, (defined by nuclear envelope breakdown (NEB) the crescent has become fully formed at the apical half of the cell and persists through metaphase. Thus, we show that Bazooka initially forms broad crescents by direct recruitment from the cytoplasm to the apical cortex. These crescents then become tightly compacted by metaphase and spread over the cortex during equatorial constriction.

The compaction of the apical crescent observed by prometaphase appears to occur via an actin-mediated mechanism. Treatment of dividing cells with Latrunculin B, which disassembles actin filaments, leads to an initial failure of neuroblasts to exhibit this tightening (Appendix A, Fig S2). Inscuteable/Bazooka recruitment still is allowed, but formation of a tight apical cortex does not occur. After approximately 30 minutes of

treatment with Latrunculin B, Inscuteable and Bazooka lose asymmetric localization, as previously observed (Broadus and Doe, 1997). This suggests that actin is required for membrane localization of Inscuteable as well as for tightening the crescent.

The phenomenon of direct recruitment of Bazooka to the apical cortex to equivalent locations on the membrane specifically during mitosis may suggest the presence of a regulated cortical landmark that maintains polarization on the apical surface of the cell. Since Inscuteable is a known binding partner of Baz and has an implicated role in establishing Bazooka polarity, we imaged its localization by a similar approach as we used for Bazooka. Confocal imaging of fixed and stained specimens revealed that Inscuteable, unlike Baz, is polarized during interphase (Figure 2A). Cortical profiles reveal Inscuteable is polarized during interphase to the region of the cortex opposite the GMC region.

Like Baz, Inscuteable also constricts into a restricted apical crescent by metaphase (Figure 2B). Unlike Baz, however, it does not appear that Inscuteable is largely recruited from the cytoplasm. Movies of UAS-GFP-Insc reveal that the Inscuteable crescents retain a similar integration of grey values throughout the cell cycle and do not noticeably deplete the cytoplasmic pool, indicating that the crescent is largely maintained on the cortex between divisions (Figure 2C). Additionally, Inscuteable retains a polarized localization over the course of multiple divisions of a neuroblast. Like Baz, compact crescents occur at similar positions on the membrane (Appendix A, Fig S1B).

To determine whether Inscuteable is required in larval neuroblasts for Bazooka recruitment, we drove UAS-Inscuteable RNAi in neuroblasts at 30*C and fixed third-instar larval brains to examine the effect on Bazooka. Upon Inscuteable depletion,

Bazooka largely fails to form apical crescents, instead remaining as scattered puncta on the cell membrane (Figure 2D). When Bazooka is depleted, however, polarity is lost yet Inscuteable remains unaffected by the loss of Baz (Figure 2E). The observed behavior of crescent compaction is also independent of Baz, as Insc still exhibits this behavior upon Baz RNAi expression. These experiments reveal that Inscuteable is genetically upstream of Baz in larval neuroblasts and Baz is dispensable for Insc localization. These data are consistent with a role for Inscuteable as a cortical landmark for Bazooka localization.

To determine whether Baz recruitment to Inscuteable crescents is a neuroblast-specific phenomenon, we attempted to reconstitute the Bazooka localization behavior in a minimal *Drosophila* S2 cell-culture induced polarity assay. By using a heterologous cell type, we can exclude neuroblast specific factors and are able to force Inscuteable to localize at sites of cell-cell contact. We can then stain for endogenous Bazooka and observe whether the dynamic recruitment is still observed in a minimal system.

In Ed alone controls, Bazooka does not exhibit specific recruitment to the crescent (Crescent/Cytoplasmic ratio ~1) during either interphase or mitosis (Figure 2F). However, in Ed-Inscuteable systems, Ed-Insc weakly recruits Baz during interphase, compared to controls. By prophase, however, Baz becomes strongly enriched at Ed-Insc crescents. Therefore, the observed dynamic localization mechanism of Bazooka to Inscuteable crescents is common across cell types and can be recapitulated in a simple model system.

Since Inscuteable and Bazooka are thought to be direct binding partners, we sought to identify the minimal components of each protein that is required for direct interaction. Bazooka contains an NH2-terminal oligomerization domain, a “neck” region containing a

Figure 1. Bazooka forms dynamic apical crescents during mitosis.

(A) Bazooka forms apical crescents during mitosis and not during interphase. Apical crescents may be observed by prophase in wild-type larval neuroblasts.
(B) Cortical profiles may be generated from confocal slices by selecting and straightening the cell cortex. Intensity plots can then be generated from fixed images.
(C) Cortical profiles of fixed specimens reveal that Baz forms cytoplasmic puncta during interphase, while it forms large contiguous regions during mitosis.
(D) Bazooka forms broad crescents that become compacted into smaller crescents by metaphase. During equatorial constriction, Bazooka becomes uniformly distributed to the neuroblast cortex.
(E) Bazooka is recruited from the cytoplasm. Live two-color confocal imaging of UAS-GFP-Baz and Histone 2A-RFP reveals that Bazooka enrichment to the apical cortex is correlated with loss of cytoplasmic intensity.

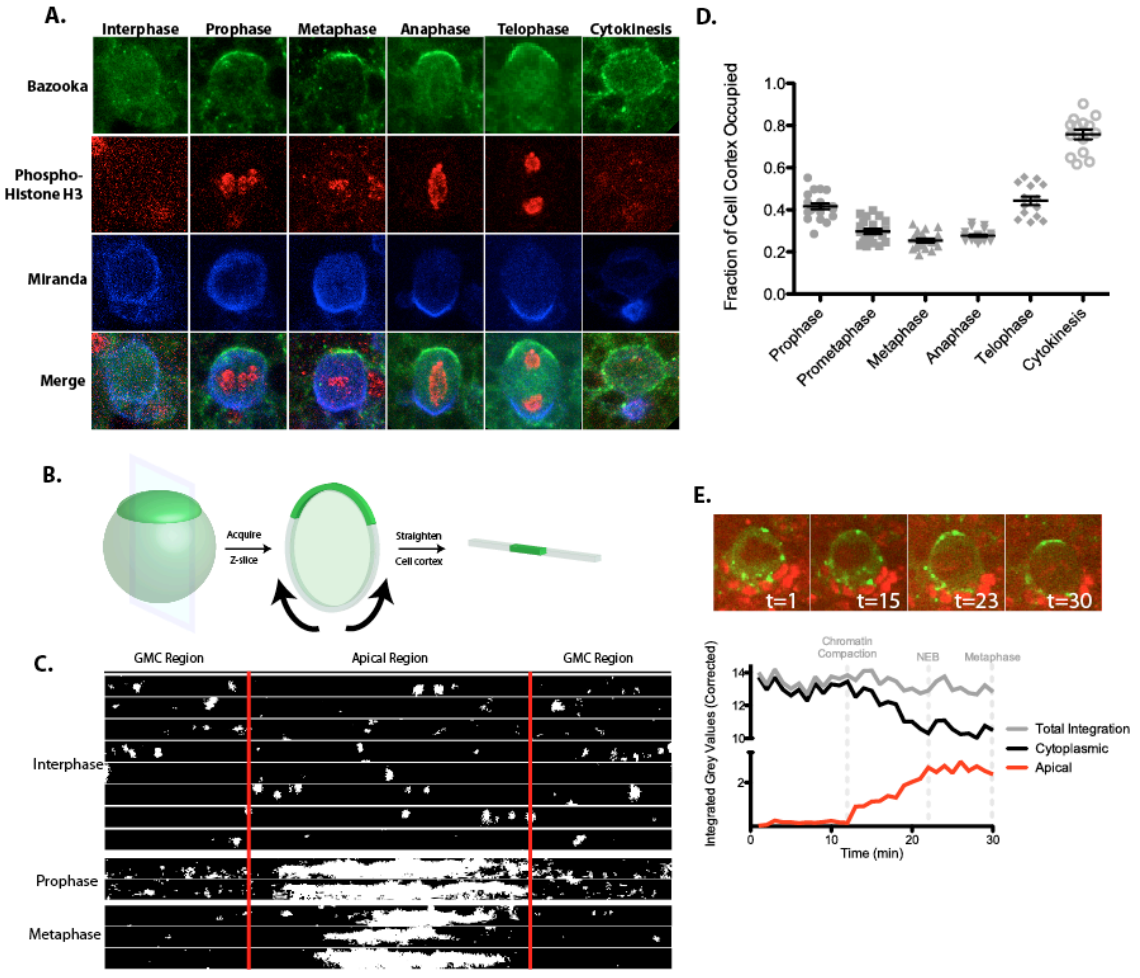

PAR-1 phosphorylation site, three central PDZ domains, and a COOH-terminal tail containing a lipid binding motif and aPKC/PAR-1 phosphorylation sites (Figure 3A). Large portions of Bazooka were cloned and purified *in vitro* and subjected to affinity pulldowns with MBP-Inscuteable. Bazooka pulled down with fragments in the NH2-terminus of Bazooka, with the fragment from 1-314 (comprising the oligomerization and neck domains) having the greatest affinity (Figure 3B). Finer dissection of this fragment revealed the neck region of Baz (amino acids 117-314) to be sufficient for interaction in the pulldown assay (Figure 3C). Complementary dissection of Insc revealed that the full set of Ankyrin repeats is required for the Baz interaction (Data not shown).

To determine whether these components were also required for Baz recruitment to Insc, we overexpressed Bazooka constructs in Ed-Insc expressing S2 cells and quantified recruitment to Insc crescents. Expression of HA-Bazooka exhibited significant recruitment specificity to Ed-Insc compared to Ed-GFP controls (Figure 3 D-E, K). Deletion of the NH2-terminal 316 amino acids of the Bazooka sequence resulted in a return of Bazooka recruitment to the Ed-GFP level with no specific recruitment observed to Insc crescents (Figure 3 F-G,K).

Therefore, the NH2-terminus of Baz is required for recruitment to Inscuteable crescents. However, expression of any known binding fragment of Baz, including the full OD+Neck region (Figure 3H), the neck domain itself (Figure 3I), or the PDZ domains (Figure 3J) did not result in specific recruitment to Insc (Figure 3K). This behavior suggests that the neck region is required, but is insufficient for Insc recruitment in our induced-polarity cell culture system. Previous studies have indicated that Bazooka

requires PIP binding through its PIP binding motif in the COOH-terminal region to become correctly localized in dividing neuroblasts (Krahn et al., 2010).

Since the mitotic localization behavior of Bazooka is controlled by a general cell factor and appears to be specific to the G2/M transition of the cell cycle, we sought to identify the effector that allows for interaction in order to understand the mechanism controlling Baz dynamics. We screened candidate mitotic kinases (Cdc2, Polo, Aurora) for defects in Baz localization by expressing neuroblast-specific RNAi against these factors. Depletion of Aurora A, and not Polo or Cdc2, was sufficient to cause defect in Baz recruitment (Figure 4A). Aurora A depletion caused an increase in Baz recruitment to the crescent during interphase, prophase, and metaphase.

Figure 2 (next page). Inscuteable maintains polarized localization throughout the cell cycle and is required for Baz localization.

(A) Costains of Inscuteable (Insc) and Bazooka (Baz) reveal that Inscuteable exhibits a polarized localization during interphase. By prophase, Inscuteable and Baz colocalize as apical crescents.
(B) Inscuteable becomes increasingly polarized by Metaphase/Anaphase, and becomes distributed over the cortex during telophase.
(C-D) Live Imaging of GFP-Insc reveal that, unlike Baz, Insc is maintained as a cortical crescent and is not recruited from the cytoplasm.
(E) Neuroblast-specific expression of Insc RNAi results in a loss of Bazooka enrichment during mitosis.
(F) Neuroblast-specific expression of Baz RNAi has no effect on Inscuteable localization.
(G) Bazooka RNAi has largely the same polarity dynamics as WT.

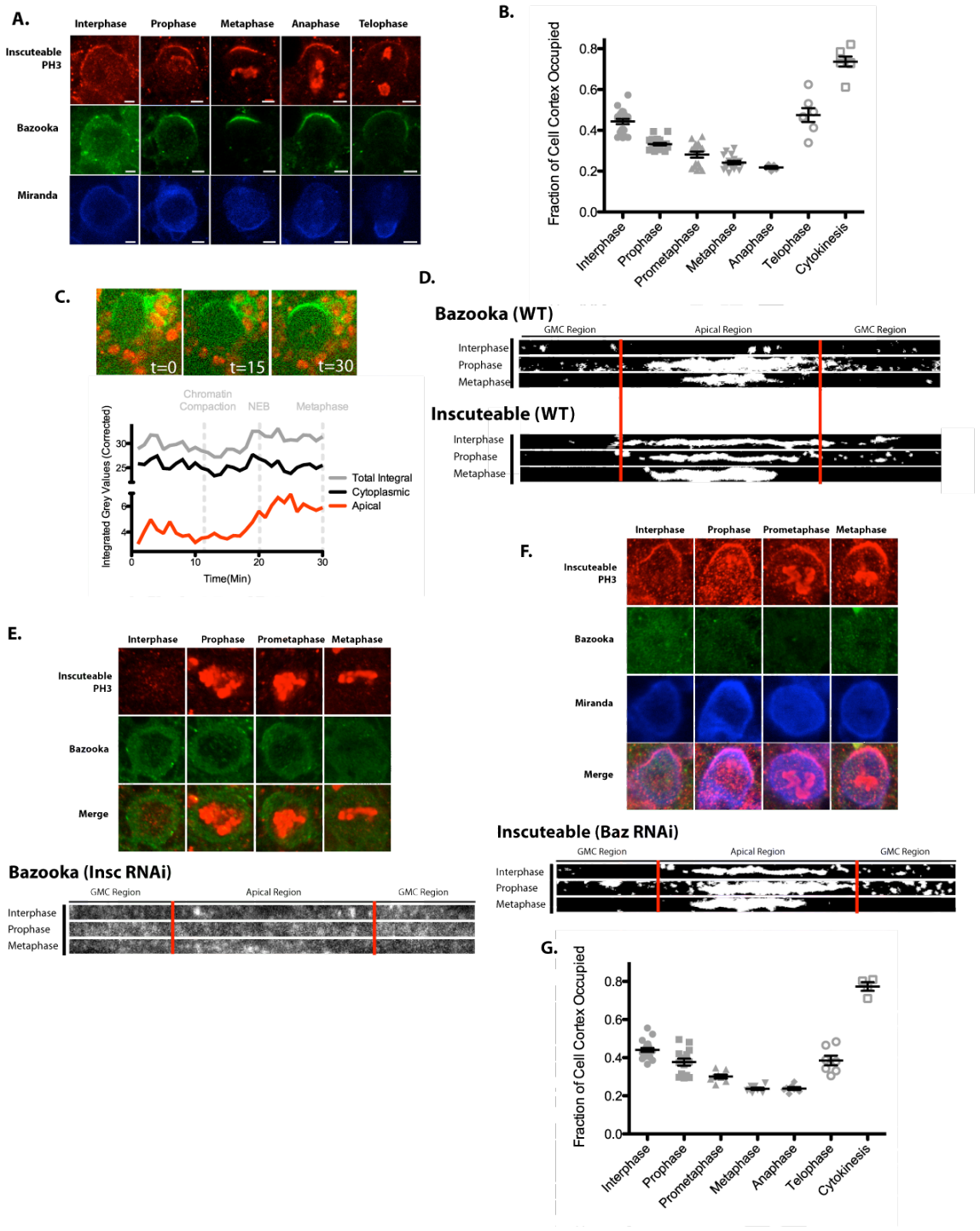
A.
Interphase
Prophase
Metaphase
Anaphase
Telophase
Inscuteable PH3
Bazooka
Miranda
B.
Fraction of Cell Cortex Occupied
0.0
0.2
0.4
0.6
0.8
Interphase
Prophase
Prometaphase
Metaphase
Anaphase
Telophase
Cytokinesis
C.
t=0
t=15
t=30
Chromatin Compaction
NEB
Metaphase
Integrated Grey Values (Corrected)
Time(Min)
Total Integral
Cytoplasmic
Apical
D.
Bazooka (WT)
GMC Region
Apical Region
GMC Region
Interphase
Prophase
Metaphase
Inscuteable (WT)
Interphase
Prophase
Metaphase
E.
Interphase
Prophase
Prometaphase
Metaphase
Inscuteable PH3
Bazooka
Merge
Bazooka (Insc RNAi)
GMC Region
Apical Region
GMC Region
Interphase
Prophase
Metaphase
F.
Interphase
Prophase
Prometaphase
Metaphase
Inscuteable PH3
Bazooka
Miranda
Merge
Inscuteable (Baz RNAi)
GMC Region
Apical Region
GMC Region
Interphase
Prophase
Metaphase
G.
Fraction of Cell Cortex Occupied
0.0
0.2
0.4
0.6
0.8
Interphase
Prophase
Prometaphase
Metaphase
Anaphase
Telophase
Cytokinesis

Figure 3. Bazooka requires the NH2-terminal "Neck" region in order to bind Inscuteable.

(A) Schematic of Bazooka (Baz) structural motifs. Baz contains an NH2-terminal oligomerization domain, three central PDZ domains, and a motif near the COOH-terminus that contains aPKC/PAR-1 phosphorylation sites and a phosphoinositide binding motif.
(B) Affinity pulldowns with MBP-Inscuteable (Insc) reveal direct binding between the NH2-terminal portion and the Insc ankyrin repeats.
(C) The region from 117-314, comprising most of the "Neck" region is sufficient for interaction with Insc.
(D-E, K) Baz is recruited to induced polarity crescents of Ed-Insc and not of Ed-GFP.
(F-G,K) Deletion of the NH2-terminal domain is sufficient to cause a loss of specific recruitment to Insc.
(H-K) Expression of NH2-terminal fragments alone are insufficient for interphase recruitment of Baz to Ed-Insc crescents.

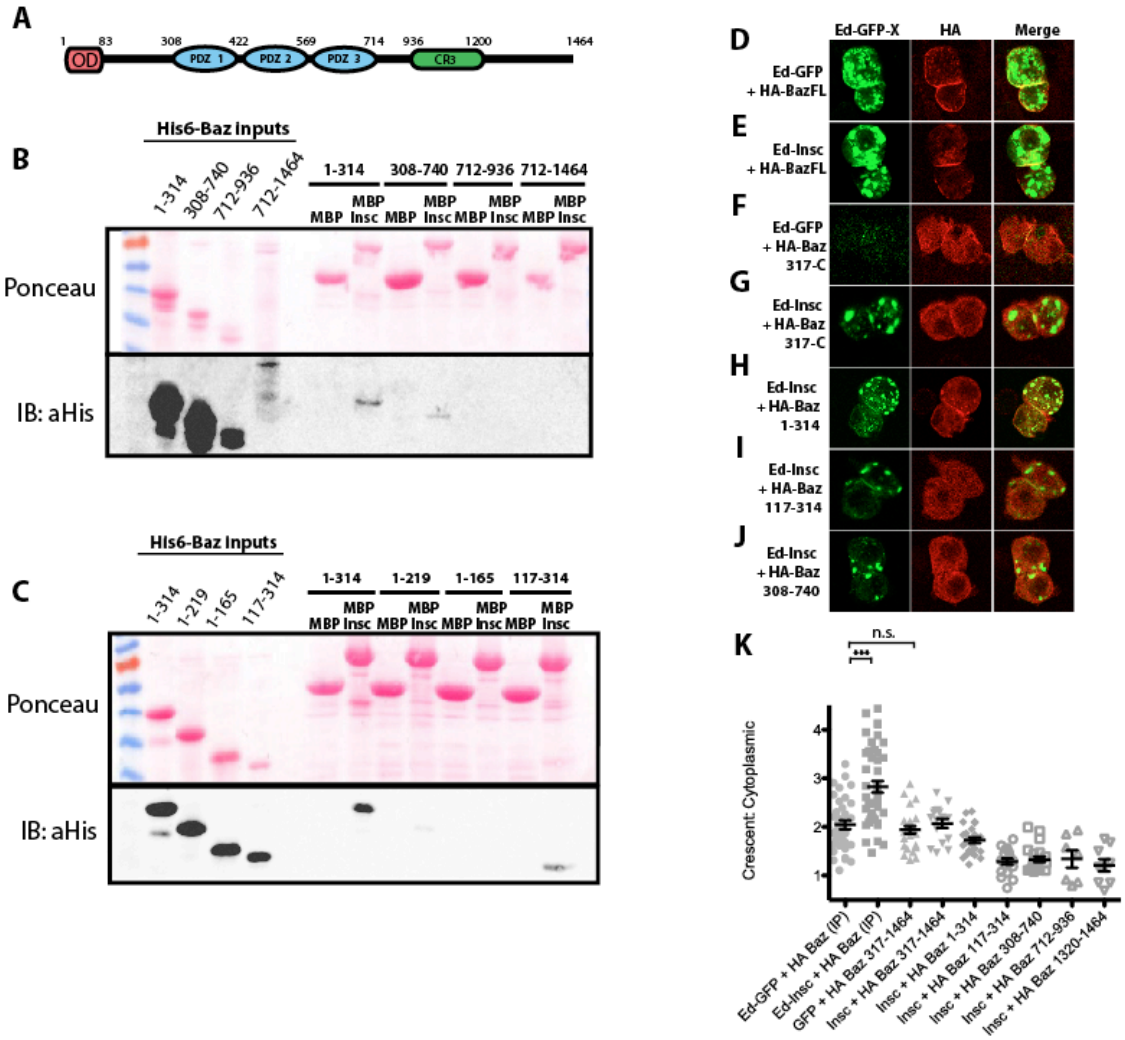

We next applied Aurora A RNAi to induced-polarity S2 cells to assess whether we could recapitulate the same defect in Bazooka localization behavior in our cell culture system. Overexpression of HA-tagged Bazooka exhibited the same mitotic localization dynamics as endogenous Bazooka was shown to have previously (Figure 4 B-C, F). Application of Aurora A RNAi to these cells, however, resulted in Bazooka recruitment to Insc crescents during Interphase to a similar degree as in mitotic S2 cells in the absence of RNAi (Figure 4D, F). Overexpression of the Aurora A Kinase domain in a non-RNAi context was also able to reduce Baz recruitment to crescents (Figure 4E-F). These data suggest that Aurora A is a repressor of the Insc-Baz interaction.

To determine whether Aurora is a direct repressor of the interaction between Inscuteable and Bazooka, we expressed and purified full-length Aurora A and performed γ32P-ATP autoradiogram assays using Insc and Bazooka fragments as substrates. Treatment of Bazooka with Aurora A resulted in a strong phosphorylation in the "neck" region comparable to our positive control Pins (Figure 5A). Strikingly, this region is the same as is sufficient for Insc interaction in pull-down assays. To determine whether phosphorylation in this region is able to affect the formation of the Insc-Baz complex, we performed MBP-Insc pulldowns in the presence and absence of Aurora A phosphorylation. MBP-Insc pulled down untreated Baz, but not Aurora-A phosphorylated Baz (Figure 5B). These data indicate that Aurora is a direct repressor of the Insc-Baz complex and phosphorylation of Baz is sufficient to disrupt the complex.

To identify the Aurora A phosphorylation site on Bazooka, we searched the sequence of the Bazooka neck region for consensus sequence elements required for Aurora phosphorylation. The sequence elements around Serine 239 of the Bazooka neck

Figure 4. Aurora A regulates Bazooka recruitment to Inscuteable crescents.

(A) Schematic of Bazooka (Baz) structural motifs. Baz contains an NH2-terminal oligomerization domain, three central PDZ domains, and a motif near the COOH-terminus that contains aPKC/PAR-1 phosphorylation sites and a phosphoinositide binding motif.
(B-C, F) Overexpression of soluble, HA-tagged Bazooka in S2 cells polarized for Insc results in a recapitulation of the phenotype of mitotic Bazooka recruitment.
(D,F) Application of in vitro transcribed Aurora A RNAi results in enhanced recruitment of Bazooka during interphase.
(E-F) Expression of the soluble Aurora A Kinase domain results in a reduction of Bazooka at the induced Insc crescent.

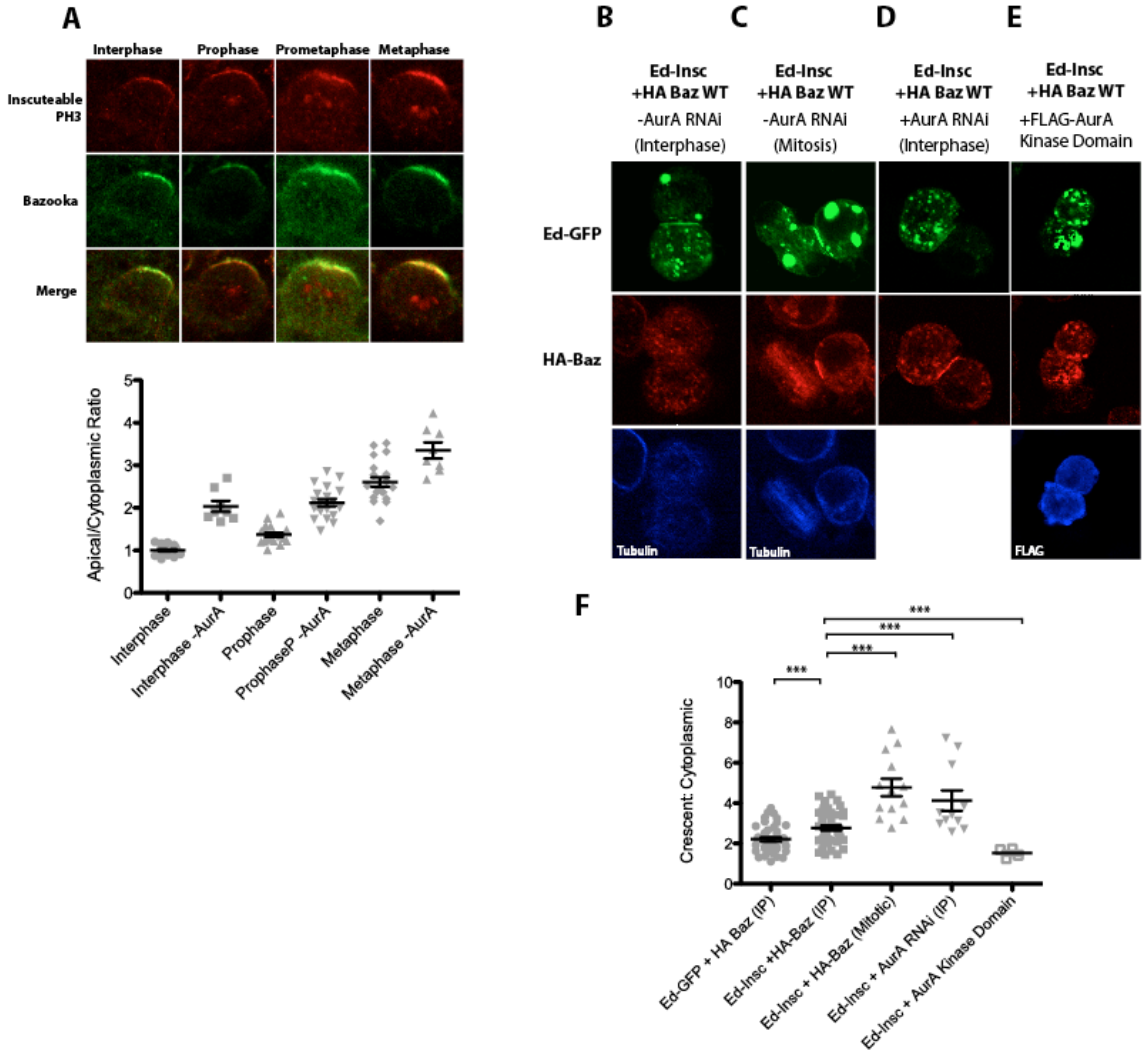

domain fit the consensus compared to other known substrates of AurA (Figure 5C). Mutation of S239 to alanine resulted in a loss of Aurora A phosphorylation (Figure 5D). Treatments of S239A phosphodead mutants resulted in a reduced level of AurA regulation in pulldown assays (Figure 5E). To determine whether S239 phosphorylation is required for the regulation of Baz recruitment, we placed it into our induced polarity assay. Compared to WT controls, Baz S239A resulted in a nearly three-fold enhancement of interphase recruitment and was more effective than Aurora A RNAi in allowing for interphase recruitment (Figure 5F-G). Therefore, we conclude that S239 phosphorylation is required for regulation of the Insc-Baz complex and may be required for the disruption of polarity at the end of the cell cycle.

DISCUSSION

The temporal dynamics of Par complex polarization in neuroblasts are reminiscent of other cell cycle regulated polarities, such as the *C. elegans* zygote and the SOP lineages. In these types, the entry of the cell into mitosis coincides with polarization. In these cell types, cortical flows of actin and myosin away from some point on the cortex seem to be responsible for polarity. Fertilization of the zygote at the posterior cortex induces flows of actin and myosin toward the anterior cortex (Zonies et al., 2010), while *Frizzled* and *Disheveled* signaling is responsible for localizing Bazooka to the posterior cortex in SOP cells (Segalen et al., 2010). Symmetry breaking in these cells therefore results from induction of Baz localization from a negative regulatory cue at the

opposite cortex. This seems to results in large, broad regions of polarity in these cells. It is not known whether a basal polarity cue also exists in neuroblasts.

Neuroblast lineages are unique due to their repression of Notch signaling (Udolph et al., 2001), the loss of adherens junctions (Cappello et al., 2006), and no known involvement of planar cell polarity factors. In the absence of normal cell polarity cues, what factors might control Baz polarization to the apical cortex? Inscuteable is known to play an important role in neuroblast cell polarity. In a rather novel mechanism, Inscuteable acts a regulated intramolecular cue for Bazooka at the apical cortex localization in larval neuroblasts. This cue persists at the apical cortex over the course of multiple divisions and couples the mitotic spindle axis to polarity by acting as a common interaction node. This allows for the stereotyped division axis of the neuroblast observed *in vivo*.

In delaminated neuroblasts, Bazooka seems to be completely dispensable for polarized Inscuteable localization (This work; Schober et al., 1999; Wodarz et al, 1999). However, during the process of delamination, loss of Insc has no effect on the recruitment of Bazooka to the apical delamination stalk. The role for Bazooka in directing Inscuteable polarity may be early and indirect. Apical-basal epithelial polarity is disrupted in a *bazooka* mutant. Failure to establish correct epithelial apical-basal polarity domains may lead to incorrect neuroblast polarity.

The colocalization of the two factors may result from the initial involvement of adherens junctions during the delamination process. Adherens junction components, such as Armadillo, are known to bind Bazooka with high affinity. This suggests that junctional

Figure 5. Phosphorylation of Bazooka by Aurora A at S239 causes disruption of the Inscuteable-Bazooka complex.

(A) Bazooka is phosphorylated by Aurora A in the "Neck" region of the protein.
(B) Treatment of the Baz "neck" domain with purified Aurora A kinase results in the loss of the Inscuteable interaction.
(C) Analysis of the sequence of the "neck" domain reveals a sequence around S239 similar to other known Aurora A substrates.
(D) Mutation of S239 to alanine results in a loss of Baz phosphorylation by AurA.
(E) Baz S239A exhibits reduced levels of Aurora regulation in MBP-Insc pulldowns.
(F) Baz S239A recruits robustly to Ed-Insc crescents during interphase.

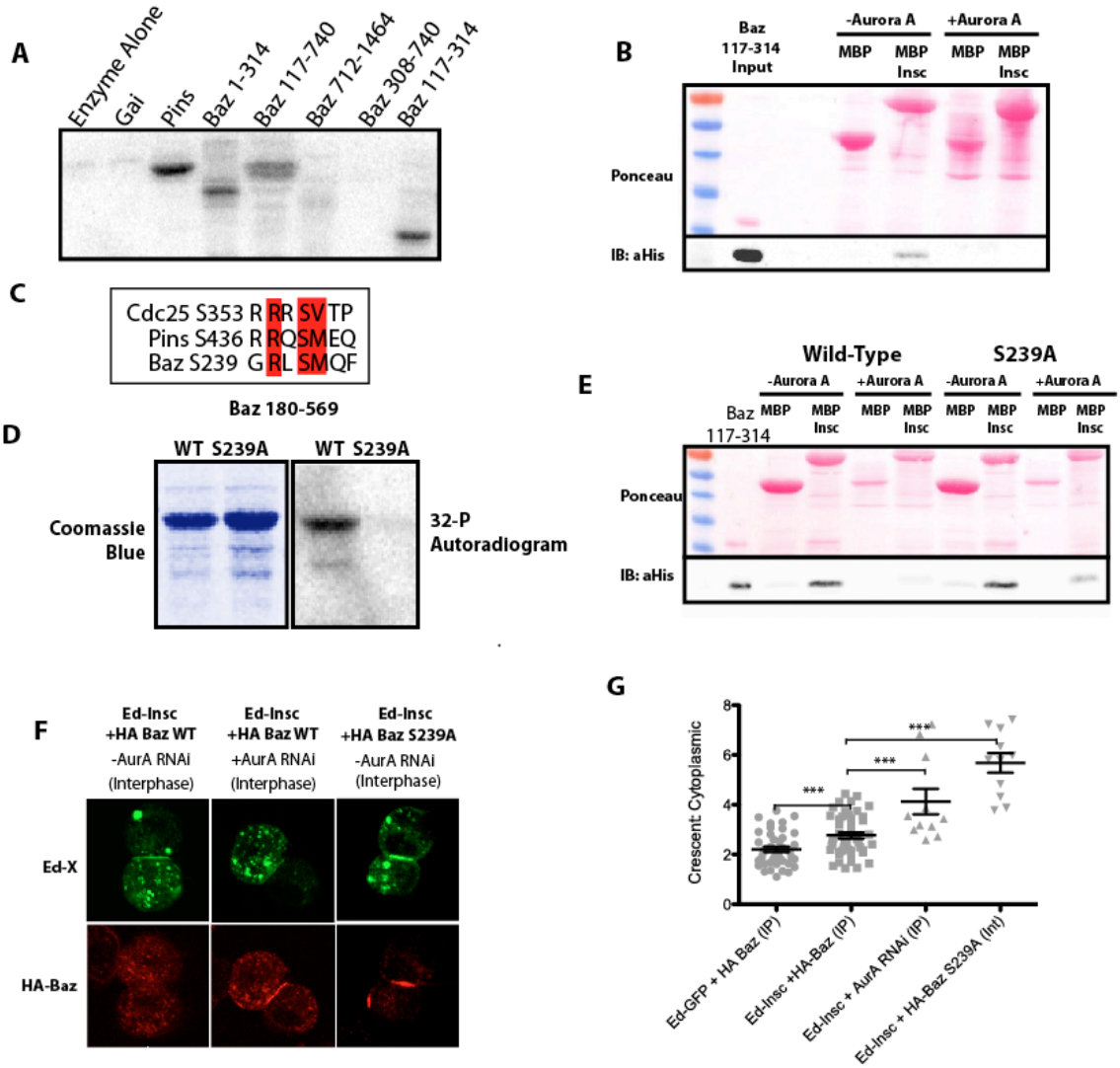

cues may override Inscuteable-mediated polarity cues. Consistent with this model, adherens junctions have been shown to play a role in preventing the onset of asymmetric cell divisions (Lu, Roegiers, 2001). In adherens junction-free systems, such as the pI SOP cell, Inscuteable is able to relocalize Baz to the posterior cortex (Bellaiche et al., 2001; Wirtz-Peitz et al., 2008). In contrast, in the pIIa cell, which utilizes adherens junction, Baz is localized during interphase (LeBorgne et al., 2002).

When misexpressed in epithelia, which exhibit adherens junction-mediated polarity, Inscuteable is sufficient to reorient the mitotic spindle and relocalize Pins to the apical domain (Kraut et al., 1996). Since delamination typically coincides with Inscuteable expression, it is possible that Inscuteable becomes apical through the activation of Pins/Gai, as in Insc-misexpressing epithelia and Bazooka retains junctional localization. Thus, the two may enrich at the apical membrane by independent mechanisms and may not be directly associated. Once junctions disappear post-delamination Inscuteable and Bazooka may be allowed to interact.

Like in Insc-misexpressing pI SOP cells, the pathway upstream of localizing Inscuteable in neuroblasts may be mediated by Pins. Pins and Gai are known to be absolute requirements for Inscuteable localization to the cortex. How Pins and Gai might lead to polarization of Inscuteable is, so far, unresolved. The GPCR receptor Tre1 has been implicated in controlling Gai localization and subsequent Pins recruitment in neuroblasts and S2 cells (Yoshiura et al., 2012). However, the localization of Tre1 is unknown within cell types. In epithelia, Tre1 may localize to the apical domain, similar to other known GPCRs (Saunders and Limbird, 1997). Polarity in this model would derive from persistent extracellular gradients of GPCR ligands that activate Gai apically

leading to Pins and Inscuteable localization. Bazooka polarity is subsequently controlled by repression of binding to Inscuteable, giving rise to temporal polarity. Further RNAi-mediated studies of the roles of Tre1, Pins, and Gai in establishing Inscuteable polarity in neuroblasts are needed to further clarify this model.

Aurora A is thought to act as a repressor of the Insc-Baz interaction which allows for disruption of the complex. Other systems, such as the pI SOP cell, Aurora A is required for the establishment of Baz localization while in neuroblasts, Aurora A is required for the disruption of the Insc-Baz complex. This may be a result of the unique mechanisms by which the Par complex is localized in these cell types. In the pI cell, Aurora A phosphorylation of aPKC is thought to lead to the formation of the Bazooka-bound Par complex. Once the complex is assembled, the Par complex enriches at the posterior of the cell. Loss of Aurora A leads to a complete failure of polarity (Wirtz-Peitz et al., 2008).

In neuroblasts, however, Aurora A plays an opposite role of disrupting the association between Insc and Baz at the end of mitosis. Additionally, Aurora A is known to become active much earlier in the cell cycle, during prophase. However, Aurora seems to act on the Insc-Baz complex later in the cell cycle, during telophase, where it assists the resolution of cytokinesis (Marumoto, 2003). Sequestration of Aurora A to the mitotic spindle apparatus may lead to the delay of activity to telophase. As the centrosome is drawn towards the apical pole of the cell and the spindle breaks down, local concentrations of Aurora A increase and may become involved in disassembling the Insc-Baz complex. Aurora localization dynamics may explain the differences in the timing of onset between different systems. Additional activation of players such as Cdc42 may help

enhance the association and polarity observed in the wild-type system. Like many regulated systems, the antagonism of protein phosphatases is often involved in counteracting the effects of the kinase. Known Aurora A antagonists include PP1 (Ghosh and Cannon, 2013), yet these have no described polarity roles in the neuroblast. Further studies will be required to identify phosphatase factors involved in the dynamic polarity observed in neuroblasts.

The roles that dynamic polarity may play in the correct division of the *Drosophila* neuroblast remains unknown. Cells with broad regions of persistent polarity, such as in the *Drosophila* oocyte and follicular epithelia, often result in polarized domains which directly contact one another. For cells with large size asymmetric cell divisions, as in neuroblasts, broad regions may make effective segregation of fate determinants difficult to achieve. Utilizing dynamic polarity may allow for a burst of activity which leads to effective segregation of fate determinants. Additional actin-mediated compaction of the polarity crescent may assist in segregating fate determinants into the daughter cells. Prolonged polarity may lead to expansion of basal determinants and errors in fate determination.

BRIDGE TO CHAPTER III

Inscuteable plays an important role in establishing the cell polarity axis in the Drosophila neuroblast. After delamination, Inscuteable maintains a polarized localization and sets the mark for Bazooka polarity over the course of multiple divisions. Inscuteable acts to set a stereotyped axis of polarity that generates daughter cell lineages toward the interior of the brain. The Inscuteable-Bazooka interaction is regulated by Aurora A

kinase, a key member of the cell cycle apparatus, and phosphorylation of Bazooka in the interaction region is sufficient to disrupt the Insc-Baz complex. This behavior allows for dynamic polarity during the cell cycle and may lead to compact regions of polarity during cell division. Aside from its role in polarity, Inscuteable is also known to play a key role in the alignment of the mitotic spindle to the polarity axis. In the following chapter, I describe the regulatory role played by Inscuteable in the alignment of the mitotic spindle through competition with spindle alignment machinery for binding to Pins.

CHAPTER III

INSCUTEABLE MODULATES THE OUTPUT OF PINS BY COMPETING WITH MUD FOR PINS BINDING

This chapter contains previously published co-authored material taken with permission from:

Mauser, J. F. & Prehoda, K. E. (2012) Inscuteable regulates the Pins-Mud spindle orientation pathway. *PLoS ONE* **7**, e29611.

Author contributions: J.F.M and K.E.P. designed research; J.F.M. performed research; J.F.M. and K.E.P. analyzed data; and J.F.M. and K.E.P. wrote the paper.

During asymmetric cell division, alignment of the mitotic spindle with the cell polarity axis ensures that the cleavage furrow separates fate determinants into distinct daughter cells. The protein Inscuteable (Insc) is thought to link cell polarity and spindle positioning in diverse systems by binding the polarity protein Bazooka (Baz; aka Par-3) and the spindle orienting protein Partner of Inscuteable (Pins; mPins or LGN in mammals). Here we investigate the mechanism of spindle orientation by the Insc-Pins complex. Previously, we defined two Pins spindle orientation pathways: a complex with Mushroom body defect (Mud; NuMA in mammals) is required for full activity, whereas

binding to Discs large (Dlg) is sufficient for partial activity. In the current study, we have examined the role of Inscuteable in mediating downstream Pins-mediated spindle orientation pathways. We find that the Insc-Pins complex requires Gαi for partial activity and that the complex specifically recruits Dlg but not Mud. *In vitro* competition experiments revealed that Insc and Mud compete for binding to the Pins TPR motifs, while Dlg can form a ternary complex with Insc-Pins. Our results suggest that Insc does not passively couple polarity and spindle orientation but preferentially inhibits the Mud pathway, while allowing the Dlg pathway to remain active. Insc-regulated complex assembly may ensure that the spindle is attached to the cortex (via Dlg) before activation of spindle pulling forces by Dynein/Dynactin (via Mud).

INTRODUCTION

Precise positioning of the mitotic spindle is critical for a broad range of processes, including cell type differentiation and tissue organization (Cabernard and Doe, 2009; Baena-Lopez et al, 2005). For example, in the asymmetric division of Drosophila neuroblasts proper segregation of fate determinants requires that the spindle align with the axis of apical/basal cell polarity (Siller and Doe, 2009; Knoblich, 2010). Incorrect spindle orientation has been implicated in a number of pathologies, including tumorigenesis (Prehoda, 2009).

During the neuroblast asymmetric division, cell fate determinants become polarized by metaphase. Factors important for differentiation of the basal daughter cell localize to the basal cell cortex, whereas factors that maintain neuroblast identity localize to the apical cortex (Prehoda, 2009). During cytokinesis, the two polarity domains

become separated by the cleavage furrow such that the apical daughter cell retains the neuroblast identity and the basal cell differentiates into a neuron or glial cell. The mitotic spindle plays a crucial role in specifying the position of the cleavage furrow and thus proper fate determinant segregation requires alignment of the spindle with the polarity axis (Chia et al., 2008; Glotzer, 2004; Cabernard et al., 2010).

Coupling of polarity and spindle orientation is thought to be mediated by the protein Inscuteable (Insc) because of its ability to bind components from both systems (Fig. 1A) (Siller and Doe, 2009). The functional region of Inscuteable, the central Ankyrin-repeat-like domain, has been previously characterized (Schober et al., 1999). Insc interacts with Bazooka (Baz; aka Par-3), a component of the apical Par polarity complex that also includes the proteins Par-6, and atypical Protein Kinase C (aPKC) (Siller and Doe, 2009; Schober et al., 1999; Wodarz et al., 1999). Insc also binds Partner of Inscuteable (Pins), which regulates neuroblast spindle orientation (Yu et al., 2000; Schaefer et al., 2000). In *insc* mutant neuroblasts, both cell polarity and spindle orientation are defective (Kraut et al., 1996; Siegrist and Doe, 2005).

Insc is thought to act as a localization signal for Pins. Pins, in turn, activates two downstream pathways that participate in mitotic spindle positioning. The Pins tetratricopeptide repeats (TPR) motifs bind Mushroom body defect (Mud; NuMA in mammals) (Siller et al., 2006). In mammals, NuMA (Nuclear Mitotic Apparatus), the Mud ortholog, has been previously been shown to be abundant in the nuclei of interphase cells and to play an essential role during mitotic spindle assembly and alignment during mitosis. Mud/NuMA in turn are thought to recruit the Dynein/Dynactin complex, which can generate pulling forces on astral microtubules from its minus-end directed motor

activity (Siller and Doe, 2008). Pins also contains a central Linker domain that is phosphorylated by the mitotic kinase Aurora A. The phosphorylated Linker domain binds Discs large (Dlg, PSD-95 in mammals) which acts to recruit the plus-end directed kinesin Khc73 (Kinesin-3, GAKIN, Kif13B in mammals) (Siegrist and Doe, 2005; Johnston et al., 2007).

Whether Insc is a passive scaffold that simply provides a physical link between polarity and spindle position, or if Insc somehow actively regulates the two pathways downstream of Pins has been unclear. Here we examine the effect of Insc on Pins-mediated spindle orientation using an induced polarity cell culture system (Johnston et al., 2007). This system allows for precise control of the components that are placed on the cortex and can be subsequently interrogated for spindle orienting activity.

MATERIALS AND METHODS

Molecular Cloning, Protein Expression and Purification

Constructs encoding Drosophila Pins, Inscuteable, and Mud have been described (Schober et al., 1999; Tio et al., 1999). Residues 252–600 of Inscuteable, including the central Ankyrin-repeat containing region, were used for all experiments. Residues 1–466 of Pins, corresponding to the TPR+LINKER domains, 42–398, corresponding to the TPR domain, and 372–658, corresponding to the three GoLoco domains were used for Inscuteable binding studies. Mud residues 1825–2016, which includes the minimal Pins-binding domain, were also amplified for binding assays.

Echinoid (Ed) fusion constructs were made in pMT-V5 (Invitrogen, Carlsbad, CA), replacing the Ed cytoplasmic domain with a visualization tag and the protein of

interest at the COOH terminus (e.g., Ed-GFP-Insc). Proteins for pull down and anisotropy experiments were expressed in Escherichia coli strain BL21(DE3) using pGEX 4T-1-based vectors for GST fusions, pMAL-c2 based-vectors for MBP fusions, and pBH-based vectors for hexahistidine fusions. GST-fusion proteins were purified on glutathione-agarose resin and washed with a large excess of GST pulldown buffer (10 mM HEPES pH 7.5/100 mM NaCl/1 mM DTT). The resin was then used for subsequent GST-pulldowns. MBP-fusion proteins were purified on amylose resin (New England Biolabs), washed with three bed-volumes of PBS+1% Triton X-100 and one bed-volume of PBS. Proteins were eluted using PBS+1M Methyl-α-D-glucopyranoside (Sigma-Aldrich). Hexahistidine-fusion proteins were purified on Ni-NTA agarose resin (Qiagen). The incubated resin was then washed with a large excess of cell lysis buffer (50 mM NaPO4/150 mM NaCl/10 mM imidazole). Samples were then eluted with elution buffer (50 mM NaPO4/150 mM NaCl/300 mM imidazole).

Transfection and S2 Cell Experiments

S2 cells were grown and cultured at room temperature in Schneider's Insect Media (Sigma) supplemented with 10% fetal bovine serum. Echinoid polarity assays were carried out as described previously (Siegrist and Doe, 2005). In short, 1×10∧6 cells were transiently transfected with pMT-V5 fusion constructs (400 ng each) using Effectene (QIAGEN) reagent according to manufacturer protocol. 24–48 hrs after transfection, protein expression was induced by incubation with CuSO4 (500 μM) for 24 hr. Cells were harvested by centrifugation and the media was replaced. These cells were then shaken (175 RPM) for 2–3 hr to induce Ed-mediated cell-cell clusters. These cells

were then were plated on glass coverslips and allowed to incubate for 3 hr to allow for cell divisions to occur.

Immunostaining

For immunostaining, S2 cells were fixed for 20 min in 4% paraformaldehyde, stained, and imaged on a Leica SP2 confocal microscope with a 63×1.4 NA lens. Antibodies and dilutions were as follows: rabbit Gαi, 1:1000 (Johnston et al., 2007), mouse Dlg, 1:250 (Developmental Studies Hybridoma Bank, Iowa); rabbit Mud 1:1000 (gift from Y. Bellaiche); rat Pins, 1:500 (Wodarz et al., 1999), rat tubulin, 1:1000 (Abcam); rabbit Insc 1:1000 (gift from W.Chia), rabbit HA, 1:1000 (Covance).

Immunoprecipitation and Western Blots

For western blot lysate inputs, 20 μg of total protein from brain extracts were used per lane. Immunoprecipitation from larval brain extracts was carried out using antibodies bound to protein G sepharose (GE Healthcare) according to the manufacturer's instructions. 40 brains from L3 larvae were dissected and homogenized by douncing in 300 uL sample buffer (50 mM HEPES pH 7.5/150 mM NaCl/1 mM DTT/0.1% Triton X-100/EDTA-free Protease Inhibitors (Roche)). Extracts were then centrifuged twice for 10 minutes each at 10,000 rpm to pellet insoluble cell debris. The resulting supernatant was then precleared with protein G sepharose and incubated with antibody-bound resin. Following three washes in sample buffer, the resin was heated to 95°C in SDS loading buffer (1% SDS/100 mM DTT/50 mM Tris pH. 7.5/0.003% bromophenol blue). Immunoprecipitates were resolved on SDS-PAGE followed by western blotting.

Measuring Cortical Polarity, Spindle Orientation, and Centrosome Alignment

Spindle alignment measurements were made as described previously (Johnston et al., 2007). Briefly, spindle angles were measured with a vector perpendicular to the center of the Ed crescent and a vector matching the spindle or connecting the spindle poles. The angle between these two vectors was then assessed.

In Vitro Binding Assays

GST pull-down assays have been described (Nipper et al., 2007). Briefly, ligands were added to glutathione agarose with adsorbed GST fusion proteins in binding buffer (10 mM Hepes/100 mM NaCl/1 mM DTT) at the indicated concentrations to a final reaction volume of 50 µl and incubated at room temperature for 15 min before washing, elution, and analysis by gel electrophoresis.

Fluorescence anisotropy binding assays were as described (Nipper et al., 2007). A peptide containing the sequence of Mud residues 1955–1970 and an NH2-terminal cysteine was labeled with tetramethylrhodamine maleimide (Life Technologies) according to the manufacturer's instructions. The labeled protein was purified by reverse-phase HPLC. For binding experiments, solutions were prepared with increasing amount of ligand and constant dye-labeled component (100 nM) in binding buffer with the temperature maintained at 20°C by using a circulating water bath. Data series were fit to an equation describing 1:1 binding.

In Vitro Kinase Assays

Recombinant Aurora-A kinase was purchased from Millipore (Billerica, MA). Pins constructs (10 μg) and Aurora-A (100 ng) were diluted in ice-cold assay buffer (20 mM Tris [pH 7.4], 100 mM NaCl, 1 mM DTT, 10 mM MgCl2, and 10 μM ATP). These reactions were then moved to room temperature for 30 minutes. Reactions were then chilled on ice and added to affinity pulldown resin for pulldown experiments.

RESULTS

Polarized Inscuteable Recruits Pins but Lacks Spindle Orientation Activity

In the current model for Insc-based coupling of polarity and spindle orientation, Insc recruits Pins, which in turn recruits the downstream effectors Mud and Dlg (Fig. 1A) (Yu et al., 2000; Siller et al., 2006; Johnston et al, 2007; Tio et al., 2000). In previous work, we found that Insc lacked activity in an induced polarity spindle orientation assay (Johnston et al., 2007). In this assay, proteins are fused to the cytoplasmic domain of the adhesion protein Echinoid (Ed) and transiently transfected into cultured Drosophila S2 cells. Cell clustering leads to polarization of the Ed fusion protein at sites of cell-cell contact and the angle of the spindle to the center of the induced crescent can be measured. Although we have observed that the spindle aligns with polarized Ed-PinsTPR-LINKER fusions, the spindle is randomly oriented in cells with polarized Ed-Insc fusions (Fig. 1B, D).

To investigate why Ed-PinsTPR-LINKER orients the spindle but Ed-Insc fails to do so, we first determined if Pins is recruited to Ed-Insc. Endogenous Pins protein strongly colocalizes with Ed-Insc (Fig. 1E). However in cells with polarized Ed alone

Pins remains in the cytoplasm (Fig. 1F). Thus, we conclude that Ed-Insc recruits Pins, yet is unable to orient the spindle. Pins is known to be autoinhibited for Mud-binding by an intramolecular interaction between its NH2- and COOH termini (Nipper et al., 2007; Du and Macara, 2004). This autoinhibition is relieved by binding of the heterotrimeric G-protein subunit, Gαi. Ed-Insc may not exhibit spindle orientation activity because the Pins that it recruits has not been activated. We expressed Gαi with Ed-Insc to ensure that Insc-bound Pins is activated. Ed-Insc and Gαi co-expression leads to the formation of an Insc-Pins-Gαi complex at the crescent, but only a moderate amount of spindle orienting activity, similar to cells with polarized Pins in which only the downstream Dlg pathway, but not the Mud pathway, has been activated (Johnston et al., 2007) (Fig. 1C, D, G).

Insc-Pins recruits Dlg but not Mud

The Insc-Pins-Gαi complex may not fully orient the mitotic spindle because of failure to recruit downstream effectors that are normally brought to the cortex by Pins. We tested for recruitment of the two known Pins spindle orientation pathways, Dlg and Mud. In cells expressing Ed-Pins, Dlg is robustly recruited to the cell-cell contacts (Fig. 1H) and co-expression of Ed-Pins with Gαi results in strong Mud recruitment (Fig. 1I). Dlg and Mud recruitment is specific as it is not observed in cells expressing Ed-GFP (Fig. 1 J, K).

We next examined whether Dlg and Mud are recruited to Ed-Insc. Dlg is recruited to Ed-Insc in a similar manner as Ed-Pins (Fig. 1L). However, while Pins-Gαi can recruit Mud, Insc-Pins-Gαi is unable to do so (Fig. 1M). Thus, Insc appears to regulate Pins complex assembly, leading to preferential activation of only one of the two spindle

Figure 1 (next page). Inscuteable-mediated orientation of the mitotic spindle requires Gαi.

(A) Current model of Inscuteable function. Inscuteable serves as a link between the apical PAR complex and the spindle-orienting Pins- Gαi complex.
(B) Echinoid-Inscuteable (green) transfected S2 cells randomly orient the mitotic spindle (red) with respect to the region that is enriched in Echinoid. Spindle alignment is measured by drawing a vector from the center of the crescent (arrow) to the center of the mitotic spindle and then along the axis (dashes).
(C) Expression of Gαi (blue) with Echinoid-Inscuteable (green) is able to confer moderate spindle orienting activity.
(D) Cumulative percentage plot of spindle angles measured in the S2 Echinoid induced-polarity assay for Echinoid-Inscuteable and Echinoid-Inscuteable+ Gαi compared to previously published data (Johnston et al., 2007). In these plots, the cumulative percentage of cells with a spindle angle below a particular value (x-axis) is shown. High spindle orienting activity corresponds to a deflection to lower spindle angles whereas no activity is a line across the diagonal.
(E) Echinoid-Inscuteable expression in S2 cells is sufficient to robustly recruit endogenous Pins from the cytoplasm to the region of Echinoid enrichment.
(F) Echinoid alone is unable to polarize endogenous Pins.
(G) Echinoid-Inscuteable induces colocalization of endogenous Pins with overexpressed Gαi
(H) Ed-Pins is able to recruit endogenous Dlg.
(I) Co-expression of Gαi with Ed-Pins results in robust recruitment of endogenous Mud.
(J,K) Ed-GFP is unable to recruit endogenous Dlg or Mud to the induced-polarity cortical domains.
(L) Ed-Insc is able to recruit Dlg to the cortex, similar to cells expressing Ed-GFP-Pins.
(M) Ed-Insc is not able to recruit Mud (red) to the Ed-crescent, even in the presence of Gai. Scale bars for all panels represent 5 μm.

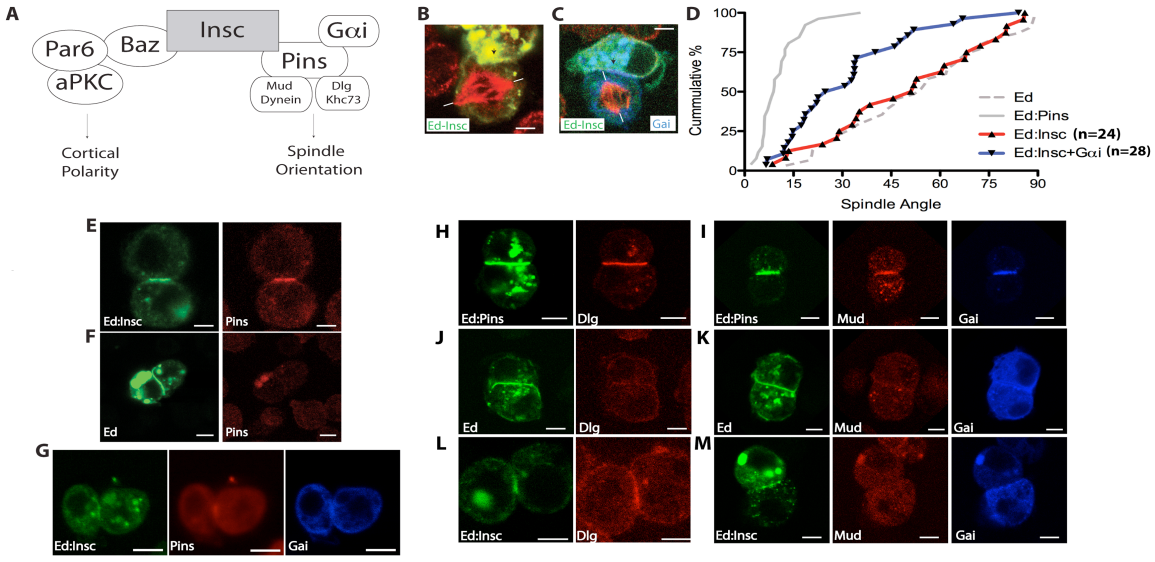

orientation pathways, with the effect of an overall reduction in spindle orientation activity.

Insc Represses Pins-Mediated Spindle Orientation

Ed-Insc cannot fully orient the spindle even though it recruits Pins and Gαi. Polarized Ed-Pins coexpressed with Gαi, however, has full spindle-orienting activity (Johnston et al., 2007). These data suggest that Insc preferentially inhibits Pins spindle orienting activity. To further investigate if Insc inhibits Pins-mediated spindle orientation, we expressed Insc in cells with polarized Ed-PinsTPR-LINKER, a construct lacking autoinhibition that, when expressed on its own, fully aligns the mitotic spindle (Fig. 2A) (Johnston et al., 2007). We observed that Insc is recruited to Ed-PinsTPR-LINKER crescents (Fig. 2A, inset) and that the presence of Insc reduces its spindle orienting activity to a level indistinguishable from the Dlg pathway alone (Fig. 2B). Thus, we conclude that Insc inhibits the spindle-orienting activity of PinsTPR-LINKER.

The Pins TPR Domains Bind Inscuteable

Why might Insc-Pins recruit Dlg, but not Mud? One possible explanation is that Insc and Mud compete for binding to Pins. Mud is known to bind the Pins tetratricopeptide repeats (TPRs) (Siller et al., 2006; Nipper et al., 2007; Du and Macara, 2004). To identify the Pins region responsible for binding Insc, we performed a deletion analysis using affinity pulldowns with purified proteins. Pins contains seven TPR repeats followed by a flexible Linker domain and three GoLoco motifs that bind Gαi. GST-fusions of full-length Pins, the GoLoco region, and the TPR region were generated and incubated with a purified MBP-fusion of the central Ankyrin-repeat containing domain of Inscuteable (MBP-Insc) (Schober et al., 1999).

All constructs containing the full set of 7 Pins TPRs are able to bind Insc, whereas those lacking these repeats, such as the COOH-terminal GoLoco domains, are unable to bind Insc (Fig. 3A). Further TPR truncations were also performed to find the minimal TPR region required for binding to Insc. While binding of Insc to Pins is detectable using a constructs consisting of the full set of TPRs as well as TPRs 1–5, all seven TPRs are required for high-affinity association with Insc (Fig. 3A). Since Mud/NuMA have also been shown to require a full array of TPRs for high-affinity binding both Insc and Mud bind to the Pins TPR motifs (Siller et al., 2006).

Mud and Insc Compete for Binding to Pins

As Insc and Mud both bind the Pins TPRs, we examined whether Insc and Mud could bind simultaneously to Pins. Extracts were prepared from the brains of wild-type third-instar larvae and complex formation was examined by immunoprecipitation of the

endogenous components. As expected, we observed both Insc and Mud in Pins immunoprecipitates. However, in Insc immunoprecipitates, we observed Pins but Mud was not present (Fig. 3B). The lack of Mud in Insc immunoprecipitates suggested that Pins forms mutually exclusive complexes with Insc and Mud. Likewise Insc was also not observed in Mud immunoprecipitates (Fig. 3B). Thus, Insc and Mud appear to form mutually exclusive complexes with Pins.

Figure 2. Expression of Inscuteable in cells expressing constitutively-active Pins reduces spindle orientation to Dlg-like levels.

(A) Co-expression of Ed-Pins 1–466 (green), which robustly orients the mitotic spindle, with Inscuteable (inset), reduces the levels of spindle orientation in adherent, polarized S2 cells.
(B) Cumulative percentage plot of spindle angles measured in cells co-expressing Ed-Pins 1–466 and Inscuteable compared to published data (Johnston et al., 2007).

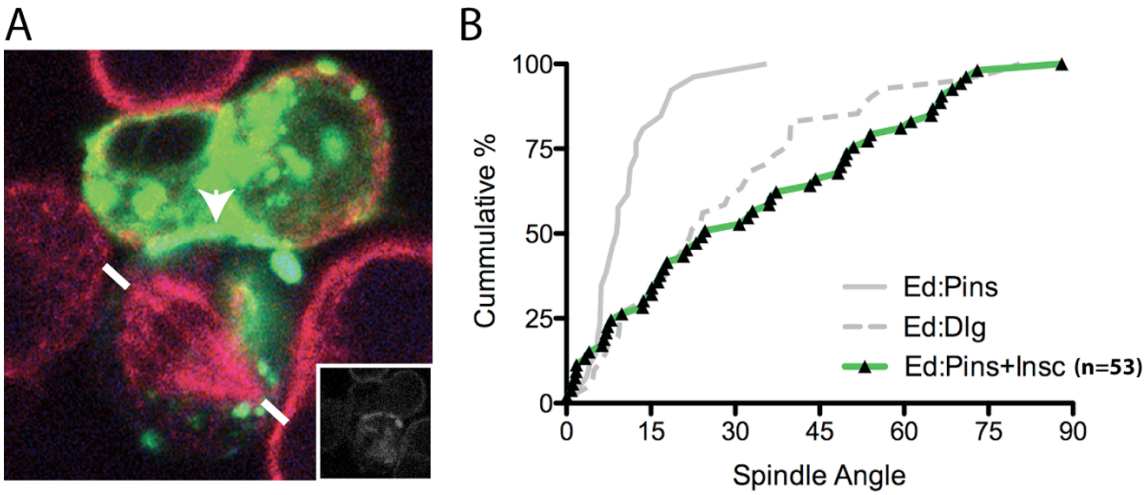

We further tested for competition between Insc and Mud for Pins using qualitative pull-downs with purified proteins. The Mud-Pins complex can be readily formed on glutathione agarose, using GST-PinsTPR and a purified Mud fragment containing the minimal TPR binding domain (Fig. 3C) (Siller et a., 2006). Introduction of MBP-Insc to these reactions dissociates Pins from Mud, resulting in switching to the Pins-Insc complex, a result consistent with competition between Insc and Mud for Pins. This effect is not observed with identical concentrations of MBP alone (Fig. 3D). GST- pulldowns with pre-formed complexes of GST-Mud and Pins TPR were likewise disrupted by addition of MBP-Insc (Fig. 3E). This effect is not observed when MBP alone is titrated into identical reactions (Fig. 3F).

Finally, we examined Insc and Mud competition using fluorescence anisotropy. We labeled a peptide representing the minimal region of Mud that binds Pins with the fluorophore tetramethylrhodamine (TMR-Mud). Binding of Pins causes a significant increase in TMR-Mud anisotropy due to complex assembly (Fig. 3G). Insc addition to a pre-formed complex of Pins & Mud leads to a decrease in TMR-Mud anisotropy to a value consistent with free peptide. No effect of Insc was observed when Pins is not present, indicating that TMR-Mud does not bind directly to Insc (Fig. 3H).

The decrease in anisotropy is a further indication that Insc competes for Mud binding and allows for calculation of the Insc affinity for Pins of Kd = 5 μM. Interestingly, this affinity is somewhat lower than the Pins-Mud interaction (Kd = 1.1 μM). Together, the immunoprecipitation, pull-down, and fluorescence anisotropy results indicate that Mud and Insc compete for Pins binding.

Figure 3 (next page). Inscuteable competes with Mud, but not Dlg, for binding to Pins.

(A) Glutathione-(S)-transferase (GST)-pulldowns of Inscuteable with different Pins constructs reveals that Inscuteable binds specifically to constructs containing the full array of Pins tetratricopeptide repeats (TPRs).
(B) Coimmunoprecipitations of endogenous proteins from wild-type L3 brain extracts demonstrate that Inscuteable and Mud form exclusive complexes with Pins.
(C) GST-pulldown using GST-Pins TPRs incubated with a constant amount of Mud and increasing Maltose Binding Protein (MBP)-Inscuteable reveals effective competition between Mud & Insc for binding to Pins.
(D) Control titrations of MBP alone do not result in dissociation of Mud from GST-Pins.
(E) GST-pulldown using GST-Mud incubated with constant 2 uM Pins TPR and increasing amounts of MBP-Insc results in an approximately 1:1 stoichiometric dissociation of Pins TPRs from GST-Mud.
(F) A control titration of MBP alone does not result in disruption of Pins-Mud binding.
(G) Fluorescence anisotropy of TMR-Mud with increasing amounts of Pins TPRs exhibits a robust association profile.
(H) Addition of Inscuteable to a pre-formed complex of 100 nM TMR-Mud & 1 uM Pins causes a dissociation of the Mud-Pins complex & reduction of TMR-Mud anisotropy.
(I) GST-pulldown using *in vitro* Aurora-A (AurA) phosphorylated Pins 1–466 results in complex formation with the Dlg GK domain. AurA treatment of a pre-formed MBP-Insc/Pins 1–466 complex likewise is able to form a complex with the Dlg GK domain.

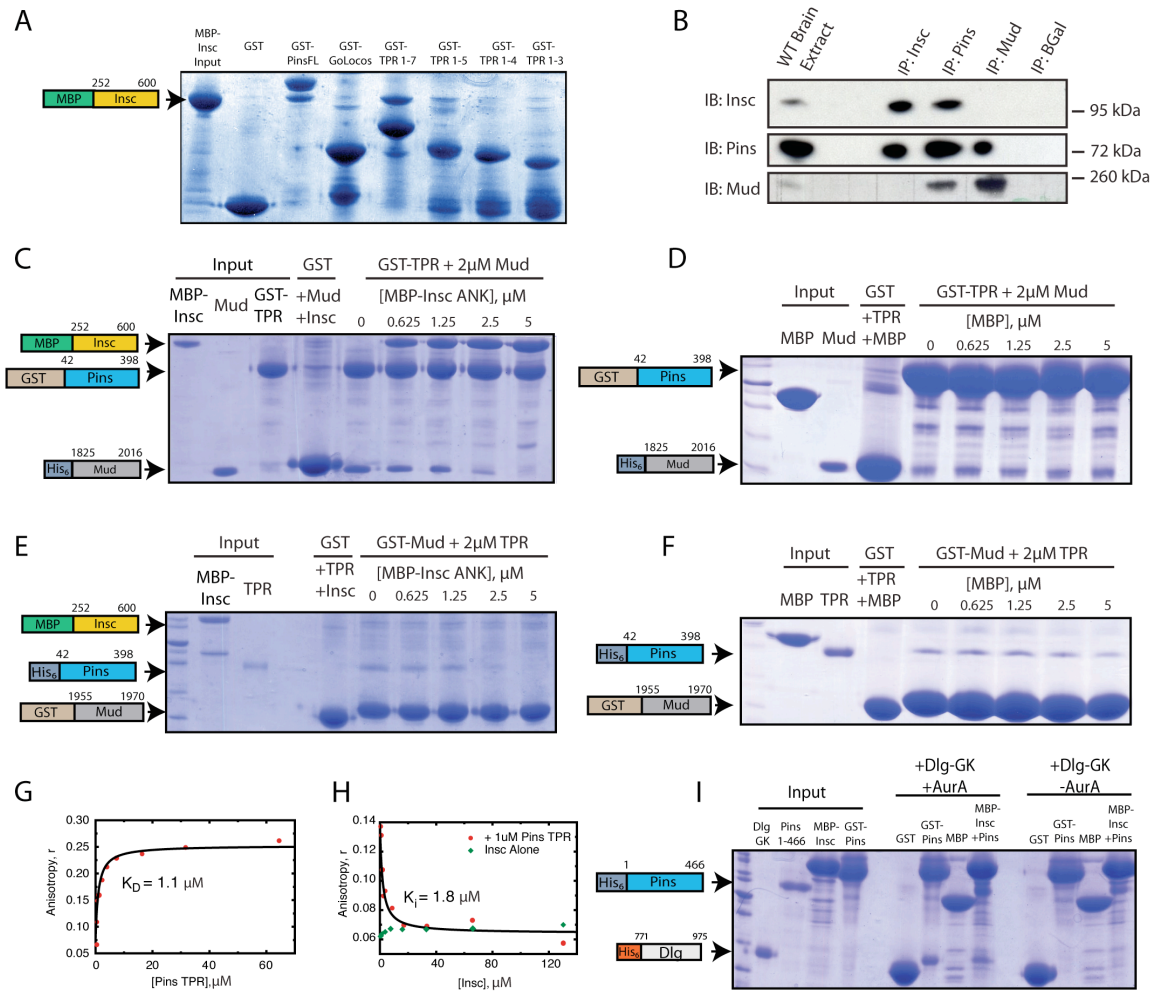

Discs large, Inscuteable, and Pins form a stable ternary complex

Pins can also bind the downstream effector Dlg through its phosphorylated Linker domain. Activation of the Dlg pathway leads to partial spindle orienting activity, similar to that observed for the Insc-Pins complex. To determine if Insc-Pins can bind Dlg, we examined their binding in a pull-down experiment. Interaction of Pins with Dlg requires Aurora-A phosphorylation of the Pins Linker domain and we observed phosphorylation-dependent formation of an Insc-Pins-Dlg ternary complex (Fig. 3I). This result indicates

that while Insc represses Mud binding to the Pins TPRs, it has no effect on regulating the downstream Dlg pathway.

DISCUSSION

Spindle positioning is important in many physiological contexts (Moore and Cooper, 2010; Lechler and Fuchs, 2005; Reinsch and Karsenti, 1994). At a fundamental level, spindle orientation determines the placement of the resulting daughter cells in the developing tissue, which is important for correct morphogenesis and tissue organization (Gray et al., 2010; Pease and Tirnauer, 2011). In other contexts, such as asymmetric cell division, spindle position ensures proper segregation of fate determinants and subsequent differentiation of daughter cells. We have examined the function of a protein thought to provide a "passive" mark on the cortex for subsequent recruitment of the spindle orientation machinery. During neuroblast asymmetric cell division, Insc has been thought to mark the cortex based on the location of the Par polarity complex.

Ectopic expression of Insc in cells that normally do not express the protein has revealed that it is sufficient to induce cell divisions oriented perpendicular to the tissue layer, reminiscent of neuroblast divisions (Kraut et al., 1996; Egger et al., 2007; Poulson and Lechler, 2010). Expression of the mammalian ortholog of Inscuteable, mInsc, in epidermal progenitors has shown that this phenotype is not completely penetrant over time (Poulson and Lechler, 2010). Expression of mInsc leads to a transient re-orientation of mitotic spindles, in which mInsc and NuMA initially co-localize at the apical cortex. After prolonged expression, however, the epidermal progenitors return to dividing along

the tissue polarity axis, a scheme in which mInsc and NuMA no longer co-localize. These results indicate that Insc and Mud can be decoupled from one another.

We have examined the effect of Insc-Pins complex formation both in an induced polarity spindle orientation assay and in *in vitro* binding assays. Our results indicate that Insc plays a more active role in spindle positioning than previously appreciated. Rather than passively coupling polarity and spindle positioning systems, Insc acts to regulate the activity of downstream Pins pathways. We have shown that the Dlg pathway is unaffected by Inscuteable expression while the Mud pathway is inhibited by Insc binding.

Recent work on the mammalian versions of these proteins explains the structural mechanism for competition between the Insc-Pins and Pins-Mud complexes (Zhu et al., 2011). The binding sites on Pins for these two proteins overlap making binding mutually exclusive because of steric considerations. The observation of Insc dissociation of the Pins-Mud complex in Drosophila (this work) and mammalian proteins (LGN-NuMA) suggests that Insc regulation of Mud-binding is a highly conserved behavior (Zhu et al., 2011).

This competition between Mud and Insc for Pins binding is consistent with previous work done with a chimeric version of Inscuteable/Pins (Yu et al., 2000). This protein, in which the Pins TPR domain was replaced with the Inscuteable Ankyrin-repeat domain, bypasses the Insc-Pins recruitment step of apical complex formation. In these cells, the chimeric Insc-Pins protein was able to rescue apical/basal polarity and spindle orientation in metaphase *pins* mutant neuroblasts. As this protein lacks the Mud-binding TPR domain, Mud binding to Pins is not absolutely necessary for spindle alignment. Importantly, the PinsLINKER domain is still intact in the Insc-Pins fusion, implying that

Dlg, not Mud, function is sufficient for partial activity, as observed in the S2 system (Johnston et al., 2007).

The Mud and Dlg pathways may play distinct roles in spindle positioning. The Dlg pathway, through the activity of the plus-end directed motor Khc73, may function to attach the cortex to the spindle through contacts with astral microtubules (Siegrist and Doe, 2005). In contrast, the Mud pathway, through the minus-end directed Dynein/Dynactin generates force to draw the centrosome towards the center of the cortical crescent (Siller and Doe, 2008). Fusion of the Pins TPR motifs, which recruit Mud, to Echinoid does not lead to spindle alignment, indicating that the Mud pathway is not sufficient for spindle alignment. The PinsLINKER domain does have partial activity on its own, however, and when placed in cis with the TPRs leads to full alignment (Johnston et al., 2007) In this framework, the function of Insc may be temporal control, ensuring that microtubule attachment by the Dlg pathway occurs before the force generation pathway is activated.

In the temporal model of Insc function, what might cause the transition from the Insc-Pins-Dlg complex, which mediates astral microtubule attachment, to the Mud-Pins-Dlg complex, which generates spindle pulling forces? By early prophase, Inscuteable recruits Pins and Gαi to the apical cortex (Siegrist and Doe, 2005). During this phase of the cell cycle, Mud is localized to the nucleus in high concentration (Du et al., 2001; Kisurina-Evgenieva et al., 2004). Apically-localized Pins binds Dlg, creating an apical target for astral microtubules (Fig. 4A). During early phases of mitosis, Inscuteable would serve to inhibit binding of low concentrations of cytoplasmic Mud to the Pins TPRs to prevent spurious activation of microtubule shortening pathways. After nuclear

envelope breakdown, Mud enters the cytoplasm in greater concentrations (Kisurina-Evgenieva et al., 2004) and could then act to compete with Insc for binding to Pins (Fig. 4B), allowing Pins output to be directed into microtubule-shortening pathways. Future work will be directed towards testing additional aspects of this model.

Figure 4. Proposed model for Inscuteable regulation of spindle orientation.

(A) In early interphase, Inscuteable recruits cortical Gαi-Pins to the apical cortex. Inscuteable (Insc)-bound Pins can scaffold for Discs Large (Dlg), allowing for early microtubule attachment, but inhibits binding of Mud, preventing ectopic microtubule shortening.
(B) After nuclear envelope breakdown and trafficking along the mitotic spindle, Mud from astral microtubules competes Pins away from Insc and allows for microtubule shortening.

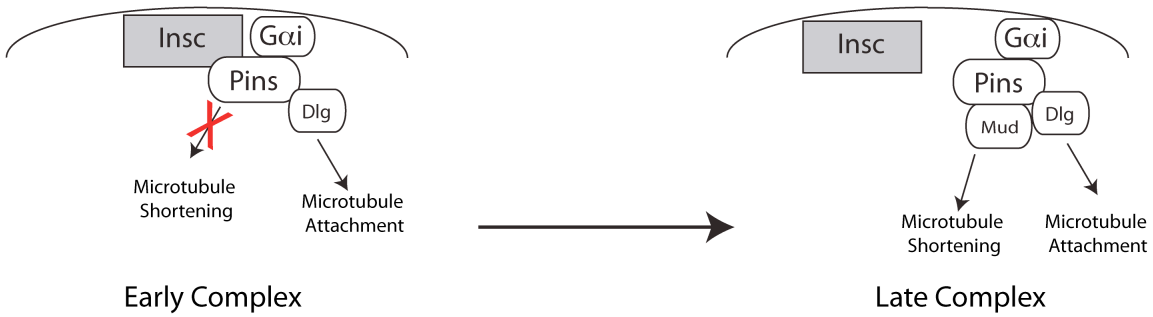

BRIDGE TO CHAPTER IV

Competition between factors for binding *in trans* to a common domain is a common mechanism by which signaling outputs may be modulated in biological systems. Inscuteable competition with Mud for binding to Pins may allow for temporal control of two parallel pathways with different biological functions. However, individual signaling components also are capable of exhibiting repression by intramolecular interaction of protein motifs *in cis* in a mechanism known as autoinhibition. This repression may be

relieved by binding of an activator to give rise to complex signaling output behavior. Pins is known to bind multiple Gai molecules, which relieves the autoinhibition between the COOH-terminal GoLoco region and the TPR domain. When this occurs, an ultrasensitive response profile is generated which can orient the mitotic spindle. The shape of this curve is very similar to systems which exhibit cooperativity. The mechanism by which cooperativity may arise in this system, however, is unclear. In the following chapter, I explain my work in generating a synthetic protein construct designed to mimic the signaling response profile of Pins by introducing the "decoy domain" mechanism of ultrasensitive activation. This contribution draws a distinction between classical cooperativity and non-cooperative mechanisms that generate similar response profiles.

CHAPTER IV

MODELING COMPLEX SPINDLE-ORIENTATION ACTIVITY USING A MODULAR SYNTHETIC PROTEIN SWITCH

This chapter contains previously published co-authored material taken with permission from:

Lu, M.S., Mauser, J. F. & Prehoda, K. E. (2011) Ultrasensitive synthetic regulatory networks using mixed decoys. ACS synthetic biology 1 (2), 65-72

Author contributions: J.F.M., M.S.L., and K.E.P. designed research; J.F.M. and M.S.L. performed research; J.F.M., M.S.L., and K.E.P. analyzed data; and M.S.L. and K.E.P. wrote the paper.

Cellular protein interaction networks exhibit sigmoidal input–output relationships with thresholds and steep responses (i.e., ultrasensitivity). Although cooperativity can be a source of ultrasensitivity, we examined whether the presence of "decoy" binding sites that are not coupled to activation could also lead to this effect. To systematically vary key parameters of the system, we designed a synthetic regulatory system consisting of an autoinhibited PDZ domain coupled to an activating SH3 domain binding site. In the absence of a decoy binding site, this system is non-ultrasensitive, as predicted by

modeling of this system. Addition of a high-affinity decoy site adds a threshold, but the response is not ultrasensitive. We found that sigmoidal activation profiles can be generated utilizing multiple decoys with mixtures of high and low affinities, where high affinity decoys act to set the threshold and low affinity decoys ensure a sigmoidal response. Placing the synthetic decoy system in a mitotic spindle orientation cell culture system thresholds this physiological activity. Thus, simple combinations of non-activating binding sites can lead to complex regulatory responses in protein interaction networks.

INTRODUCTION

Ultrasensitivity is a common property of cellular signaling systems, yet its molecular origins are poorly understood. Koshland and Goldbeter proposed the term "ultrasensitivity" to describe any system that exhibits a sigmoidal input-output relationship (Koshland et al., 1982; Ferrell, 1996; Tyson et al., 2003)(Fig. 1*A*). Sigmoidal activation profiles contain thresholds and steep activation profiles, both of which are thought to be important for biological regulatory systems (Goldbeter and Koshland, 1981). Thresholds serve to buffer input noise and offset the response to higher concentration regimes, while sharp responses lead to large output changes over a narrow range of input. These two qualities are necessary for many biological phenomena that exhibit all-or-none behavior including *Xenopus* oocyte maturation (Ferrell, 1996; Ferrell and Machleder, 1998), cell-cycle regulation (Pomerening et al., 2003), and oxygen-binding to hemoglobin (Koshland et al., 1966). While ultrasensitive responses are crucial

for the regulation of cell signaling, the molecular mechanisms responsible for translating input gradients into sharp responses are still being uncovered.

Ultrasensitive responses are generally thought to be a product of complex regulatory mechanisms such as feedback loops or cooperativity (Koshland et al., 1982; Novak and Tyson, 1993). While cooperative, multistep, and zero-order mechanisms are common sources of ultrasensitivity (Ferrell, 1996), simpler mechanisms can also generate sigmoidal response profiles. For example, the sequestration of transcriptional activators is sufficient to generate the ultrasensitive response of a synthetic genetic network (Buchler and Cross, 2009), whose ultrasensitivity is measured by the commonly used Hill coefficient (Hill, 1910). Competition effects are not limited to genetic networks, and can provide a means of ultrasensitive regulation of enzyme activity. Competition for substrate phosphorylation sites by the kinase Cdk1 has been reported as the source for the ultrasensitive inactivation of Wee1 (Kim and Ferrell, 2007).

While it has been shown that basic mechanisms such as protein sequestration and substrate competition can generate ultrasensitive profiles, they have been demonstrated in systems controlled either transcriptionally or by post-translational modifications. Transcription and post-translational modifications are common means of cellular regulation, but many cellular decisions rely on rapid simple binary protein interactions (Pawson and Nash, 2003; Staub and Rotin, 1997; Mellman and Nelson, 2008; Kholodenko, 2006). Binary protein interactions produce graded binding behaviors (hyperbolic, Michaelis-Menten-type) because they are the product of individual binding interfaces (Buchler and Louis, 2008). However, combinations of simple protein interactions can produce complex, non-linear behaviors such as ultrasensitivity through a

Figure 1. Defining ultrasensitivity, and the design and construction of the synthetic regulatory systems

(A) Ultrasensitive profiles (black) are sigmoidal in shape, exhibiting a threshold and are generally characterized by a Hill coefficient greater than one, unlike hyperbolic profiles (red). Both hyperbolic and ultrasensitive curves can behave as efficient switches (solid lines) or poor switches (dashed).

(B) Overlapping sequences allow for mutually exclusive binding of the SH3 domain or the *cis* PDZ domain to the C-terminal region of the synthetic regulatory system.

(C) Simplified graphical representation of the end states in the activation process. The PDZ domain forms an intramolecular interaction with a *cis* PDZ ligand (COOH) to produce an autoinhibited state. SH3 binding to the polyproline motif (PxxP) occludes the intramolecular interaction, exposing the PDZ domain allowing it to bind a *trans* PDZ ligand. Fluorescent dye-labeled *trans* PDZ ligand (TMR-COOH) binding can be followed by anisotropy to measure the "activated" state (activated, but SH3-unbound state is omitted for clarity, but was included in the analytical modeling in Appendix B).

(D) The synthetic regulatory system exhibits a non-ultrasensitive activation profile with a Kact of 31μM (error bars represent SEM from three independent measurements). The synthetic regulatory system is present at 50 μM; 400 μM SH3 corresponds to eight times the repressed polyproline site. The solid line represents the predicted behavior of the system based on the analytical model (see methods and Appendix B) for the system shown in the schematic using the parameters shown in Table 1. It is not the best fit to the data. All affinities used in the modeling correspond to experimentally measured affinities listed in table 1.

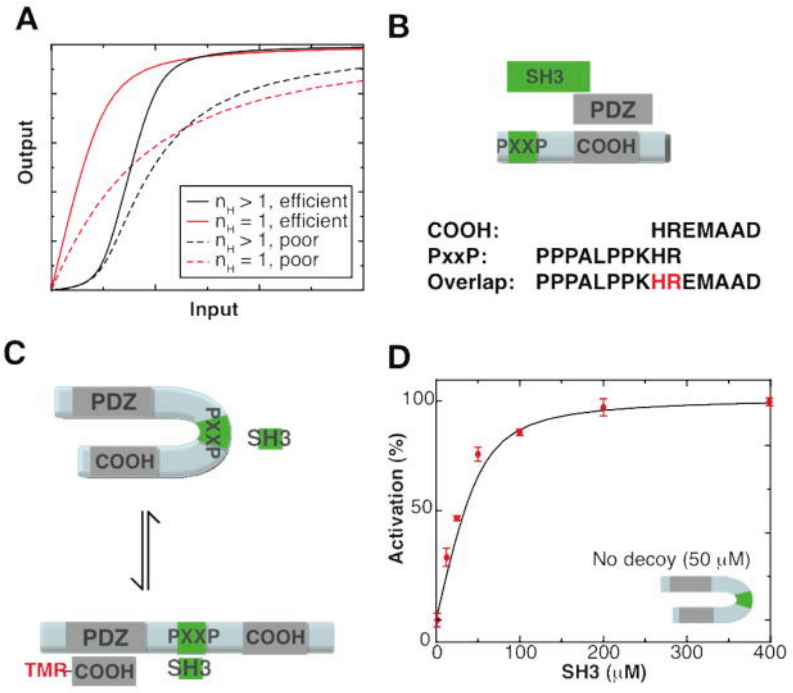

simple competition mechanism, much like that seen in the ultrasensitive inactivation of Wee1.

The MAPK and Wee1 signaling cascades utilize “decoy” phosphorylation sites to generate ultrasensitivity. Decoy phosphorylation sites are recognized by the upstream kinase but are not coupled to functional output, instead functioning to buffer the input signal to generate an ultrasensitive response. Much like decoy phosphorylation sites, protein interaction domains can also serve as sequestering agents to buffer the input signal to generate complex, non-linear responses. While mathematical modeling supports protein-protein interaction decoy-based ultrasensitivity (Buchler and Louis, 2008), the only example of a natural protein-protein interaction pathway to utilize the decoy mechanism to generate ultrasensitivity is the mitotic spindle orientation protein Partner of Inscuteable (Pins) (Smith and Prehoda, 2008). Pins contains three GoLoco motifs, one of which is coupled to activation by the heterotrimeric G-protein α subunit Gαi, while the remaining two GoLoco motifs serve as decoy binding sites for the activating Gαi molecule. The decoy sites bind and sequester Gαi from the activation site, thresholding Pins activation to generate an ultrasensitive profile that can be fit to the Hill equation. The relative affinities and the quantity of decoy domains in a system determine the degree of thresholding, and in the case of Pins, the affinities of the GoLoco domains for Gαi have been appropriately “tuned” to generate an ultrasensitive response. Thus, simple binary protein interactions can be a source of ultrasensitivity.

While Pins has supplied valuable insight into the decoy mechanism, it remains the only example, natural or otherwise, of a protein-interaction based competition mechanism capable of generating ultrasensitivity. Is it possible to construct a synthetic system to

thoroughly study the decoy mechanism? The construction of synthetic systems that exhibit complex input/output behaviors using protein modularity has been previously reported, where multiple modular domains of an engineered protein were reported to act cooperatively to generate ultrasensitive input/output control (Dueber et al., 2007). Here we generate an artificial regulatory system using simple protein interaction domains and overlapping binding sites to systematically examine how decoy domains contribute to the input threshold and ultrasensitivity of a system.

We use a synthetic regulatory pathway, along with a modeling approach, to examine whether ultrasensitivity can be generated in synthetic protein interaction networks without cooperativity. We find that the relative affinity of the decoy domains determines the overall shape of the activation profile. Although the synthetic decoy-based systems can be ultrasensitive with large apparent Hill coefficients, we find that the threshold is the most readily manipulated in this type of regulatory system. In contrast, the steepness of the input/output relationship is limited to a relatively narrow range in this type of pathway. By independently altering these two characteristics, thresholds and steepness, we evaluate their relative contribution to the Hill coefficient, which is the most commonly used measure of ultrasensitivity. Finally, we examine the effects of decoys in our synthetic regulatory pathways in a physiological context using a cell culture assay. We find that decoys can threshold biological activities, such as the spindle orientation activity of Partner of Inscuteable (Pins) in S2 cells. Together, the *in vitro* studies, analytical modeling, and *in vivo* work demonstrate that simple binary protein interactions can tune several parameters of a response.

MATERIALS AND METHODS

Protein Construction and Purification

Protein domains were expressed in the *Escherichia Coli* BL21(DE3) strain, fused to a cleaveable N-terminal 6xHis (pBH4-based vector). The fusion proteins were purified on Ni-NTA resin (Qiagen) and further purified by anion exchange FPLC.

1. SH3 (activator) and PDZ domain. The mouse *Crk* (Accession: NP_598417.2) SH3 domain (residues 134–191) was subcloned from vector A5.5a (gift from J. Dueber, UC Berkeley) into the pBH4-based vector. *D. melanogaster Par-6*(Accession: NP_573238.1) PDZ domain (residues 156–255) was subcloned by PCR into a pBH4-based vector.
2. Synthetic Regulatory Systems. The PDZ domain of *Par-6* (residues 156–255) was subcloned by PCR and modified by using 5′ and 3′ overhanging primers that introduced desired restriction sites and ligand sequences. The 3′ primer contains a polyproline sequence overlapped with a PDZ-ligand peptide, LPPPALPPKHREMAAD, fusing these overlapping ligands to the C-terminus of the PDZ domain. The 5′ primer contains sequential BamHI and XhoI restriction sites immediately before the first codon of the PDZ domain. Oligonucleotide cassettes encoding various polyproline motifs containing a 5′ BamHI overhang and a 3′ XhoI/SalI overhang and were ligated to the 5′ end of the PDZ domain. Cassettes were added sequentially in manner if desired.
3. Peptide Labeling. The peptides CGYPKHREMAVDSP and CGYPKHREMAAD (N-terminally acetylated and C-terminally amidated) were synthesized by EZ-Biolabs. Both peptides' N-terminal cysteines were conjugated to

tetramethylrhodamine-maleimide (Invitrogen) as instructed by the manufacturer. Labeled peptides were further purified by RP-HPLC, characterized by MALDI-ToF, and suspended in 0.1% Trifluoroacetic Acid.

Fluorescence Anisotropy

50, 75, or 100 μM synthetic regulatory protein was incubated with 0.5μM TMR-labeled peptide in binding buffer (20mM HEPES pH 7.5, 100mM NaCl, 1mM DTT). Increasing concentrations of SH3 domain were introduced into the reaction to a final volume of 70μl. The final reactions were incubated in a 25ºC water bath for 10 minutes. Anisotropy measurements were conducted using the ISS-PC1 spectrofluorometer equipped with polarizers, with an excitation of TMR at 555nm and emission recorded at 580nm over ten iterations (average reading taken). Background anisotropy was measured using SH3 domain alone from 0–1mM; these values served as the baseline for anisotropy background and were subtracted from experimental measurements to obtain "corrected anisotropy" values. Corrected anisotropy values were percentage normalized to the highest and lowest anisotropy values of each synthetic regulatory pathway tested. Fluorescence anisotropy was also used to measure the dissociation constants of the TMR-labeled peptides CGYPKHREMAAD and CGYPKHREMAVDSP for the PDZ domain and repressed PDZ domain. For these measurements, 0–400 μM PDZ domain or repressed PDZ domain were incubated with 0.5 μM of the labeled peptides.

Echinoid plasmid construction and Echinoid cell-adhesion assays

Synthetic regulatory systems (see Protein Construction and Purification section 2) were cloned into a pMT/V5-HisA vector (Invitrogen) containing Echinoid and GFP

upstream of the multiple cloning site (Wu, 1995). *Drosophila melanogaster Pins*(Accession: NP_524999.2) residues 1–466, with the C-terminal sequence HREMAVDCP, was cloned into pMT containing an N-terminal HA epitope tag. Mouse *Crk* SH3 residues 134–191 was cloned into pMT containing an N-terminal FLAG epitope tag.

S2 cell maintenance and cell adhesion assays have been detailed elsewhere (Wu, 1995). Briefly, S2 cells were transfected using Effectene reagent (Qiagen, Germantown, MD) with 1.5 μg total DNA for 24 hours. Subsequent protein expression was induced by the addition of 500 μM CuSO4 for 24 hours. Cell adhesion clustering was induced by shaking at 175 RPM for 2 hours.

Immunostaining, Immunofluorescence Microscopy, and Data Analysis

All synthetic regulatory constructs tested were transfected, fixed, and stained concurrently to minimize variations. Clustered cells were fixed in 4% paraformaldehyde in PBS for 20 min, washed (0.1% saponin in PBS), and incubated with primary antibodies in buffer (0.1% saponin, 1% BSA in PBS) overnight at 4ºC. Coverslips were then washed and incubated with fluorescently-linked secondary antibodies for two hours at room temperature. The coverslips were washed again and mounted onto microscope slides using Vectashield Hardset medium (Vector Laboratories, Burlingame, CA). Antibodies were used as follows: rat anti-HA (Roche; 1:1000), rat anti-α-tubulin (Abcam; 1:500), and mouse anti-FLAG (Sigma; 1:1000), Alexa Fluor 555 goat anti-rat IgG (H+L) (Invitrogen; 5 μg/mL), and DyLight 649 AffiniPure Dnk Anti-Mouse IgG (H+L) (Jackson ImmunoResearch; 7 μg/mL).

All images were collected using a Leica TCS SP2 confocal microscope with a 60X 1.4 NA immersion-oil lens using 488 Ar laser/500–530nm emission filter, 543 HeNe laser/560–620 emission filter, and 633 HeNe laser/650–750 emission filter. The refractive index of the immersion oil is 1.518. Laser power, photomultiplier tube gain, and other imaging settings were optimized to fall within the linear range of the camera and to avoid saturation. Optimized settings were held constant throughout imaging sessions. Fluorescence intensity of a single cell was analyzed using ImageJ software. The inner boundaries of 32–33 cells of each condition were marked using the freehand selection tool and the mean intensity of the marked area was recorded. Background intensity was subtracted from these values. Spindle angles were measured using the angle tool in ImageJ, measuring the spindle angle against the center of the Echinoid crescent. For spindle angle vs. intensities plots, cells were binned at 15 A.U. intensity levels.

Analytical Modeling

We modeled binding curves for the no-decoy switch, a one-decoy switch, and a three-decoy switch using constants and concentrations reported in this paper—the curves are not a best fit. All objects, terms, and equations are presented in the supplementary information. For each switch, we plotted the fraction of the switch bound fraction-bound of peptide (*fbp*) to the readout peptide [P] as a function of total activator [A]Tot. We used the general binding equation using all states and equilibria to obtain *fbp*. [A]Tot is presented as the sum of free activator [A] and the summation of all states in which the switch is bound to the activator. In this way, we were able to vary [A] to obtain a *fbp* curve as a function of [A]Tot.

RESULTS AND DISCUSSION

We used an approach combining synthetic biology and analytical modeling to comprehensively explore decoy-based ultrasensitivity. A synthetic system can be precisely controlled to minimize the number of variables being tested (Dueber et al., 2007), whereas modeling can highlight parameters important for the phenomenon being examined (Buchler and Cross, 2009; Gunawardena, 2005). To thoroughly examine decoy-based ultrasensitivity, we built a synthetic regulatory pathway composed of readily available modular domains whose properties (binding partners, affinities, etc) have been extensively characterized. The design of the synthetic regulatory pathway is modular in nature, which allowed for its easy manipulation so that we could systematically test the effects of decoys on ultrasensitivity.

In order to characterize the synthetic regulatory pathway, we developed an *in vitro* biochemical assay as well as an *in vivo* cell biological assay to test the effects of various decoys on thresholding and ultrasensitivity. The *in vitro* assay is based on fluorescence anisotropy using bacterially purified proteins and served as a quantitative method for examining decoy-based ultrasensitivity, whereas the *in vivo* studies highlight the functional consequence of decoy-based ultrasensitivity in a more physiological context. In addition to the biochemistry and cell biology, we analytically modeled the synthetic regulatory pathways, incrementally varying several parameters to fully understand the effects of decoy domains. We found that combining analytical modeling, biochemistry, and cell biology provided a comprehensive analysis of the decoy mechanism and how decoys can be tuned to generate ultrasensitivity.

To construct a system that can be manipulated *in vitro* to test the role of decoy sites in ultrasensitive activation, we designed an "autoinhibited" protein based on a PDZ protein interaction domain. We utilized autoinhibition because it's a common mechanism in signaling pathways in which intramolecular interactions regulate activity (Pufall and Graves, 2002). We also utilized PDZ domains because they and their binding partners, short C-terminal sequences (Harris and Lim, 2001), have been well characterized and are readily available. We engineered autoinhibition into the synthetic system using a sequence overlap strategy (Sallee et al., 2007), where we constructed a fusion protein containing the *Drosophila* Par-6 PDZ domain and a modified PDZ ligand sequence HREMAAD from *Drosophila* Stardust (Sdt) (Penkert et al., 2004). Between the PDZ domain and its ligand sequence, we included an overlapping proline-rich sequence PPPALPPKHR that binds the mouse Crk SH3 domain, with a dissociation constant of 1.57 μM (Posern, 1998; Wu, 1995), with the goal of disrupting the intramolecular interaction when the SH3 domain binds its target (Fig. 1B). The overlapping PDZ ligand and proline-rich sequence permits the mutually exclusive binding of either the *cis* PDZ domain or*trans* SH3 domain at this site, forming a favorable intramolecular interaction that would occlude the SH3 binding site (Fig. 1C). The PDZ domain has an approximately three-fold lower affinity for its *cis* ligand than the fluorescently labeled *trans* ligand, when measured in *trans* (table 1) so that the system can be more readily activated (effective concentration effects favor the intramolecular interaction).

Table 1. Characteristics of the Modular Domains and Their Ligands Used for the Construction of the Synthetic Regulatory Pathways

Domain	Origin and sequence	Ligand(s)	K_d(μM)	ref
PDZ	Par-6 residues 156–255	TMR-CGYPKHREMAVDSP	6	Penkert et al., 2004
		TMR-CGYPKHREMAAD	15	measured[a]
SH3	Crk residues 134–191	PPPALPPKHR	1.57	Posern, 1998; Wu, 1995
		PPALPPKK	2.1	Posern, 1998; Wu, 1995
		PPPALPPKRRR	0.1	Posern, 1998; Wu, 1995
		PPPVPPRR	10	Wu, 1995; Nguyen and Lim, 1997
-PxxP-COOH	[Par-6 156-255]-PPPALPPKHREMAAD	-CGYPKHREMAVDSP	48	measured[a]

a) Affinities measured in *trans* (see Methods).

We used the mouse Crk SH3 domain as the activator and measured output activity using the fluorescence anisotropy of a Tetramethyl rhodamine (TMR)-labeled PDZ ligand peptide. Consistent with the presence of autoinhibition in this system, the repressed PDZ domain's affinity for its *trans* ligand is approximately eight-fold lower than the free PDZ domain because of competition with the intramolecular ligand (table 1). The SH3 domain activates the system, and the affinity of the fluorescent peptide for the PDZ domain increases upon SH3 domain binding, resulting in a graded, non-ultrasensitive activation profile (Fig. 1D). We also analytically modeled this synthetic regulatory pathway (as well as the others discussed below) using the affinities shown in table 1, and found the modeling to be in excellent agreement with the experimental findings (Fig. 1D, solid line). We next examined whether simple competition could introduce elements of ultrasensitive behavior into our system by adding various SH3 ligands.

To determine the effect of decoy sites on the activation of our synthetic regulatory system, we introduced SH3 binding sites N-terminal to the PDZ domain in regions where SH3 interaction does not influence PDZ activation (Fig. 2A). We initially examined the effect of adding a single decoy site with the sequence PPPALPPKRRR at a higher intrinsic affinity (KdSH3 = 0.1 μM) than the activating SH3 binding site (when measured in isolation, KdSH3 = 1.57 μM) and found that this introduces a threshold to the graded response (Fig. 2B). The threshold corresponds to the concentration of the the synthetic regulatory pathway (and therefore the decoy) indicating that the SH3 activator binds the

Figure 2. High-affinity decoy sites threshold activity.

(A) Graphical representation of end states in the activation sequence. The high-affinity decoy (black) becomes fully saturated with the activating SH3 domain before activation.

(B) A high-affinity decoy (Kd,SH3 = 0.1 μM, black) thresholds the activation profile by the concentration of decoy in the reaction (error bars represent SEM from three independent measurements). The total concentration of the system is 100 μM, which corresponds to a total of 100 μM decoy domains (Kd,SH3 = 0.1 μM) and 100 μM repressed polyproline motifs. The solid line represents the predicted behavior of the system based on the analytical model (see Methods and Appendix B) for the system shown in the schematic using the parameters shown in Table 1. It is not the best fit to the data. All affinities used in the modeling correspond to experimentally measured affinities listed in Table 1.

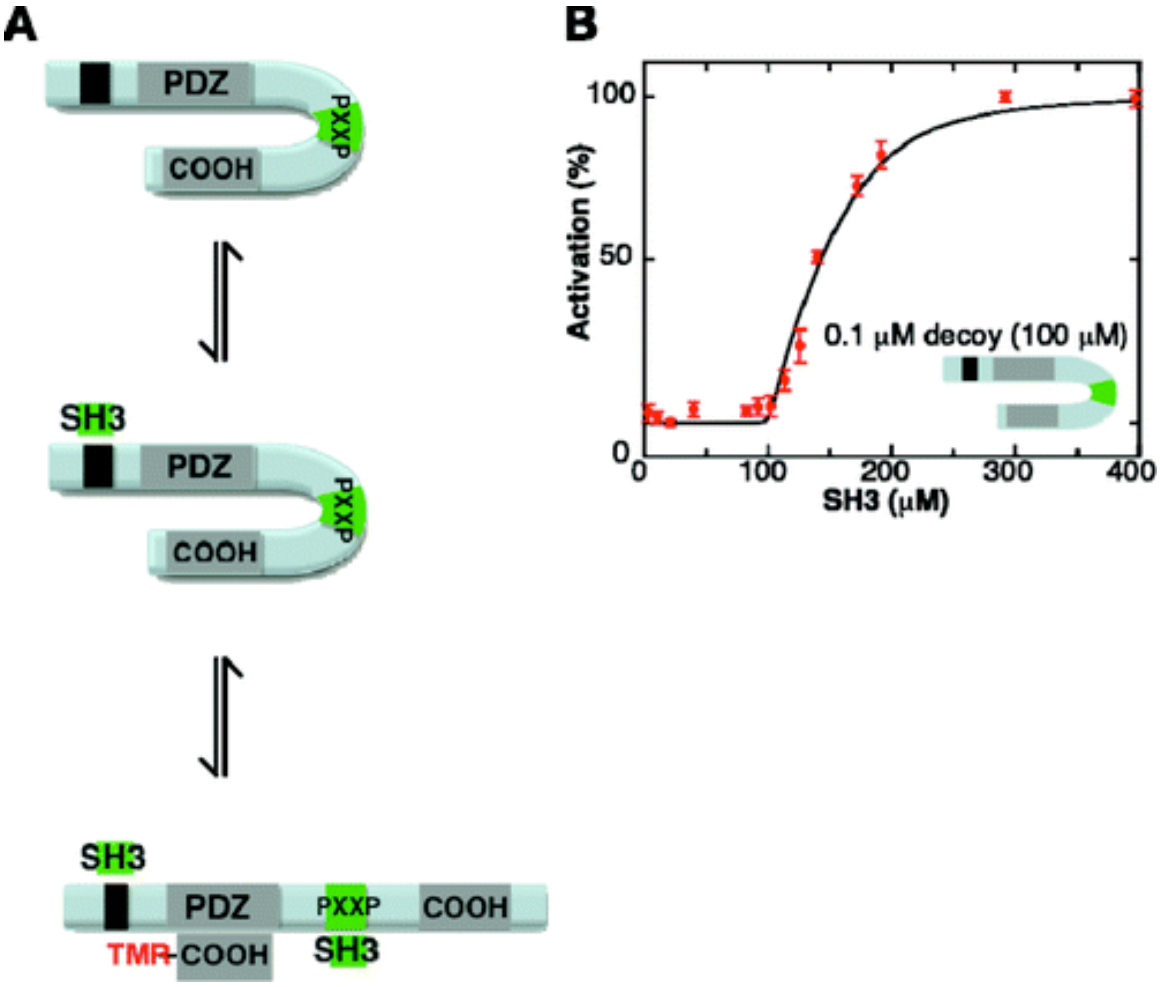

Figure 3. Tabular illustration summarizing the characteristics of synthetic regulatory pathways containing various combinations of decoy domains.

We have omitted the PDZ, COOH, and PXXP domains from the regulatory pathway depictions for clarity. The 0.1 μM affinity decoy is represented as a black square, the 2.1 μM affinity decoy as a green square, and the 10 μM affinity decoy as a red square.

Pathway	Decoys No.	Decoys K_d (μM)	K_{act} (μM)	n_H	Steepness[a] (10^{-1} % activity/SH3)	Threshold[b] [SH3] (μM)	Profile
(50 μM)	—	—	31	1	12.5	1	hyperbolic
(50 μM)	1	0.1	70	1	12.4	44	offset hyperbolic
(100 μM)	1	0.1	140	1	9	107	offset hyperbolic
(50 μM)	1	2.1	73	2.5	9.5	22	sigmoid
(50 μM)	1	10	51	1	0.4	2.5	hyperbolic
(50 μM)	2	0.1	190	1	8.3	104	offset hyperbolic
(50 μM)	2	2.1	176	3.9	5.5	55	sigmoid
(50 μM)	1 1	2.1 0.1	140	3.9	6.7	71	sigmoid
(50 μM)	1 1	2.1 10	71	2	5.3	18	sigmoid
(75 μM)	1 2	2.1 0.1	250	4.5	7.8	177	sigmoid
(50 μM)	3	2.1	122	2.8	5.3	35	sigmoid
(50 μM)	1 2	10 2.1	121	2.6	5.3	25	sigmoid
(50 μM)	1 2	0.1 2.1	202	3.7	4.8	93	sigmoid

[a] Steepness defined as slope at K_{act}
[b] Threshold defined as 10% maximal activation

decoy until it is saturated before binding the activation site. An inflection point in the response profile of this system is predicted by modeling (Appendix B) and arises because the decoy acts as a strong stoichiometric sink (Fig. 2B, solid line). Addition of another high-affinity decoy site causes the threshold to be further shifted to higher activator concentration but does not alter the overall shape of the activation profile (Fig. 3).

These results demonstrate that decoy sites can introduce thresholds, which is a hallmark feature of ultrasensitive responses. However, the profiles of the synthetic pathways containing the nanomolar high-affinity (0.1 μM) decoy are not sigmoidal and

therefore do not meet Koshland and Goldbeter's original definition of "ultrasensitive," which is still widely used today. Instead, the profile resembles an offset, graded curve that is poorly fit by the Hill equation, which serves as a common analysis method for ultrasensitivity (the use of the Hill analysis to measure ultrasensitivity is discussed below). Thus, high affinity decoys generate thresholds by shifting the start of the graded response to higher activator concentration but do not generate ultrasensitivity.

In order to generate truly sigmoidal responses, we reasoned that lower affinity (micromolar range) decoys might "blur" the transition between the threshold and activation region by allowing activation before the decoys had become fully saturated (Fig. 4A, 4B). We tested this idea by adding lower affinity (2.1 μM) decoys to the synthetic regulatory system. By lowering the affinity of the decoy site to 2.1 μM from 0.1 μM such that it approximates the affinity of the activation site (Kd SH3 = 1.57 μM), it is possible to obtain intermediate activation states where there is a mixture of decoy-bound repressed, decoy-bound activated, and decoy-unbound activated states, generating canonical ultrasensitive profiles. To determine whether a decoy site with a similar affinity as the activation site could introduce an element of ultrasensitivity, we included a decoy site whose polyproline sequence PPALPPKK (Kd SH3 = 2.1 μM) is near the affinity of the activation site PPALPPKHR (Kd SH3 = 2.1 μM)(Posern, 1998) into the synthetic regulatory system (table 1). The small disparity in affinities between these two sites for the SH3 domain allows the system to exhibit an ultrasensitive response that can be fit to an apparent Hill coefficient of 2.5 (Fig. 4C). The decoy site acts as a competitive ligand for the SH3 domain, producing an input threshold where the system is mostly in the decoy-bound state, yet allows some SH3 domain binding to the activation site. Modeling

of a single-decoy system containing a 2.1 μM decoy (see Appendix B) generates a sigmoidal input-response curve that closely matches the observed activation profiles (Fig. 4C, solid line). We conclude that tuning the affinity of decoy sites so that they are not completely saturated before the activator binds to the activating site can lead to ultrasensitivity.

Ultrasensitive responses have two key characteristics, thresholds and steepness, and we next examined how decoy-based regulatory systems can alter these parameters. For each synthetic regulatory pathway, we defined the threshold as the concentration of activator required to reach 10% output activity and steepness as the slope at the 50% activation point (Figure 5A). As shown in Figure 3, the threshold can be readily manipulated by the addition of decoys, especially with the high affinity (0.1 μM) decoys. We found that steepness, on the other hand, could not be as easily controlled. The inclusion of the lower affinity (2.1 μM) decoy site broadens the input range over which the system transitions between states, requiring more input signal than the no-decoy system to reach maximal activation (Figure 3). After testing several decoy combinations, we conclude that the threshold component of ultrasensitive profiles can be readily manipulated in decoy-based regulatory systems, but response steepness is limited to a narrow range.

In addition to steepness and threshold, we also determined each pathway's Hill coefficient as this term is popularly used to as a measure of ultrasensitivity (Koshland et al., 1982; Ferrell, 1996). The Hill coefficient was originally described as a model for cooperativity (Hill, 1910), and in addition to its use as a measure of ultrasensitivity, it is often used as a measure of activation profile steepness (Kim and Ferrell, 2007;

Figure 4. Decoys can be a source of ultrasensitivity.

(A) Graphical representation of end states in the activation sequence (decoy-unbound activated step is omitted for clarity but is included in the analytical modeling in the Appendix B). The lower-affinity decoy (green) approximates the affinity of the activation site, allowing for mixed binding states.
(B) Single-decoy modeling shows that decreasing the affinity of the decoy from nanomolar (solid line) to micromolar affinity (dashed lines) can generate sigmoidal properties.
(C) A synthetic regulatory pathway containing a decoy with similar affinity as the activation site (K_d^{SH3} = 2.1 μM, green) for the SH3 domain produces a sigmoidal activation profile and can be fit to an apparent n_H of 2.5 (error bars represent SEM from three independent measurements). The total concentration of the system is 50 μM, which corresponds to a total of 50 μM decoy domains (2.1 μM) and 50 μM repressed polyproline motifs. The solid line represents the predicted behavior of the system based on the analytical model (see Appendix B) for the system shown in the schematic using the parameters shown in Table 1. It is not the best fit to the data. All affinities used in the modeling correspond to experimentally measured affinities listed in Table 1.

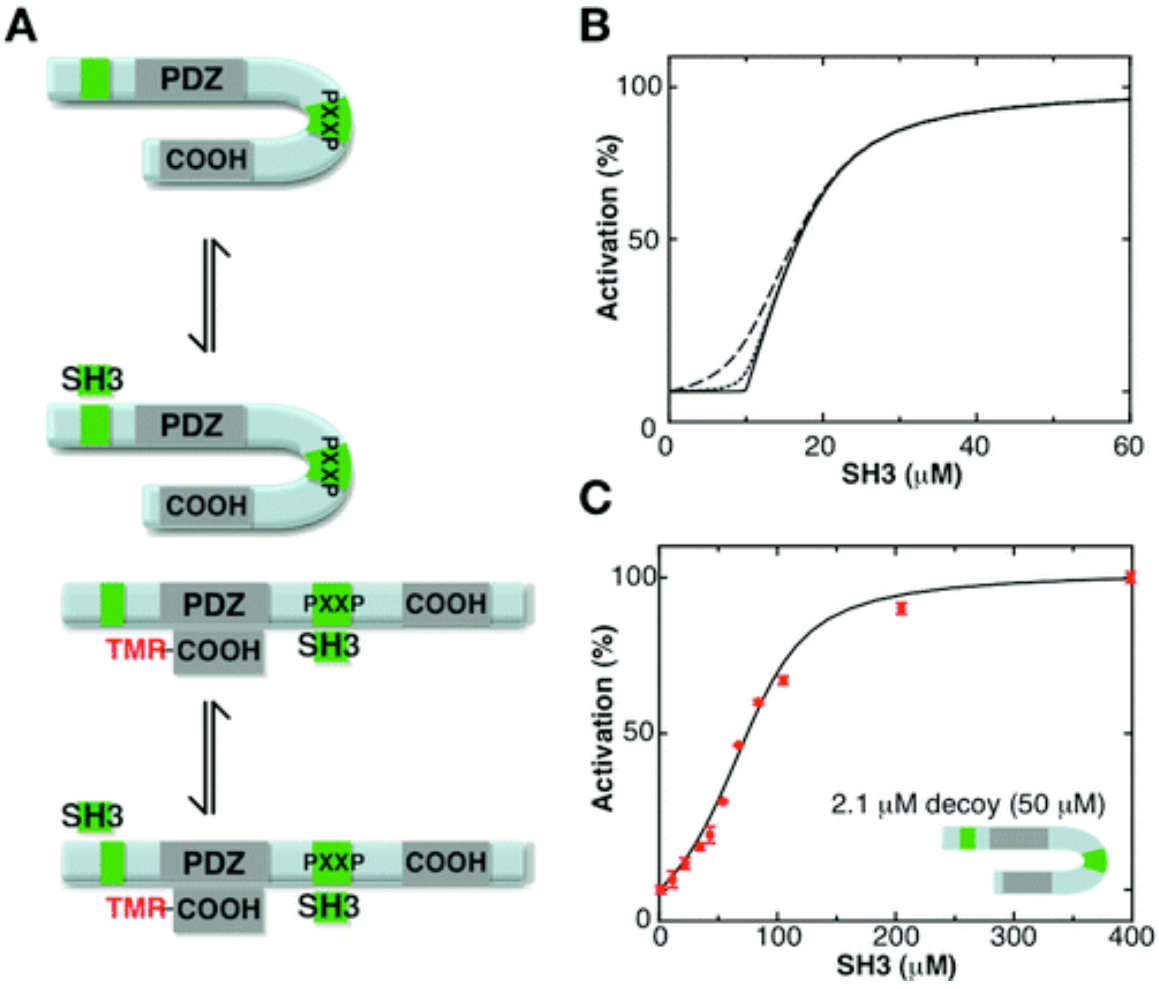

Dueber et al., 2007). Though steepness does affect the Hill coefficient, we find that increasing the threshold without increasing the steepness can also influence the magnitude of the Hill coefficient (Fig. 5B). Therefore, the Hill coefficient may not be the best term to describe how ultrasensitive a system is when other parameters, such as Kact, provide a more transparent description of an activation profile. Like the Hill coefficient, Kact is also a complex function of the threshold and steepness (Fig. 5A), and is defined as the concentration of activator required for 50% activity (Dueber et al., 2007). Combined, the Kact, slope, and threshold offer a complete description of how "ultrasensitive" an activation profile is, as opposed to the Hill coefficient, which can be misleading when thresholds are large.

We have shown that decoys can be used to tune different parameters of a response such as the sensitivity and threshold of a synthetic regulatory pathway *in vitro.* We wanted to expand the utility of the synthetic regulatory pathway into a more physiological context, so we introduced the synthetic system into the regulatory pathway that controls mitotic spindle orientation. We chose a cell culture system that uses the cell-adhesion protein Echinoid (Ed) to polarize an otherwise unpolarized S2 cell (Fig. 6A) (Johnston et al., 2009). Using this technique, it is possible to polarize any protein of interest in S2 cells, and previous work from our lab has demonstrated that Echinoid fusions of Partner of Inscuteable (Pins) robustly orients the spindle in S2 cells (Johnston et al., 2009). To explore whether Pins's spindle orientation activity can be altered by decoy-based thresholding, we fused the autoinhibited regulatory system to the cytoplasmic domain of Echinoid to induce crescents of two different synthetic regulatory

Figure 5. Tailoring response parameters with decoy combinations.

(A) Hill coefficients (n_H) are not an accurate measure of the "sensitivity" of a response. The highly thresholded, but less steep curve (red) can be fit to a n_H of 5.1, whereas the steeper but less thresholded curve (black) is fit to a lower n_H of 3.7. Measuring 10% activation (defined as threshold in this work), half-maximal activation (K_{act}), and slope at the steepest part of the curve (dashed line) can clarify ultrasensitive profiles.

(B) A synthetic regulatory system containing two 0.1 μM K_d (black) and one 2.1 μM K_d(green) decoy can threshold a sigmoidal activation profile, generating an apparent n_H of 4.5 (note *x*-axis scale, error bars represent SEM from three independent measurements). The total concentration of the system is 75 μM, which corresponds to a total of 150 μM high affinity decoy domains (K_d^{SH3} = 0.1 μM, black), 75 μM lower-affinity decoy domains (K_d^{SH3} = 2.1 μM, green), and 75 μM repressed polyproline motifs. The solid line represents the predicted behavior of the system based on the analytical model (see Appendix B) for the system shown in the schematic using the parameters shown in Table 1. It is not the best fit to the data. All affinities used in the modeling correspond to experimentally measured affinities listed in Table 1

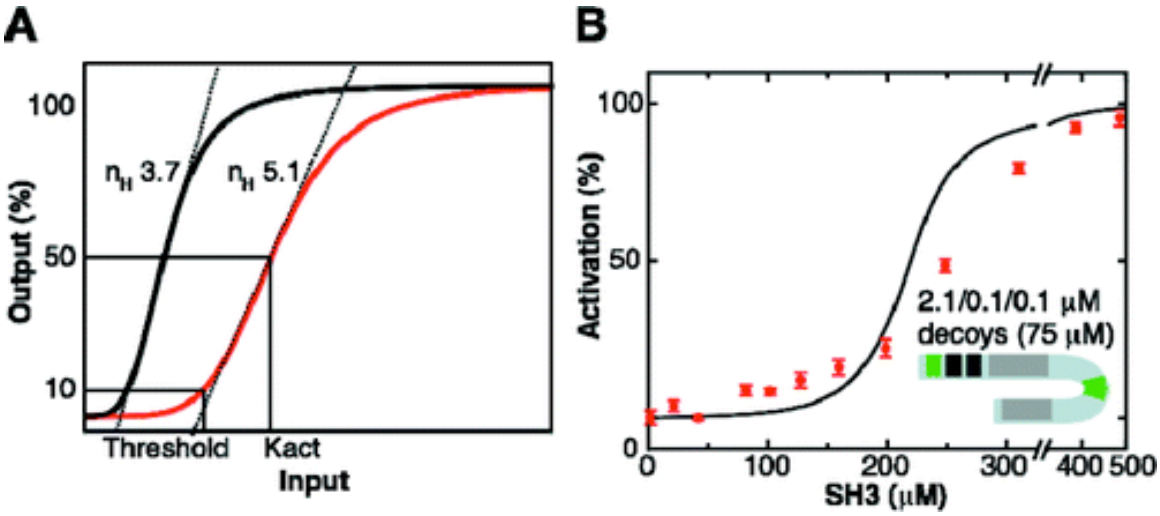

pathways (Fig. 6B). We fused the PDZ ligand HREMAVDCP to the C-terminus of soluble Pins, and also introduced soluble SH3 as the activator, with the goal of coupling the activation of the regulatory pathway to the spindle orienting activity of Pins (Fig. 6B). In this cell culture system, the activation of the regulatory pathway manifests as spindle orientation, which can be plotted as a function of the relative SH3 domain expression level in a given cell.

To determine whether the synthetic regulatory pathway transitions well into the *in vivo* system, we examined the spindle orienting activity of the no-decoy regulatory pathway. Cells expressing relatively low levels of SH3 domain display a broad range of the spindle orientations, suggesting that Pins is not recruited to the induced regulatory pathway crescents (Fig. 6C, black circles). However, cells that express higher levels of SH3 domain are restricted to aligned spindle orientation angles, indicating that the regulatory pathway is activated, thereby recruiting Pins to the induced crescents where it functions to orient the spindle. These results demonstrate that the synthetic regulatory pathway can be coupled to spindle orientation.

To examine the effect of decoys in this system, we tested the spindle orienting activity of a high-affinity 0.1μM decoy regulatory pathway. Like the no-decoy system, the high-affinity decoy system displays a range of broad spindle orientation angles at low SH3 domain expression levels, however, the random spindle angles persist to higher levels of SH3 domain, indicating that spindle orientation activity is thresholded (Fig. 6C, red squares). The high-affinity decoy system finally reaches maximal activation at high SH3 domain expression levels, at about twice the SH3 domain expression level as the no-decoy system. While the thresholding cannot be precisely controlled, as expression levels of all three components are difficult to manipulate, the decoys nevertheless offer some amount of thresholding. Thus, decoy sites can threshold biological activities at the post-translational level through simple binary interactions, and this synthetic regulatory pathway could be adopted for other biological applications.

We have described a strategy to generate ultrasensitivity in a synthetic system utilizing binary protein interactions, where a simple competition mechanism is sufficient

to create a sigmoid response curve. We showed that a decoy site, a peripheral domain of the autoinhibited PDZ domain that can bind to the activator, competes with the activation site for the input generating a stoichiometric threshold. Decoy sites with a high affinity for the input generate a threshold that reflects the concentration of the decoy in the system, while still retaining the hyperbolic response of a decoyless system, (i.e. the response is an input-offset hyperbola). When the affinity of the decoy is decreased to approximate the affinity of the activation site for the activator, the system is ultrasensitive and its output follows a sigmoidal path that can be fit to the Hill equation. Finally, because of the modular nature of the synthetic system, we can design systems with desired thresholds and switching efficiencies.

Though the decoy mechanism introduces elements of ultrasensitivity to the system such as thresholds and sigmoidal response curves, it should be noted that the response does not become more steep or switch-like. Despite generating large Hill coefficients, the addition of a competitive decoy reduces the activation slope by a quarter, broadening the range over which the system switches from the inactive to active state increasing the overall Kact of the system. The large apparent Hill coefficients are the result of limitations in describing the two key components of ultrasensitivity, thresholds and steepness. A similar observation was reported in the case of multisite phosphorylation, where multiple phosphorylation sites that act as stoichiometric inhibitors of a kinase introduce a threshold while making the response more graded after the threshold is achieved (Gunawardena, 2005).

Figure 6 (next page). Decoys can threshold spindle orientation activity of Pins.

(A) Induced polarity spindle orientation assay. S2 cells adhere through the homophilic, intercellular membrane-associated Echinoid protein (Ed), which redistributes on the cortex to points of cell–cell contact, inducing polarity of the Ed:Regulatory Pathway (shown in green using intrinsic GFP fluorescence). The orientation of the spindle (shown in red with anti-α-tubulin stain) is measured (white dashed line) with respect to the center of the Ed:Regulatory Pathway crescent (white arrowhead). Flag-SH3 expression levels (shown in blue with antiflag antibody, merged with red and green) were determined by measuring the fluorescence intensity of each cell using ImageJ software (see Methods). HA-Pins expression was confirmed by anti-HA antibody stain in red.

(B) Regulatory pathways fused to Ed are co-expressed with soluble Pins containing a C-terminal PDZ ligand and soluble SH3 domain in S2 cells. Induced regulatory pathway crescents can be activated by the soluble SH3 molecules, leading to the recruitment of soluble Pins by its C-terminal PDZ ligand fusion. Induced Pins crescents are sufficient to robustly orient the mitotic spindle coupling the activation of the regulatory pathway to spindle orientation.

(C) Measurements of the binned intensities (A.U.; intensity corresponds to relative SH3 intracellular concentration) versus spindle orientation angle (deg) of 32 cells expressing the Ed:Regulatory pathway (black, filled circles) and 33 cells expressing the Ed:Regulatory pathway with high-affinity decoy (red, filled squares). Cells were binned at 15 A.U. intensities. Lower spindle angle values represent an aligned phenotype.

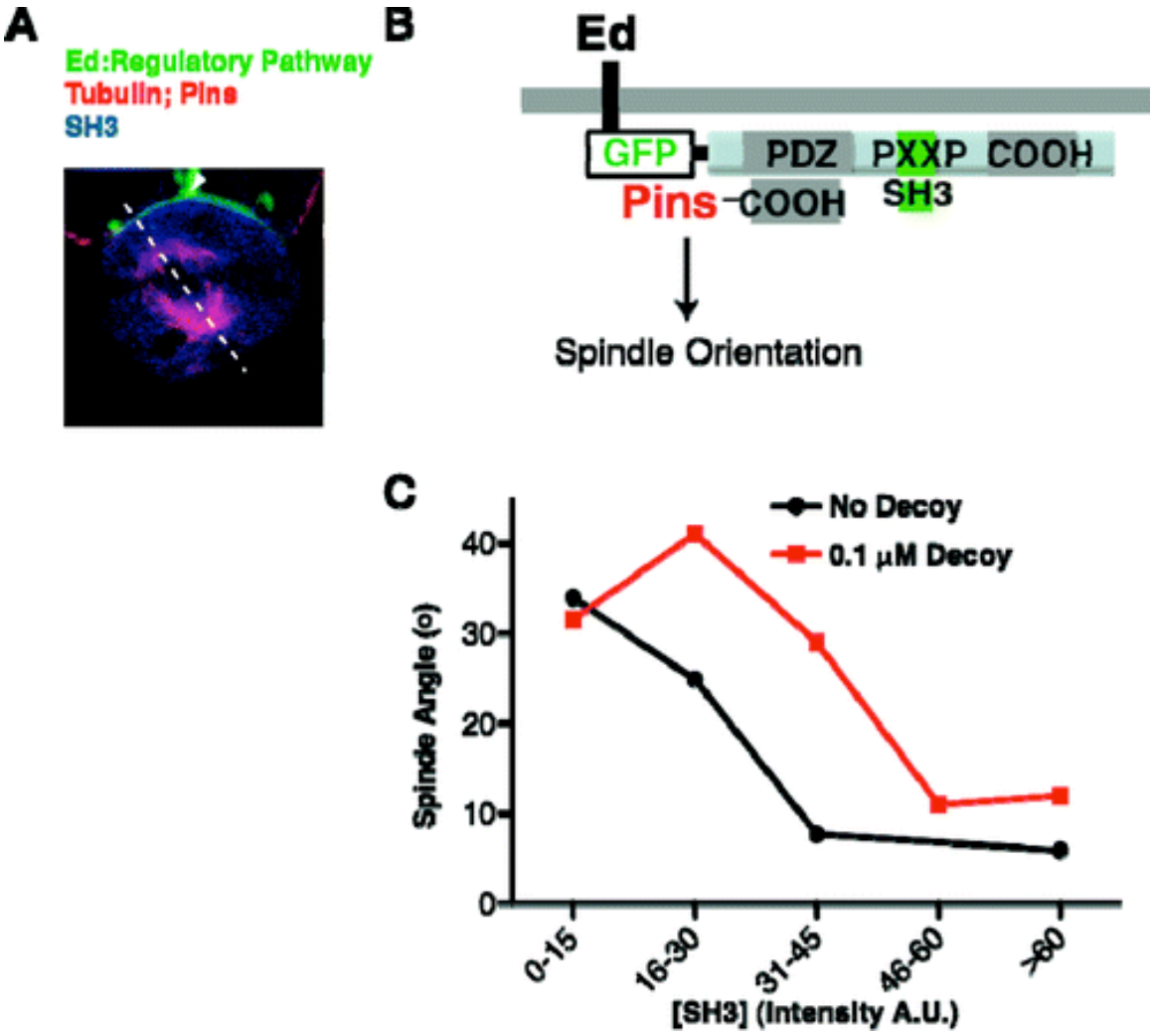

The addition of a high affinity decoy, on the other hand, does not negatively affect the steepness, but merely introduces a stoichiometric threshold while retaining the original switch-like transition of the system, which is ultimately determined by the isomerization constant. The response profile could be easily modulated with the addition or removal of these high-affinity decoy domains to achieve a desired input concentration at which the system will abruptly switch from the inactive to active state. This mechanism is also attractive because the modular nature of the decoy system allows the incorporation or removal of domain repeats through genetic recombination events in

natural systems. We showed that the synthetic regulatory pathway generated in this study can be adopted in a physiological context, and may be useful for other synthetic biologists.

BRIDGE TO CHAPTER V

In the preceding chapter, I detailed the construction of a synthetic protein that is able to mimic the behavior of Pins without the involvement of cooperativity. This model indicates that while two signaling responses may have a similar shape and output behavior, they may arise by different mechanisms. In the following chapter, I will summarize the contributions made in this dissertation and discuss how these results increase our understanding of regulatory mechanisms that control cell polarity and spindle orientation. I also discuss future studies that could arise from the questions these results raise.

CHAPTER V

SUMMARY AND FUTURE CONSIDERATIONS

Summary

My thesis work focused on identifying regulatory mechanisms controlling the establishment of cell polarity and the orientation of the mitotic spindle in the *Drosophila* neuroblast. These regulatory mechanisms include phosphorylation control of cell-cell interactions as well as intermolecular and intramolecular competition between effector proteins for a common binding site. I focused on the protein Inscuteable, a key player in both polarity and spindle orientation in the *Drosophila* neuroblast. Inscuteable was previously thought to serve as a passive physical bridge between the processes of cell polarity and spindle orientation by physically binding members of both the polarity and spindle orientation complexes. Connecting the pathways allows for high fidelity alignment of the apical-basal polarity axis and allows for cell-type differentiation in the nervous system.

Contrary to the passive bridge model, I found that Inscuteable exhibits robust regulation of its interactions with both Par-3 and Pins that may have important biological ramifications in neuroblasts. Unlike the polarity machinery, which is cytoplasmic during interphase, Inscuteable is apically polarized throughout the cell cycle and serves to mark the apical cortex for the polarity machinery at the onset of cell division. The Inscuteable-

Bazooka complex can be disrupted by the activity of the mitotic kinase Aurora A phosphorylation of Bazooka at S239, facilitating depolarization at the end of mitosis. The control of the Insc-Baz interaction ensures that polarity and spindle orientation attain their stereotyped directionality over the course of multiple divisions and that neural tracts are generated towards the interior of the brain.

Inscuteable also exhibits strong competition with the spindle orientation effector Mud for binding to Pins. This competition likely establishes two phases of spindle orientation in the neuroblast. When Inscuteable is bound to Pins, spindle-shortening pathways are repressed while spindle targeting and attachment pathways remain active. When Mud is bound to Pins, Inscuteable is released from Pins and the spindle can shorten and align. Allowing targeting and attachment of the mitotic spindle prior to shortening likely contributes to the fidelity of spindle orientation. This competition may grant temporal control to the system by allowing the complex to switch between Insc- and Mud-bound states as a function of the assembly of the spindle. This Insc-bound complex may contribute to the anchoring and alignment of the G2 apical centrosome during interphase (Siegrist and Doe, 2006).

Aside from competition-mediated regulation, Pins exhibits an intrinsic regulation mode. To explain the mechanism of the regulated spindle orientation mediated by Pins, we built a model of the spindle-orienting system from modular components to generate a regulated synthetic construct. This switch can mimic the spindle orientation behavior of Pins without invoking cooperativity. Even though the response profile of Pins resembles classical cooperative systems, it has been unclear how the thermodynamic contributions of cooperativity may act in this system. Pins may work by utilizing a simple “decoy

domain" mechanism, which prevents early activation by adding high-affinity sites for activator binding. Addition of these sites prevents activation by signaling noise and by chance encounters between activator and effector. This mechanism works by drawing activator molecules away from the activating site until activator concentration reaches a certain level (Smith and Prehoda, 2010). These regulatory mechanisms, when combined, contribute to high levels of temporal and spatial control of polarity and spindle orientation in the *Drosophila* neuroblast.

Future Considerations

The findings in chapter II detail a model where Inscuteable acts as a permanently localized cue for Bazooka enrichment. Formation of the Insc-Baz complex is directly regulated by the cell cycle machinery and allows for polarity crescents to form specifically during mitosis. Inscuteable also retains polarized localization over the course of multiple divisions, while Bazooka is repeatedly depolarized and repolarized from the cytoplasm to the apical cortex. This phenomenon may help to explain the stereotyped division axis observed in dividing neuroblasts (Siegrist and Doe, 2006).

Inscuteable exhibits polarized localization throughout the cell cycle, yet it is unclear what factors promote this continuous localization behavior. Inscuteable lacks any clear membrane-binding domains, and therefore it is likely that this behavior may be due to protein-protein interactions. Only two direct binding partners are known for Inscuteable: Pins and Bazooka. Given that Bazooka is not localized during interphase, Pins seems to be an obvious candidate to explain this behavior. Observations from previous studies support this prediction. Pins is known to be required for Insc localization

to the cortex after delamination (Schaefer et al., 2000). Gai likewise is known to be required for Pins cortical localization. These data suggest a model by which Gai at the apical cortex is activated to recruit constitutively bound Pins and Inscuteable. Therefore, the site of activated Gai may ultimately set the mark for Inscuteable localization. This prediction is supported by Inscuteable misexpression in the pI SOP cell. Inscuteable in this cell is recruited to Pins at the anterior cortex and brings Bazooka to this cortex as well. Thus, Gai/Pins/Insc may be upstream of Bazooka in other model systems as well.

Continuous polarity behaviors as observed for Inscuteable tend to result from extracellular signaling gradients that induce the polarity machinery to localize asymmetrically, as in epithelial layers. Asymmetric Gai activation in neuroblasts may likewise be the result of tissue-derived signaling gradients from outside of the neuroblast. Extrinsic cues are known to be required for the directionality of neuroblast divisions (Siegrist and Doe, 2006; Broadus and Doe, 1997). Dissociated clusters of neuroblasts ehxibit sequential divisions over a small region of the cell membrane. Once isolated, neuroblasts exhibit a randomized axis of division.

G-protein coupled receptor (GPCR) signaling has recently been implicated in establishing asymmetric localization of Pins in induced polarity S2 cells (Yoshiura et al., 2012). The GPCR Tre1 was shown to be important in maintaining the axis of neuroblast division during development and to be able to asymmetrically localize Pins in a Ga-specific manner. This leads to a potential model where a signaling gradient of GPCR ligands is able to cause asymmetric localization of Gai along the signaling axis and thus polarizes Pins/Inscuteable.

However, the presence of Tre1 in neural lineages has not been detected, nor has asymmetric localization of Pins and Gai during interphase been described previously. Other GPCRs may also serve redundant roles in activating Gai in neural lineages. Determining the pathway upstream of Insc interphase localization is likely to more thoroughly explain the directionality of neuroblast division and the role of cross-membrane signal transduction and translation of extracellular signals into intracellular phenotypes. A similar immunofluorescence study as was detailed in Chapter II examining Pins, Gai, Tre1, and Insc localization behavior may be able to verify or exclude this model for interphase Inscuteable polarization.

Another important and outstanding question in cell polarity are the biological ramifications of dynamic cell cycle controlled polarity. Yeast and *C. elegans* model systems exhibit cell cycle control of polarity by different mechanisms. In the *C. elegans* zygote, the cell cycle and polarity mechanisms are triggered by inheritance of activators during fertilization. Yeast use the cell cycle machinery to give rise to short bursts of polarity during the cell cycle as a means of accomplishing cell division by targeting bud growth to specific regions of the cell membrane. Other model systems, such as the *Drosophila* follicular epithelium, exhibit long lasting polarity in response to intercellular signaling gradients. Why the neuroblast stem cell utilizes the cell cycle machinery to exhibit dynamic Par complex polarity, while cells nearby exhibit consistent polarity remains unknown.

Localizing an active Par complex during interphase may lead to broad regions of polarity, similar to that observed in the *Drosophila* oocyte, which is polarized by the nurse cells around it. In stem cell lineages such as SOP cells and neuroblasts, tightly

compacted regions of polarity proteins are likely to be required, especially given the small size of the basal daughter cell (Cabernard et al, 2010; Connell and Prehoda, 2011). Par complex components are also known to be involved in the development of cell membrane processes and in cell motility. Preventing membrane localization of the polarity machinery may also assist in deactivating unneeded cellular functions, such as cytoskeletal growth, that involve activation by the Par complex.

The data in chapter III present a role for Inscuteable in controlling Pins-mediated spindle orientation. Inscuteable/Mud competition adds an additional level of regulation over the triggering of spindle shortening. Inscuteable binds to Pins regardless of numbers of Gai bound while Mud requires Gai activation. Even when autoinhibition is relieved, Mud must outcompete Inscuteable for binding. This may lead to the timing of spindle orientation to a point in the cell cycle where Mud is high enough in concentration to displace Inscuteable at the cortex.

A strong prediction of this model is that Pins begins the cell cycle bound to Inscuteable and ends the cell cycle bound to Mud. The switch presumably occurs by the time the spindle is fully oriented during metaphase. Now that the spindle apparatus is decoupled from polarity, it is unclear what is preventing spindle rotation due to loss of Pins enrichment. Inscuteable binding of Pins may be dispensible once the spindle is formed. Physical connections between astral microtubules and Pins-Mud-Gai complexes may prevent lateral diffusion of the polarized domain. Alternatively, like the proposed model for polarizing Inscuteable, GPCR response

To test the ramifications of the switching between Insc- and Mud- bound complexes, a hybrid Pins molecule could be generated with two sets of TPR repeats, one

of which is repressed by the GoLoco domains. Point mutants could be introduced to the TPR domains such that each only allows Mud or Inscuteable binding, thus preventing competition. Defects in asymmetric cell division would indicate that this switch between complexes has important biological relevance.

The material presented in Chapter IV truly tests our understanding both of cell signaling in general as well as the mechanisms by which Pins orients the spindle in the absence of Insc/Mud competition in specific. Ultrasensitive Pins activation has been shown to be important for high-fidelity spindle orientation (Smith and Prehoda, 2011). Our synthetic model system demonstrates that ultrasensitivity can be generated in a noncooperative manner. Evolutionarily speaking, adding and modifying decoy domains is theoretically simpler than evolving thermodynamic coupling between subsequent binding events. While cooperativity may arise in a decoy-domain system, decoy domains themselves are capable, if properly tuned, of generating similar response profiles as cooperative systems. Decoy mechanisms may be common in switch-like proteins such as Pins and LGN and perhaps in other proteins containing tandem domain repeats. To further prove the decoy-domain hypothesis of Pins, a fully synthetic signaling pathway with the decoy-domain containing switch could be engineered and tested for spindle orientation rescue in mutant flies, as was done in polarized S2 cells. Reconstituting pathway output would be a remarkably strong proof of principle that decoy-domain mechanisms have the potential to be functionally relevant in extant organisms.

Concluding Remarks

My thesis research has shed light on the mechanisms that control neuroblast polarity and spindle orientation using the regulated scaffolding protein Inscuteable. Contrary to a previous model, where Inscuteable serves as a passive link between spindle-orientation and polarity complexes, Inscuteable exhibits highly regulated interactions with both polarity and spindle orientation components and uses these regulations to grant temporal and spatial control of polarity and spindle orientation. Additionally, from our synthetic switch work, we understand more about how spindle orientation response profiles may be shaped by evolution to give a desired output. These mechanisms together cooperate to give rise to the high-fidelity phenotypes we observe during neuroblast asymmetric cell division.

APPENDIX A

SUPPLEMENTAL FIGURES FOR CHAPTER II

Figure S1. Inscuteable and Bazooka repeatedly localize to equivalent positions on the membrane over the course of sequential divisions.

(A) Neuroblast-specific expression of GFP-Bazooka reveals polarization dynamics during cell division. Bazooka localizes to the membrane before nuclear envelope breakdown (NEBD) and disappears from the membrane after telophase. Subsequent divisions establish polarity at similar membrane positions.

(B) Neuroblast-specific expression of GFP-Inscuteable reveals that Inscuteable exhibits constant membrane association, which becomes increasingly polarized between cell divisions. Regions of strong localization are formed at similar regions of the cell membrane over subsequent divisions.

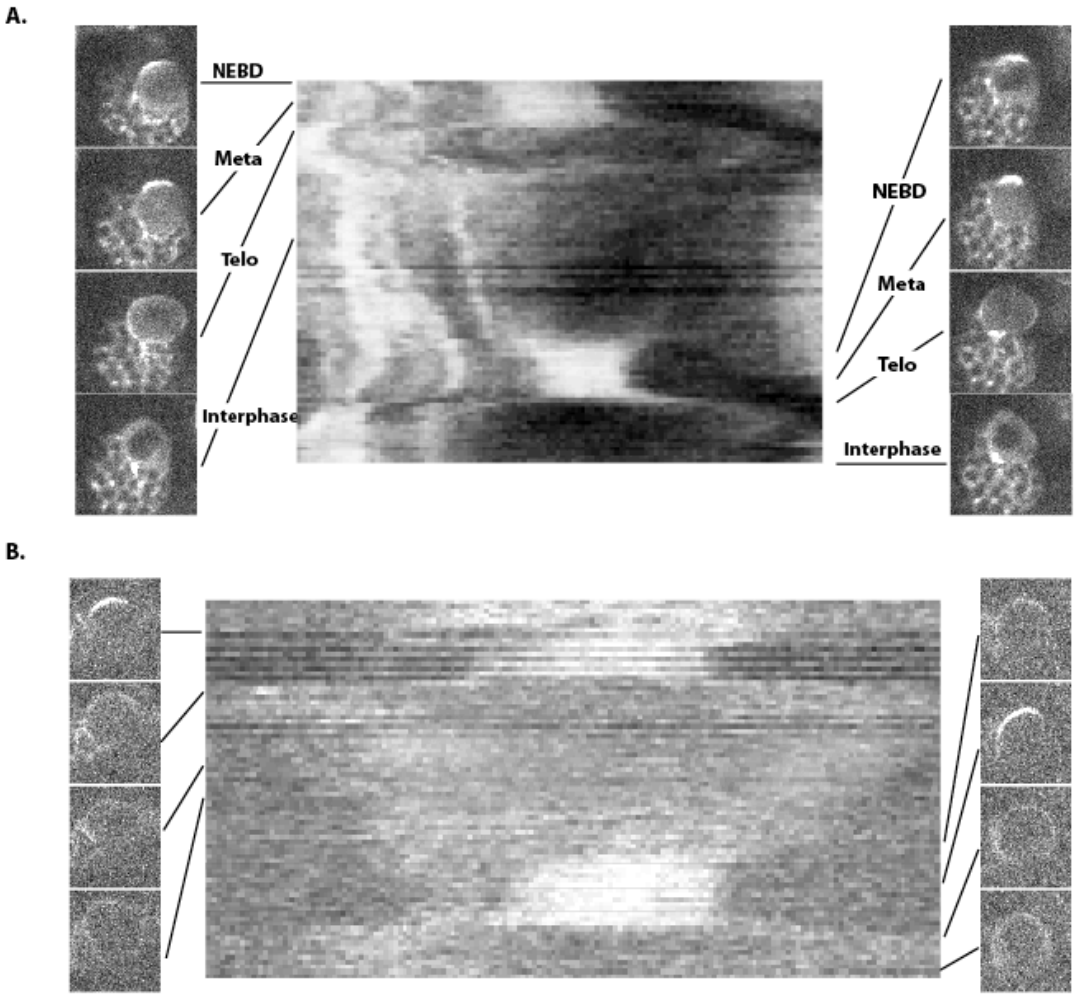

Figure S2. Treatment of neuroblasts with Latrunculin B results in failure to form compact apical crescents.

(A) Neuroblast-specific expression of GFP-Inscuteable results in compact cortical crescents by metaphase.
(B) Addition of Latrunculin B to GFP-Inscuteable expressing neuroblasts during prophase results in a broader and weaker apical crescent of Inscuteable.
(C) Neuroblast-specific expression of GFP-Bazooka results in compact cortical crescents by metaphase.
(D) Addition of Latrunculin B to GFP-Bazooka expressing neuroblasts during prophase results in a broader and weaker apical crescent of Bazooka.

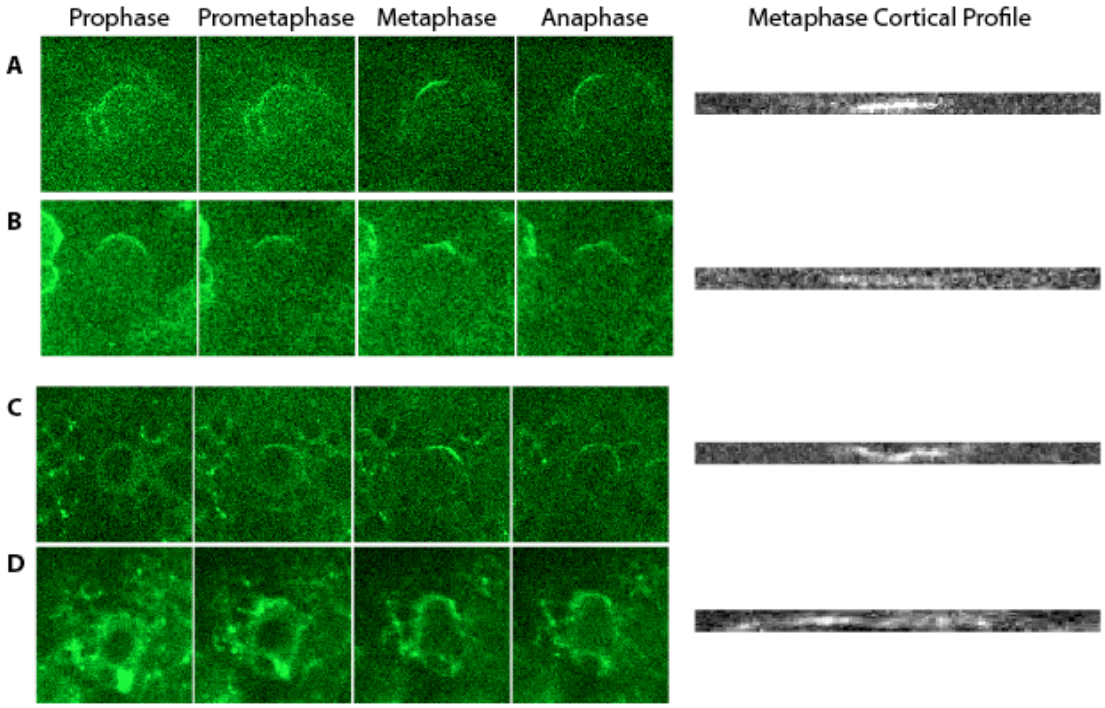

APPENDIX B

SUPPLEMENTAL METHOD FOR CHAPTER IV

SUPPORTING INFORMATION

Modeling of Zero-, One-, and Three-Decoy Systems

Zero-decoy system:

Notation

Objects:

A Activator

R Decoy-containing auto-inhibited synthetic construct

P Readout peptide

Terms:

KdP Equilibrium constant for free peptide-repressed PDZ ligand site. Measured in isolation (this study)

KdAS Equilibrium constant for Activator-activation site. Measured in isolation (this study; Harris and Lim, 2001; Sallee et al., 2007)

c Cooperativity effect.

Obtain activation curves by plotting total activator concentration against fraction bound:

fbAS fraction R bound to A at activation site

fbPo fraction R bound to readout peptide in absence of A

$$f_{b}AS = (1 - f_{b}P_{o})\left(\frac{[A]}{K_{d}AS + [A]}\right) + \left(\frac{f_{b}P_{o}[A]}{[A] + \frac{K_{d}AS}{c}}\right)$$

$$f_{b}P_{o} = \left(\frac{1}{2[R]_{tot}}\right)\left(K_{d}P + [R]_{tot} + [P]_{tot} - \sqrt{\left(-K_{d}P - [P]_{tot} - [R]_{tot}\right)^{2} - 4[P]_{tot}[R]_{tot}}\right)$$

$$f_{b}P = (1 - f_{b}AS)\left(\frac{[P]_{tot}}{[P]_{tot} + K_{d}P}\right) + f_{b}AS\left(\frac{[P]_{tot}}{[P]_{tot} + \frac{K_{d}P}{c}}\right)$$

$$[A]_{tot} = [A] + [R]_{tot}\left(f_{b}AS(1 - f_{b}P) + f_{b}ASf_{b}P\right)$$

One-Decoy System:

Notation

Objects:

A Activator

R Decoy-containing auto-inhibited synthetic construct

P Readout peptide

Terms:

KdAD Equilibrium constant for Activator-Decoy site. Measured in isolation (Harris and Lim, 2001; Sallee et al., 2007; Penkert et al., 2004).

KdP Equilibrium constant for free peptide-repressed PDZ ligand site. Measured in isolation (this study).

KdAS Equilibrium constant for Activator-activation site. Measured in isolation (this Study; Harris and Lim, 2001; Sallee et al., 2007)

c Cooperativity effect.

Obtain activation curves by plotting total activator concentration against fraction bound:

fbAS fraction R bound to A at activation site

fbAD fraction R bound to A at decoy site

fbPo fraction R bound to readout peptide in absence of A

fbP fraction R bound to readout peptide

$$f_bAS = (1 - f_bP_o)\left(\frac{[A]}{K_dAS + [A]}\right) + \left(\frac{f_bP_o[A]}{[A] + \frac{K_dAS}{c}}\right)$$

$$f_bAD = \frac{[A]}{K_dAD + [A]}$$

$$f_bP_o = \left(\frac{1}{2[R]_{tot}}\right)\left(K_dP + [R]_{tot} + [P]_{tot} - \sqrt{(-K_dP - [P]_{tot} - [R]_{tot})^2 - 4[P]_{tot}[R]_{tot}}\right)$$

$$f_bP = (1 - f_bAS)\left(\frac{[P]_{tot}}{[P]_{tot} + K_dP}\right) + f_bAS\left(\frac{[P]_{tot}}{[P]_{tot} + \frac{K_dP}{c}}\right)$$

$$[A]_{tot} = [A] + [R]_{tot}\begin{pmatrix} f_bAD(1 - f_bAS)(1 - f_bP) + (1 - f_bAD)f_bAS(1 - f_bP) \\ +2f_bADf_bAS(1 - f_bP) + f_bAD(1 - f_bAS)f_bP \\ +(1 - f_bAD)(f_bAS)(f_bP) + 2f_bADf_bASf_bP \end{pmatrix}$$

Three-Decoy System:

Objects:

A Activator

R Decoy-containing auto-inhibited synthetic construct

P Free peptide

Terms:

KdAD1 Equilibrium constant for Activator-Decoy site 1. Measured in isolation (Harris and Lim, 2001; Sallee et al., 2007; Penkert et al., 2004).

KdAD2 Equilibrium constant for Activator-Decoy site 2. Measured in isolation (Harris and Lim, 2001; Sallee et al., 2007; Penkert et al., 2004).

KdAD3 Equilibrium constant for Activator-Decoy site 3. Measured in isolation (Harris and Lim, 2001; Sallee et al., 2007; Penkert et al., 2004).

KdP Equilibrium constant for free peptide-repressed PDZ ligand site. Measured in isolation (this study).

KdAS Equilibrium constant for Activator-activation site.

c Cooperativity effect.

Obtain activation curves by plotting total activator concentration against fraction bound:

fbAS fraction R bound to A at activation site

fbAD1 fraction R bound to A at decoy site 1

fbAD2 fraction R bound to A at decoy site 2

fbAD3 fraction R bound to A at decoy site 3

fbPo fraction R bound to readout peptide in absence of A

fbP fraction R bound to readout peptide

$$f_bAS = (1 - f_bP_o)\left(\frac{[A]}{K_dAS + [A]}\right) + \left(\frac{f_bP_o[A]}{[A] + \frac{K_dAS}{c}}\right)$$

$$f_bAD_1 = \frac{[A]}{K_dAD_1 + [A]}$$

$$f_bAD_2 = \frac{[A]}{K_dAD_2 + [A]}$$

$$f_bAD_2 = \frac{[A]}{K_dAD_2 + [A]}$$

$$f_bP_o = \left(\frac{1}{2[R]_{tot}}\right)\left(K_dP + [R]_{tot} + [P]_{tot} - \sqrt{(-K_dP - [P]_{tot} - [R]_{tot})^2 - 4[P]_{tot}[R]_{tot}}\right)$$

$$f_bP = (1 - f_bAS)\left(\frac{[P]_{tot}}{[P]_{tot} + K_dP}\right) + f_bAS\left(\frac{[P]_{tot}}{[P]_{tot} + \frac{K_dP}{c}}\right)$$

$$[A]_{tot} = [A] + [R]_{tot}\begin{pmatrix}
(f_bAD_1)(1 - f_bAD_2)(1 - f_bAD_3)(1 - f_bAS)(1 - f_bP) + (1 - f_bAD_1)(f_bAD_2)(1 - f_bAD_3)(1 - f_bAS)(1 - f_bP) \\
+(1 - f_bAD_1)(1 - f_bAD_2)(f_bAD_3)(1 - f_bAS)(1 - f_bP) + (1 - f_bAD_1)(1 - f_bAD_2)(1 - f_bAD_3)(f_bAS)(1 - f_bP) \\
+2(f_bAD_1)(f_bAD_2)(1 - f_bAD_3)(1 - f_bAS)(1 - f_bP) + 2(f_bAD_1)(1 - f_bAD_2)(f_bAD_3)(1 - f_bAS)(1 - f_bP) \\
+(f_bAD_1)(1 - f_bAD_2)(1 - f_bAD_3)(f_bAS)(1 - f_bP) + (f_bAD_1)(1 - f_bAD_2)(1 - f_bAD_3)(1 - f_bAS)(f_bP) \\
2(1 - f_bAD_1)(f_bAD_2)(f_bAD_3)(1 - f_bAS)(1 - f_bP) + (1 - f_bAD_1)(f_bAD_2)(1 - f_bAD_3)(f_bAS)(1 - f_bP) \\
+(1 - f_bAD_1)(f_bAD_2)(1 - f_bAD_3)(1 - f_bAS)(f_bP) + (1 - f_bAD_1)(1 - f_bAD_2)(f_bAD_3)(f_bAS)(1 - f_bP) \\
+(1 - f_bAD_1)(1 - f_bAD_2)(f_bAD_3)(1 - f_bAS)(f_bP) + (1 - f_bAD_1)(1 - f_bAD_2)(1 - f_bAD_3)(f_bAS)(f_bP) \\
+3(f_bAD_1)(f_bAD_2)(f_bAD_3)(1 - f_bAS)(1 - f_bP) + 2(f_bAD_1)(f_bAD_2)(1 - f_bAD_3)(f_bAS)(1 - f_bP) \\
+2(f_bAD_1)(f_bAD_2)(1 - f_bAD_3)(1 - f_bAS)(f_bP) + 2(f_bAD_1)(1 - f_bAD_2)(f_bAD_3)(f_bAS)(1 - f_bP) \\
+2(f_bAD_1)(1 - f_bAD_2)(f_bAD_3)(1 - f_bAS)(f_bP) + (f_bAD_1)(1 - f_bAD_2)(1 - f_bAD_3)(f_bAS)(f_bP) \\
+2(1 - f_bAD_1)(f_bAD_2)(f_bAD_3)(f_bAS)(1 - f_bP) + 2(1 - f_bAD_1)(f_bAD_2)(f_bAD_3)(1 - f_bAS)(f_bP) \\
+(1 - f_bAD_1)(f_bAD_2)(1 - f_bAD_3)(f_bAS)(f_bP) + (1 - f_bAD_1)(1 - f_bAD_2)(f_bAD_3)(f_bAS)(f_bP) \\
+3(f_bAD_1)(f_bAD_2)(f_bAD_3)(f_bAS)(1 - f_bP) + 3(f_bAD_1)(f_bAD_2)(f_bAD_3)(1 - f_bAS)(f_bP) \\
+2(f_bAD_1)(1 - f_bAD_2)(f_bAD_3)(f_bAS)(f_bP) + 2(f_bAD_1)(f_bAD_2)(1 - f_bAD_3)(f_bAS)(f_bP) \\
+2(1 - f_bAD_1)(f_bAD_2)(f_bAD_3)(f_bAS)(f_bP) + 3(f_bAD_1)(f_bAD_2)(f_bAD_3)(f_bAS)(f_bP)
\end{pmatrix}$$

REFERENCES CITED

Achilleos, A., Wehman, A. M., and Nance, J. (2010) PAR-3 mediates the initial clustering and apical localization of junction and polarity proteins during C. elegans intestinal epithelial cell polarization. Development *137(11)*:1833-42.

Albertson, R. and Doe, C. Q. (2003) Dlg, Scrib and Lgl regulate neuroblast cell size and mitotic spindle asymmetry. Nat. Cell Biol. *5(2)*:166-170.

Altschuler, S. J., Angenent, S. B., Wang, Y., and Wu, L. F. (2008) On the spontaneous emergence of cell polarity. Nature 454(7206):886-9.

Atwood, S. X., Chabu, C., Penkert, R. R., Doe, C. Q., and Prehoda, K. E. (2007) Cdc42 acts downstream of Bazooka to regulate neuroblast polarity through Par-6 aPKC. J Cell Sci *120(18):*3200-6.

Atwood S. X. and Prehoda, K. E. (2009) aPKC phosphorylates Miranda to polarize fate determinants during neuroblast asymmetric cell division. Curr Biol *19(9):*723-9.

Baena-López, L. A., Baonza, A., and García-Bellido, A. (2005) The orientation of cell divisions determines the shape of Drosophila organs. Curr Biol *15*:1640–1644.

Baker, J. and Garrod, D. (1993) Epithelial cells retain junctions during mitosis. J Cell Sci *104(2)*:415-25.

Barnes, A. P., Lilley, B. N., Pan, Y. A., Plummer, L. J., Powell, A. W. et al. (2007) LKB1 and SAD kinases define a pathway required for the polarization of cortical neurons. Cell *129(3)*:549-63.

Bellaïche, Y., Radovic, A., Woods, D. F., Hough, C. D., Parmentier, M. L., et al. (2001) The Partner of Inscuteable/Discs-large complex is required to establish planar polarity during asymmetric cell division in Drosophila. Cell *106(3)*:355-66.

Benton, R. and St Johnston, D. (2003) Drosophila PAR-1 and 14-3-3 inhibit Bazooka/PAR-3 to establish complementary cortical domains in polarized cells. Cell *12*;115(6):691-704.

Betschinger, J., Mechtler, K., and Knoblich, J. A. (2006) Asymmetric segregation of the tumor suppressor brat regulates self-renewal in Drosophila neural stem cells. Cell *124(6)*:1241-1253.

Bhat, K. M. (1998) Cell-cell signaling during neurogenesis: some answers and many questions.Int J Dev Biol 42(2):127-39.

Broadus, J. and Doe, C. Q. (1997) Extrinsic cues, intrinsic cues and microfilaments regulate asymmetric protein localization in Drosophila neuroblasts. Curr Biol. *7(11):*827-35.

Buchler, N. E. and Louis, M (2008) Molecular titration and ultrasensitivity in regulatory networks J. Mol. Biol. 384 (5): 1106–1119.

Buchler, N. E. and Cross, F. R. (2009) Protein sequestration generates a flexible ultrasensitive response in a genetic network. Mol. Syst. Biol. *5:*272.

Cabernard, C., and Doe, C. Q. (2009) Apical/basal spindle orientation is required for neuroblast homeostasis and neuronal differentiation in Drosophila. Dev Cell *17*: 134–141.

Cabernard, C., Prehoda, K. E., and Doe, C. Q. (2010) A spindle-independent cleavage furrow positioning pathway. Nature *467*: 91–94.

Cappello, S., Attardo, A., Wu, X., Iwasato, T., Itohara, S., et al., (2006) The Rho-GTPase cdc42 regulates neural progenitor fate at the apical surface. Nat Neurosci *9(9)*:1099-107.

Chau, A. H., Walter, J. M., Gerardin, J., Tang, C., and Lim, W.A. (2012) Designing synthetic regulatory networks capable of self-organizing cell polarization. Cell *151(2*): 320-32.

Chia, W., Somers, W. G., and Wang, H. (2008) Drosophila neuroblast asymmetric divisions: cell cycle regulators, asymmetric protein localization, and tumorigenesis. J Cell Biol *180*: 267–272.

Connell, M., Cabernard, C., Ricketson, D., Doe, C. Q., and Prehoda, K. E. (2011) Asymmetric cortical extension shifts cleavage furrow position in Drosophila neuroblasts. Mol Biol Cell *22(22)*:4220-6.

Cuenca, A. A., Schetter, A., Aceto, D., Kemphues, K. and Seydoux, G. (2003) Polarization of the C. elegans zygote proceeds via distinct establishment and maintenance phases. Development *130(7)*:1255-65.

David, D. J., Wang, Q., Feng, J. J., and Harris, T. J. (2013). Bazooka inhibits aPKC to limit antagonism of actomyosin networks during amnioserosa apical constriction. Development *140(23)*: 4719-4729.

Doe, C. Q. (2008) Neural stem cells: balancing self-renewal with differentiation. Development *135(9)*:1575-87.

Du. Q., Stukenberg, P. T., and Macara, I. G. (2001) A mammalian Partner of inscuteable binds NuMA and regulates mitotic spindle organization. Nature Cell Biol *3*: 1069–1075.

Du, Q., and Macara, I. G. (2004) Mammalian Pins is a conformational switch that links NuMA to heterotrimeric G proteins. Cell *119*: 503–516.

Dueber, J. E., Mirsky, E. A., and Lim, W. A. (2007) Engineering synthetic signaling proteins with ultrasensitive input/output control. Nat. Biotechnol. *25(6):* 660–662.

Egger, B., Boone, J. Q., Stevens, N. R., Brand, A. H., and Doe, C. Q. (2007) Regulation of spindle orientation and neural stem cell fate in the Drosophila optic lobe. Neural Dev *2*: 1.

Emery, G., Hutterer, A., Berdnik, D., Mayer, B., Wirtz-Peitz, F., et al. (2005) Asymmetric Rab 11 endosomes regulate delta cycling and specify cell fate in the Drosophila nervous system. Cell *122*:763–773.

Ferrell, J. E., Jr. (1996) Tripping the switch fantastic: how a protein kinase cascade can convert graded inputs into switch-like outputs. Trends Biochem. Sci. *21 (12):* 460–466.

Ferrell, J. E., Jr. and Machleder, E. M. (1998) The biochemical basis of an all-or-none cell fate switch in Xenopus oocytes. Science *280 (5365):* 895–898.

Ferrell, J. E., Jr. (1999) Building a cellular switch: more lessons from a good egg. Bioessays *21(10):* 866–870.

Fletcher, G.C., Lucas, E.P., Brain, R., Tournier, A., and Thompson, B.J. (2012) Positive feedback and mutual antagonism combine to polarize crumbs in the Drosophila follicle cell epithelium. Curr. Biol *22(12)*: 1116-1122.

Gambardella L. and Vermeren S. (2013) Molecular players in neutrophil chemotaxis--focus on PI3K and small GTPases. J Leukoc Biol *94(4)*: 603-12.

Glotzer M (2004) Cleavage furrow positioning. J Cell Biol *164(3):* 347–351.

Goehring, N. W., Hoege, C., Grill, S. W., and Hyman, A. A. (2011) PAR proteins diffuse freely across the anterior-posterior boundary in polarized C. elegans embryos. J Cell Biol *193(3)*:583-94.

Goldbeter, A. and Koshland, D. E., Jr. (1981) An amplified sensitivity arising from covalent modification in biological systems. Proc. Natl. Acad. Sci. U.S.A. *78(11):* 6840–6844.

Goldstein, B. and Hird, S. N. (1996) Specification of the anteroposterior axis in Caenorhabditis elegans. Development *122(5)*:1467-74.

Goryachev, A. B. and Pokhilko, A. V. (2009) Dynamics of Cdc42 network embodies a Turing-type mechanism of yeast cell polarity. FEBS Lett. *582(10):*1437-43.

Gotta, M., Abraham, M. C., and Ahringer, J. (2001) CDC-42 controls early cell polarity and spindle orientation in C. elegans.Curr Biol *11(7)*:482-8.

Grabher, C., von Boehmer, H., and Look, A. T. (2006) Notch 1 activation in the molecular pathogenesis of T-cell acute lymphoblastic leukaemia. Nat Rev Cancer *6(5)*:347-59.

Gray, R. S., Cheung, K. J., and Ewald, A. J. (2010) Cellular mechanisms regulating epithelial morphogenesis and cancer invasion. Curr Opin Cell Biol *22*: 640–650.

Gunawardena, J. (2005) Multisite protein phosphorylation makes a good threshold but can be a poor switch. Proc. Natl. Acad. Sci. U.S.A. *102(41):* 14617–14622.

Hao, Y., Boyd, L., and Seydoux, G. (2006) Stabilization of cell polarity by the C. elegans RING protein PAR-2. Dev Cell *10(2)*:199-208.

Harris, B. Z. and Lim, W. A. (2001) Mechanism and role of PDZ domains in signaling complex assembly. J. Cell Sci. *114 (18):* 3219–3231.

Harris, K. P. and Tepass, U. (2008) Cdc42 and Par proteins stabilize dynamic adherens junctions in the Drosophila neuroectoderm through regulation of apical endocytosis. J Cell Biol *183(6)*:1129-43.

Heath, J. P. and Holifield, B. F. (1993) On the mechanisms of cortical actin flow and its role in cytoskeletal organisation of fibroblasts. Symp Soc Exp Biol *47*: 35-56.

Higuchi, M., Masuyama, N., Fukui, Y., Suzuki, A., and Gotoh, Y. (2001) Akt mediates Rac/Cdc42-regulated cell motility in growth factor-stimulated cells and in invasive PTEN knockout cells. Curr Biol *11(24)*: 1958-62.

Hill, A. (1910) The possible effects of the aggregation of the molecules of haemoglobin on its dissociation curves. J. Physiol. *40(Supplemental):* iv–vii.

Horikoshi, Y., Suzuki, A., Yamanaka, T., Sasaki, K., Mizuno, K. et al. (2009) Interaction between PAR-3 and the aPKC-PAR-6 complex is indispensable for apical domain development of epithelial cells. J Cell Sci *122(10)*:1595-606.

Hurov, J. B., Watkins, J. L. and Piwnica-Worms, H. (2004) Atypical PKC phosphorylates PAR-1 kinases to regulate localization and activity. Curr Biol *14(8):*736-41.

Hutterer, A., Betschinger, J., Petronczki, M., and Knoblich, J. A. (2004) Sequential roles of Cdc42, Par-6, aPKC, and Lgl in the establishment of epithelial polarity during Drosophila embryogenesis. Dev Cell *6(6):*845-54.

Huynh, J. R., Petronczki, M., Knoblich, J. A., and St Johnston, D. (2001) Bazooka and PAR-6 are required with PAR-1 for the maintenance of oocyte fate in Drosophila. Curr Biol *11(11)*:901-6.

Iden, S., van Riel, W. E., Schäfer, R., Song, J. Y., Hirose, T., Ohno, S., and Collard, J. G. (2012) Tumor type-dependent function of the par3 polarity protein in skin tumorigenesis. Cancer Cell *22(3)*:389-403.

Irazoqui, J. E., Gladfelter, A. S., and Lew, D. J. (2003) Scaffold-mediated symmetry breaking by Cdc42p. Nat Cell Biol *5(12)*:1062-70.

Izumi, Y., Ohta, N., Itoh-Furuya, A., Fuse, N., and Matsuzaki, F. (2004) Differential functions of G protein and Baz-aPKC signaling pathways in Drosophila neuroblast asymmetric division. J Cell Biol *164(5)*:729-38.

Joberty, G., Petersen, C., Gao, L. and Macara, I. G. (2000). The cell-polarity protein Par6 links Par3 and atypical protein kinase C to Cdc42. Nat. Cell Biol. *2*, 531-539.

Johnson, J. M., Jin, M., and Lew, D. J.. (2011) Symmetry breaking and the establishment of cell polarity in budding yeast. Curr Opin Genet Dev. *21(6)*: 740-6.

Johnston, C. A., Hirono, K., Prehoda, K. E., and Doe, C. Q. (2009) Identification of an Aurora-A/PinsLINKER/Dlg spindle orientation pathway using induced cell polarity in S2 cells. Cell *138(6):* 1150–1163.

Kato, Y. (2011). The multiple roles of Notch signaling during left-right patterning. Cell Mol Life Sci *68(15):* 2555-67.

Kholodenko, B. N. (2006) Cell-signalling dynamics in time and space. Nat. Rev. Mol. Cell. Biol. *7(3):*165–176.

Kibar, Z., Capra, V., and Gros, P. (2007) Toward understanding the genetic basis of neural tube defects. Clin Genet *71(4)*:295-310.

Kim, S. Y. and Ferrell, J. E., Jr. (2007) Substrate competition as a source of ultrasensitivity in the inactivation of Wee1. Cell *128(6):* 1133–1145.

Kisurina-Evgenieva, O., Mack, G., Du, Q., Macara, I., Khodjakov, A., et al. (2004) Multiple mechanisms regulate NuMA dynamics at spindle poles. J Cell Sci *117*: 6391–6400.

Knoblich, J. A. (2010) Asymmetric cell division: recent developments and their implications for tumour biology. Nat Rev Mol Cell Biol *11*: 849–860.

Koshland, D. E., Jr., Nemethy, G., and Filmer, D. (1966) Comparison of experimental binding data and theoretical models in proteins containing subunits. Biochemistry *5(1):* 365–385.

Koshland, D. E., Jr., Goldbeter, A, and Stock, J. B. (1982) Amplification and adaptation in regulatory and sensory systems Science *217(4556):* 220–225.

Krahn, M. P., Egger-Adam, D., and Wodarz, A. (2009) PP2A antagonizes phosphorylation of Bazooka by PAR-1 to control apical-basal polarity in dividing embryonic neuroblasts. Dev Cell *16(6)*:901-8.

Krahn, M. P., Bückers, J., Kastrup, L., and Wodarz, A. (2010) Formation of a Bazooka-Stardust complex is essential for plasma membrane polarity in epithelia. J Cell Biol *190(5)*:751-60.

Kraut, R., Chia, W., Jan, L. Y., Jan, Y. N., and Knoblich, J. A. (1996) Role of inscuteable in orienting asymmetric cell divisions in Drosophila. Nature *383*: 50–55.

Le Borgne, R. and Schweisguth, F. (2003) Unequal segregation of Neuralized biases Notch activation during asymmetric cell division. Dev Cell *5(1)*:139-48.

Lee, C. Y., Andersen, R. O., Cabernard, C., Manning, L., Tran, K. D., et al. (2006) Drosophila Aurora-A kinase inhibits neuroblast self-renewal by regulating aPKC/Numb cortical polarity and spindle orientation. Genes Dev *20(24)*:3464-74.

Lechler, T. and Fuchs, E. (2005) Asymmetric cell divisions promote stratification and differentiation of mammalian skin. Nature *437:* 275–280.

Lee, W. L., Oberle, J. R., and Cooper, J. A. (2003) The role of the lissencephaly protein Pac1 during nuclear migration in budding yeast. J Cell Biol *160(3)*:355-64.

Leibfried, A., Müller. S., and Ephrussi, A. (2013) A Cdc42-regulated actin cytoskeleton mediates Drosophila oocyte polarization. Development *140(2)*:362-71.

Lu, B., Roegiers, F., Jan, L. Y., and Jan, Y. N. (2001) Adherens junctions inhibit asymmetric division in the Drosophila epithelium. Nature *409(6819)*:522-5.

Ma, W., Trusina, A., El-Samad, H., Lim, W. A., and Tang, C. (2009) Defining network topologies that can achieve biochemical adaptation. Cell *138(4):*760-73.

McCusker, D., Denison, C., Anderson, S., Egelhofer, T. A., Yates, J. R. 3rd, et al., (2007) Cdk1 coordinates cell-surface growth with the cell cycle. Nat Cell Biol *9(5*):506-15.

McKinley, R. F. and Harris, T. J. (2012). Displacement of basolateral Bazooka/PAR-3 by regulated transport and dispersion during epithelial polarization in Drosophila. Mol. Biol. Cell *23(22)*: 4465-4471.

McKinley, R. F., Yu, C. G., and Harris, T. J. (2012). Assembly of Bazooka polarity landmarks through a multifaceted membrane-association mechanism. J. Cell Sci. 125(5): 1177-1190.

Meinhardt, H. and Gierer, A. (2000) Pattern formation by local self-activation and lateral inhibition. Bioessays *22(8)*:753-60.

Mellman, I. and Nelson, W. J. (2008) Coordinated protein sorting, targeting and distribution in polarized cells Nat. Rev. Mol. Cell. Biol. *9 (11):* 833–845.

Miller, R. K., D'Silva, S., Moore, J. K., and Goodson, H. V. (2006) The CLIP-170 orthologue Bik1p and positioning the mitotic spindle in yeast. Curr Top Dev Biol *76*:49-87.

Moore, J. K. and Cooper, J. A. (2010) Coordinating mitosis with cell polarity: Molecular motors at the cell cortex. Semin Cell Dev Biol *21:* 283–289.

Moore, T. I., Tanaka, H., Kim, H. J., Jeon, N. L., and Yi, T. M. (2013) Yeast G-proteins mediate directional sensing and polarization behaviors in response to changes in pheromone gradient direction.Mol Biol Cell *24(4)*:521-34.

Morais-de-Sa, E., Mirouse, V., and St Johnston, D. (2010) aPKC phosphorylation of Bazooka defines the apical/lateral border in drosophila epithelial cells. Cell *141*:509–523.

Motegi, F. and Sugimoto, A. (2006) Sequential functioning of the ECT-2 RhoGEF, RHO-1 and CDC-42 establishes cell polarity in Caenorhabditis elegans embryos. Nat Cell Biol *8(9)*:978-85.

Motegi, F., Zonies, S., Hao, Y., Cuenca, A. A., Griffin, E. and Seydoux, G. (2011) Microtubules induce self-organization of polarized PAR domains in Caenorhabditis elegans zygotes. Nat Cell Biol *13(11):*1361-7.

Munro, E., Nance, J. and Priess, J. R. (2004) Cortical flows powered by asymmetrical contraction transport PAR proteins to establish and maintain anterior-posterior polarity in the early C. elegans embryo. Dev Cell *7(3)*:413-24.

Nguyen, J. T. and Lim, W. A. (1997) How Src exercises self-restraint. Nat. Struct. Biol. *4 (4):* 256–260.

Nipper, R. W., Siller, K. H., Smith, N. R., Doe, C. Q., and Prehoda, K. E. (2007) Galphai generates multiple Pins activation states to link cortical polarity and spindle orientation in Drosophila neuroblasts. Proc Natl Acad Sci USA *104*: 14306–14311.

Novak, B. and Tyson, J. J. (1993) Numerical analysis of a comprehensive model of M-phase control in Xenopus oocyte extracts and intact embryos. J. Cell Sci. *106(4):* 1153–1168.

Orgogozo, V., Schweisguth, F., and Bellaïche, Y. (2001) Lineage, cell polarity and inscuteable function in the peripheral nervous system of the Drosophila embryo. Development *128(5)*:631-43.

Pawson, T. and Nash, P. (2003) Assembly of cell regulatory systems through protein interaction domains. Science *300(5618):* 445–452.

Pease, J. C. and Tirnauer, J. S. (2011) Mitotic spindle misorientation in cancer–out of alignment and into the fire. J Cell Sci *124:* 1007–1016.

Penkert, R. R., DiVittorio, H. M., and Prehoda, K. E. (2004) Internal recognition through PDZ domain plasticity in the Par-6-Pals1 complex. Nat. Struct. Mol. Biol. *11(11):* 1122–1127.

Peterson, F. C., Penkert, R. R., Volkman, B. F. and Prehoda, K. E.(2004) Cdc42 regulates the Par-6 PDZ domain through an allosteric CRIB-PDZ transition. Mol. Cell *13,* 665-676.

Petronczki, M. and Knoblich, J. A. (2001) DmPAR-6 directs epithelial polarity and asymmetric cell division of neuroblasts in Drosophila. Nat Cell Biol *3(1)*:43-9.

Pomerening, J. R., Sontag, E. D., and Ferrell, J. E., Jr. (2003) Building a cell cycle oscillator: hysteresis and bistability in the activation of Cdc2. Nat. Cell Biol. *5(4):* 346–351.

Posern, G. (1998) Development of highly selective SH3 binding peptides for Crk and CRKL which disrupt Crk-complexes with DOCK180, SoS and C3G. Oncogene *16(15):* 1903–1912.

Postiglione, M. P., Jüschke, C., Xie, Y., Haas, G. A., Charalambous, C., and Knoblich, J. A. (2011) Mouse inscuteable induces apical-basal spindle orientation to facilitate intermediate progenitor generation in the developing neocortex. Neuron *72(2)*:269-84.

Poulson, N. and Lechler, T. (2010) Robust control of mitotic spindle orientation in the developing epidermis. J Cell Biol *191*: 915–922.

Prehoda, K. E. (2009) Polarization of Drosophila neuroblasts during asymmetric division. Cold Spring Harb Perspect Biol *1*: a001388.

Pufall, M. A. and Graves, B. J. (2002) Autoinhibitory domains: modular effectors of cellular regulation. Annu. Rev. Cell Dev. Biol. *18:* 421–462.

Reinsch, S. and Karsenti, E. (1994) Orientation of spindle axis and distribution of plasma membrane proteins during cell division in polarized MDCKII cells. J Cell Biol *126*: 1509–1526.

Rida, P. C. and Chen, P. (2009) Line up and listen: Planar cell polarity regulation in the mammalian inner ear. Semin Cell Dev Biol *20(8)*:978-85.

Roegiers, F., Younger-Shepherd, S., Jan, L. Y., and Jan, Y. N. (2001) Bazooka is required for localization of determinants and controlling proliferation in the sensory organ precursor cell lineage in Drosophila. Proc Natl Acad Sci U S A *98(25)*:14469-74.

Rolls, M. M., Albertson, R., Shih, H. P., Lee, C. Y., and Doe, C. Q. (2003) Drosophila aPKC regulates cell polarity and cell proliferation in neuroblasts and epithelia. J Cell Biol *163(5)*:1089-98.

Royer, C. and Lu, X. (2011) Epithelial cell polarity: a major gatekeeper against cancer? Cell Death Differ *18(9)*: 1470–1477.

Sallee, N. A., Yeh, B. J., and Lim, W. A. (2007) Engineering modular protein interaction switches by sequence overlap. J. Am. Chem. Soc. *129 (15):* 4606– 4611.

Saunders, C. and Limbird, L. E. (1997) Disruption of microtubules reveals two independent apical targeting mechanisms for G-protein-coupled receptors in polarized renal epithelial cells. J Biol Chem *272(30)*:19035-45.

Schaefer, M., Shevchenko, A., Shevchenko, A., and Knoblich, J. A. (2000) A protein complex containing Inscuteable and the Galpha-binding protein Pins orients asymmetric cell divisions in Drosophila. Current Biol *10:* 353–362.

Schober, M., Schaefer, M., and Knoblich, J. A. (1999) Bazooka recruits Inscuteable to orient asymmetric cell divisions in Drosophila neuroblasts. Nature *402*: 548–551.

Schonegg, S. and Hyman, A. A. (2006) CDC-42 and RHO-1 coordinate acto-myosin contractility and PAR protein localization during polarity establishment in C. elegans embryos. Development *133(18):*3507-16.

Ségalen, M., Johnston, C. A., Martin, C. A., Dumortier, J. G., Prehoda, K. E., et al. (2010) The Fz-Dsh planar cell polarity pathway induces oriented cell division via Mud/NuMA in Drosophila and zebrafish. Dev Cell *19(5)*:740-52.

Sheeman, B., Carvalho, P., Sagot, I., Geiser, J., Kho, D., Hoyt, M. A., and Pellman, D. (2003) Determinants of S. cerevisiae dynein localization and activation: implications for the mechanism of spindle positioning. Curr Biol *13(5)*:364-72.

Shimizu, K., Sato, M., and Tabata, T. (2011) The Wnt5/planar cell polarity pathway regulates axonal development of the Drosophila mushroom body neuron. J Neurosci. *31(13)*:4944-54.

Siegrist S. E. and Doe C. Q. (2005) Microtubule-induced Pins/Galphai cortical polarity in Drosophila neuroblasts. Cell *123*: 1323–1335.

Siegrist, S. E. and Doe, C. Q. (2006) Extrinsic cues orient the cell division axis in Drosophila embryonic neuroblasts. Development *133(3)*:529-36.

Siller K. H., Cabernard C., Doe C. Q. (2006) The NuMA-related Mud protein binds Pins and regulates spindle orientation in Drosophila neuroblasts. Nature Cell Biol *8*: 594–600.

Siller, K. H. and Doe, C. Q. (2008) Lis1/dynactin regulates metaphase spindle orientation in Drosophila neuroblasts. Dev Biol *319*: 1–9.

Siller K. H. and Doe C. Q. (2009) Spindle orientation during asymmetric cell division. Nature Cell Biol *11*: 365–374.

Slaughter, B. D., Das, A., Schwartz, J. W., Rubinstein, B., and Li, R. (2009) Dual modes of cdc42 recycling fine-tune polarized morphogenesis. Dev Cell *17(6)*:823-35.

Smith, N. R. and Prehoda, K. E. (2011) Robust spindle alignment in Drosophila neuroblasts by ultrasensitive activation of pins Mol. Cell *43 (4):* 540–549.

St Johnston, D. and Ahringer, J. (2010) Cell polarity in eggs and epithelia: parallels and diversity. Cell *141(5)*:757-74.

Staub, O. and Rotin, D. (1997) Regulation of ion transport by protein-protein interaction domains Curr. Opin. Nephrol. Hypertens. *6(5):* 447–454.

Strutt, D. (2001) Planar polarity: getting ready to ROCK. Curr Biol *11(13)*:R506-9.

Strutt, H. and Strutt, D. (2009) Asymmetric localisation of planar polarity proteins: Mechanisms and consequences. Semin Cell Dev Biol *20(8)*:957-63.

Tian, A. G. and Deng, W. M. (2008). Lgl and its phosphorylation by aPKC regulate oocyte polarity formation in Drosophila. Development *135(3)*: 463-471.

Tio, M., Zavortink, M., Yang, X., and Chia, W. (1999) A functional analysis of inscuteable and its roles during Drosophila asymmetric cell divisions. J Cell Sci *112*: 1541–1551.

Tio, M., Udolph, G., Yang, X., and Chia, W. (2001) cdc2 links the Drosophila cell cycle and asymmetric division machineries. Nature *409(6823)*:1063-7.

Tyson, J. J., Chen, K. C., and Novak, B (2003) Sniffers, buzzers, toggles and blinkers: dynamics of regulatory and signaling pathways in the cell Curr. Opin. Cell Biol. *15(2):*221–231.

Udolph, G., Rath, P., and Chia, W. (2001) A requirement for Notch in the genesis of a subset of glial cells in the Drosophila embryonic central nervous system which arise through asymmetric divisions. Development *128(8)*:1457-66.

Vanzo, N., Oprins, A., Xanthakis, D., Ephrussi, A., and Rabouille, C. (2007) Stimulation of endocytosis and actin dynamics by Oskar polarizes the Drosophila oocyte.Dev Cell *12(4)*:543-55.

Wang, H., Ouyang, Y., Somers, W. G., Chia, W., and Lu, B. (2007) Polo inhibits progenitor self-renewal and regulates Numb asymmetry by phosphorylating Pon. Nature *449(7158)*:96-100.

Wang, W., Li, X., Huang, J., Feng, L., Dolinta, K. G., and Chen, J. (2014) Defining the protein-protein interaction network of the human hippo pathway. Mol Cell Proteomics *13(1)*:119-31.

Wedlich-Soldner, R., Altschuler, S., Wu, L., and Li, R. (2003) Spontaneous cell polarization through actomyosin-based delivery of the Cdc42 GTPase. Science *299(5610)*:1231-5.

Werts, A. D., Roh-Johnson, M., and Goldstein, B. (2011) Dynamic localization of C. elegans TPR-GoLoco proteins mediates mitotic spindle orientation by extrinsic signaling. Development *138(20)*:4411-22.

Wirtz-Peitz, F., Nishimura, T., and Knoblich, J. A. (2008) Linking cell cycle to asymmetric division: Aurora-A phosphorylates the Par complex to regulate Numb localization. Cell *135(1)*:161-73.

Wodarz A., Ramrath A., Kuchinke U., and Knust E. (1999) Bazooka provides an apical cue for Inscuteable localization in Drosophila neuroblasts. Nature *402*: 544–547.

Wu, X. (1995) Structural basis for the specific interaction of lysine-containing proline-rich peptides with the N-terminal SH3 domain of c-Crk. Structure. *3(2):*215–226.

Yoshiura, S., Ohta, N., and Matsuzaki, F. (2012) Tre1 GPCR signaling orients stem cell division in the Drosophila central nervous system. Dev Cell *22(1)*:79-91.

Yu, F., Morin, X., Cai, Y., Yang, X., and Chia, W. (2000) Analysis of partner of inscuteable, a novel player of Drosophila asymmetric divisions, reveals two distinct steps in inscuteable apical localization. Cell *100*: 399–409.

Yu, F., Ong, C. T., Chia, W., and Yang, X. (2000) Membrane targeting and asymmetric localization of Drosophila partner of inscuteable are discrete steps controlled by distinct regions of the protein. Mol Cell Biol *22*: 4230–4240.

Zallen, J. A. (2007) Planar polarity and tissue morphogenesis. Cell *129(6)*:1051-63.

Zhu, J., Wen, W., Zheng, Z., Shang, Y., Wei, Z., et al. (2011) LGN/mInsc and LGN/NuMA complex structures suggest distinct functions in asymmetric cell division for the Par3/mInsc/LGN and Gai/LGN/NuMA pathways. Mol Cell *43*: 418–431.

Zigman, M., Cayouette, M., Charalambous, C., Schleiffer, A., Hoeller, O., et al. (2005) Mammalian inscuteable regulates spindle orientation and cell fate in the developing retina. Neuron 48(4):539-45.

Zonies, S., Motegi, F., Hao, Y., and Seydoux, G. (2010) Symmetry breaking and polarization of the C. elegans zygote by the polarity protein PAR-2. Development *137(10)*:1669-77